Instytut Paleobiologii Polskiej Akademii Nauk

# The effect of geochemical parameters of the environment (Mg/Ca) and diet on the biomineralization of the echinoderm skeleton

## Wpływ geochemicznych parametrów środowiska (Mg/Ca) oraz diety na biomineralizację szkieletu szkarłupni

Dorota Kołbuk

Dissertation for the degree of PhD at the Institute of Paleobiology, Polish Academy of Sciences. The research was conducted under the supervision of Przemysław Gorzelak Ph.D., D. Sc.

Rozprawa doktorska wykonana w Instytucie Paleobiologii PAN pod kierunkiem dr. hab. Przemysława Gorzelaka

Warszawa, grudzień 2021

# Table of contents

Acknowledgements 4

Streszczenie 5

Summary 9

Introduction 13

Chapter I 31

Effects of seawater chemistry ($Mg^{2+}/Ca^{2+}$ ratio) and diet on the skeletal Mg/Ca ratio in the common sea urchin *Paracentrotus lividus*

Chapter II 45

Effects of seawater $Mg^{2+}/Ca^{2+}$ ratio and diet on the biomineralization and growth of sea urchins and the relevance of fossil echinoderms to paleoenvironmental reconstructions

Chapter III 78

Impact of seawater $Mg^{2+}/Ca^{2+}$ on Mg/Ca of asterozoan skeleton – evidence from culturing and the fossil record

Conclusions 108

Future perspectives 109

Declarations 110

# Acknowledgements

In the first place, I would like to thank my supervisor, dr hab. Przemysław Gorzelak (Institute of Paleobiology, Polish Academy of Sciences, Warsaw, Poland), who introduced me to the fascinating world of echinoderms. Thank you for being a great mentor and for the continuous support of this thesis.

I am also greatly indebted to Prof. Jarosław Stolarski (Institute of Paleobiology, Polish Academy of Sciences, Warsaw, Poland) for the opportunity to join the Biomineralization Working Group and for useful advice throughout the course of my studies.

Completion of this thesis would be impossible without help and hospitality of the staff and students of the Marine Biology Lab (Université Libre de Bruxelles, Belgium), who hosted me during biomineralization experiments. My deepest thanks go to Prof. Philippe Dubois and Saloua M'Zoudi, whose scientific expertise proved invaluable on many occasions.

Thanks are also due to Prof. Urszula Radwańska (Faculty of Geology, University of Warsaw, Poland) and Prof. Barbara Studencka (Museum of the Earth, Polish Academy of Sciences, Warsaw, Poland) for allowing me to access fossil specimens from their collections.

Finally, I would like to thank: my parents and siblings for their support, Jakub and Piotr for their outstanding patience, Samar for being a great friend, and Ludwik with family for giving me motivation to finish this thesis. I also thank my fellow PhD students from the Institute of Paleobiology – we're all in this together!

# Streszczenie

Szkarłupnie posiadają szkielet pochodzenia mezodermalnego, składający się z wielu płytek o charakterystycznej beleczkowatej (trabekularnej) strukturze (tzw. stereom). Szkielet ten zbudowany jest z kalcytu o wysokiej zawartości magnezu oraz z niewielkiej ilości związków organicznych, amorficznego węglanu wapnia (ACC) oraz wody. Powstaje on na drodze biologicznie kontrolowanej mineralizacji.

Dotychczas uważano, że jony wapnia i magnezu niezbędne do tworzenia szkieletu szkarłupni pochodzą wyłącznie z wody morskiej, a stosunek Mg/Ca w szkielecie stanowi dobre odzwierciedlenie okresowych różnic w koncentracji tych pierwiastków w środowisku. Dzięki temu na podstawie danych geochemicznych (stosunku Mg/Ca) zawartych w szkieletach szkarłupni można obliczyć stosunek molowy $Mg^{2+}/Ca^{2+}$ wody morskiej, w której zwierzęta te wzrastały. Potencjał takich rekonstrukcji został dostrzeżony przez badaczy, którzy wykorzystywali dobrze zachowane kopalne szkarłupnie do odtwarzania parametrów geochemicznych dawnych oceanów. Niemniej w ostatnich latach ukazało się kilka prac sugerujących, że na stosunek Mg/Ca w szkielecie mogą wpływać również inne czynniki środowiskowe (temperatura i zasolenie) oraz biologiczne, wynikające z fizjologii organizmu (tzw. efekt witalny, ang. *vital effect*), co oznacza, że stopień kontroli biomineralizacji przez szkarłupnie jest większy, niż dotychczas uważano. Co więcej, brak jest wiarygodnych danych eksperymentalnych na dzisiejszych szkarłupniach sugerujących związek między Mg/Ca w ich szkielecie a $Mg^{2+}/Ca^{2+}$ w wodzie morskiej. Celem pracy doktorskiej było przeprowadzenie serii eksperymentów biomineralizacyjnych na dzisiejszych szkarłupniach, które miały wykazać jaki wpływ na skład chemiczny ich szkieletu mają zmiany $Mg^{2+}/Ca^{2+}$ wody morskiej oraz diety.

W ramach pracy doktorskiej zaplanowano trzy eksperymenty biomineralizacyjne na różnych, niespokrewnionych gatunkach szkarłupni, których wyniki podsumowano w trzech rozdziałach/artykułach:

1) krótkoterminowy (14-dniowy) eksperyment dotyczący wpływu podwyższonej koncentracji $Ca^{2+}$ w wodzie morskiej oraz diety wzbogaconej w $MgCO_3$ na skład chemiczny regenerujących kolców dorosłych osobników jeżowców euechinoida *Paracentrotus lividus*;
2) rozszerzony (21-dniowy) eksperyment dotyczący wpływu obniżonego stosunku molowego $Mg^{2+}/Ca^{2+}$ w wodzie morskiej (uzyskanego poprzez podwyższanie koncentracji $Ca^{2+}$ oraz obniżanie $Mg^{2+}$) oraz diety wzbogaconej w MgO na tempo wzrostu i respiracji oraz skład chemiczny nowo wzrastających płytek pancerza, zębów,

demipiramid oraz kolców dwóch gatunków jeżowców (cidaroida *Prionocidaris baculosa* i euechinoida *Psammechinus miliaris*);

3) rozszerzony (21-dniowy) eksperyment dotyczący wpływu obniżonego stosunku molowego $Mg^{2+}/Ca^{2+}$ w wodzie morskiej (uzyskanego poprzez podwyższanie koncentracji $Ca^{2+}$ oraz obniżanie $Mg^{2+}$) na skład chemiczny nowo wzrastających płytek rozgwiazd (*Asterias rubens*) i wężowideł (*Ophiocomina nigra*).

W pierwszym eksperymencie jeżowcom odcięto końcówki kolców w celu zainicjowania ich regeneracji. Następnie szkarłupnie przetrzymywane były w wodzie o kontrolnym (~5.2 mol/mol) i obniżonym (~1.9 mol/mol) stosunku molowym $Mg^{2+}/Ca^{2+}$ oraz karmione dietą o standardowej (~0.3 wt%) i podwyższonej zawartości magnezu (~11 wt%). Po zakończeniu eksperymentu pobrano kolce, a zregenerowane końcówki poddano badaniom składu chemicznego (stosunku Mg/Ca). Kolce wzrastające w wodzie o obniżonym stosunku molowym $Mg^{2+}/Ca^{2+}$ cechował niższy stosunek Mg/Ca w zregenerowanych końcówkach, co potwierdziło hipotezę o wpływie wody morskiej na skład chemiczny szkieletu szkarłupni. Jednakże u osobników karmionych dietą wzbogaconą w magnez stwierdzono wyższy stosunek Mg/Ca w szkielecie. Oznacza to, że woda morska nie jest jedynym źródłem jonów w procesie biomineralizacji (część jonów magnezu może pochodzić również z diety). Ponadto wyniki badań sugerują, że ścieżka transportu magnezu w procesie biomineralizacji regenerujących się kolców jeżowców jest bardziej złożona niż sądzono. Dotychczas uważano, że transport magnezu z wody morskiej do sklerocytów (komórek tworzących szkielet) mediowany jest wyłącznie przez epidermę okalającą kolce. Wyniki eksperymentu sugerują jednak, że magnez pochodzący z diety mógłby być transportowany do stref wzrostu w kolcach przez fagocyty i sferulocyty (jedyne typy komórek o zdolnościach migracyjnych z jamy ciała). Badania te mogą mieć znaczenie w kontekście wiarygodności wykorzystywania kopalnych szkarłupni w rekonstrukcjach paleośrodowiskowych. Okazuje się bowiem, że rodzaj diety może wpływać na skład chemiczny szkieletu szkarłupni, co może skutkować błędami w rekonstrukcji $Mg^{2+}/Ca^{2+}$ wody morskiej na podstawie danych geochemicznych uzyskanych ze szkieletów szkarłupni.

W powyższym eksperymencie obniżanie stosunku molowego $Mg^{2+}/Ca^{2+}$ w wodzie morskiej odbywało się poprzez dodanie soli zawierającej wapń ($CaCl_2$), jednakże w przeszłości geologicznej zmiany stosunku molowego $Mg^{2+}/Ca^{2+}$ w wodzie morskiej związane były ze zmianami stężenia obu jonów ($Mg^{2+}$ oraz $Ca^{2+}$). Z tego powodu w kolejnym eksperymencie stosunek molowy $Mg^{2+}/Ca^{2+}$ obniżany był poprzez dodawanie chlorku wapnia i wody bezmagnezowej (sporządzonej poprzez rozpuszczenie soli NaCl, $Na_2SO_4$, KCl, KBr, $SrCl_2$, NaF, $H_3BO_3$ i $NaHCO_3$). Tym razem do badań wykorzystano dwa gatunki jeżowców o różnych preferencjach środowiskowych: chłodnolubny *Psammechinus miliaris* i tropikalny *Prionocidaris baculosa.* Osobnikom *P. miliaris* przycięto kolce celem wzbudzenia regeneracji (u cidaroida *P. baculosa* regeneracja kolców nie występuje). Dodatkowo u obydwu gatunków przeprowadzono znakowanie manganem (1 mg/L), a następnie obrazowanie przy użyciu mikroskopu katodoluminescencyjnego. Zaletą tej metody, oprócz łatwego i taniego przygotowania oraz braku zauważalnego negatywnego wpływu (przy niskim stężeniu Mn) na fizjologię zwierząt, jest wysoka rozdzielczość umożliwiająca precyzyjne wyznaczenie znakowanych stref wzrostu. Po znakowaniu jeżowce były przetrzymywane w wodzie o stosunku molowym $Mg^{2+}/Ca^{2+}$: ~5.2, ~2.5, ~1.5 (mol/mol) i karmione dietą o standardowej (~0.3 wt%) lub podwyższonej (~20 wt%) zawartości magnezu. Po zakończonym eksperymencie od każdego z osobników pobrano różne elementy szkieletu tj kolce, zęby, demipiramidy i płytki ambitalne. Przygotowany materiał poddano obserwacjom pod mikroskopem katodoluminescencyjnym celem wyznaczenia nowopowstałych stref szkieletu i skalibrowania tempa wzrostu, a następnie badaniom składu chemicznego (Mg/Ca). Wyniki badań pokazały, że jeżowce inkubowane w wodzie morskiej o niskim stosunku molowym $Mg^{2+}/Ca^{2+}$ rosły wolniej i wytwarzały szkielet o obniżonym stosunku Mg/Ca. Z drugiej strony, szkielety osobników karmionych dietą wzbogaconą w magnez charakteryzowały się wyższym stosunkiem molowym Mg/Ca niż szkielety osobników karmionych dietą zubożoną w magnez. Dane te potwierdzają wnioski z pierwszego eksperymentu sugerujące, że część jonów w procesie biomineralizacji może pochodzić z diety, co może mieć wpływ na stosunek Mg/Ca w szkielecie. Co istotne, stosunek Mg/Ca w kalcycie budującym szkielet jeżowców może być niejednorodny w obrębie jednego osobnika (między różnymi typami płytek), a nawet w obrębie pojedynczej płytki (między różnymi typami stereomu). Oznacza to, że rekonstrukcje stosunku molowego $Mg^{2+}/Ca^{2+}$ wody morskiej na podstawie danych geochemicznych (Mg/Ca) pochodzących ze szkieletu szkarłupni mogą być obarczone błędami wynikającymi nie tylko z efektu diety, ale także z wewnątrzosobniczego zróżnicowania wynikającego z efektów witalnych. W rozdziale omówiono błędy wynikające z takich rekonstrukcji, obliczone na podstawie danych eksperymentalnych. Omówiono także wyniki badań geochemicznych (Mg/Ca) dobrze zachowanych jurajskich i mioceńskich jeżowców, które zostały wykorzystane do rekonstrukcji stosunku $Mg^{2+}/Ca^{2+}$ ówczesnych mórz. Jurajskie jeżowce przeważnie wykazują niższy, a mioceńskie wyższy stosunek Mg/Ca w szkielecie, co jest zgodne z typem ówczesnych mórz („kalcytowe” morza w jurze i „aragonitowe” morza w miocenie), niemniej zróżnicowanie geochemiczne jest na tyle duże, że utrudnia precyzyjne odtworzenie zmian $Mg^{2+}/Ca^{2+}$ wody morskiej w fanerozoiku.

W trzeciej części rozprawy omówiono wpływ zmian składu chemicznego wody morskiej na tworzenie szkieletu dwóch rzadziej wykorzystywanych do badań biomineralizacyjnych grup szkarłupni, tj. rozgwiazd i wężowideł. W ramach eksperymentu osobniki dwóch gatunków (rozgwiazdy *Asterias rubens* i wężowidła *Ophiocomina nigra*) najpierw znakowano manganem, a następnie umieszczono w akwariach zawierających wodę o stosunku molowym ~5.2, ~2.5 i ~1.5 (mol/mol). W przypadku wężowideł w ciągu tygodnia zaobserwowano wysoką śmiertelność, autotomię oraz zahamowanie wzrostu, co uniemożliwiło pozyskanie danych z większości osobników (niemniej z nielicznych wężowideł uzyskano dane wskazujące na obniżony stosunek Mg/Ca w szkielecie). W przypadku rozgwiazd wszystkie zbadane osobniki trzymane przez 21 dni w wodzie o obniżonym stosunku molowym $Mg^{2+}/Ca^{2+}$ wytwarzały szkielet o obniżonym stosunku Mg/Ca. Wartości stosunku $Mg^{2+}/Ca^{2+}$ zastosowane w eksperymencie na dzisiejszych rozgwiazdach zostały zestawione z wartościami stosunku $Mg^{2+}/Ca^{2+}$ wody morskiej odtworzonymi na podstawie danych geochemicznych z kopalnych rozgwiazd. Rekonstrukcje bazujące na dobrze zachowanych kopalnych jurajskich i mioceńskich rozgwiazdach są zgodne z danymi geologicznymi, wskazującymi na niski stosunek $Mg^{2+}/Ca^{2+}$ w morzu jurajskim i wysoki w morzu mioceńskim. Należy pamiętać jednocześnie, że dokładność rekonstrukcji jest ograniczona różnym stopniem frakcjonowania magnezu u różnych gatunków szkarłupni oraz lokalnymi parametrami środowiska, które mogą dodatkowo wpływać na końcowy stosunek szkieletowego Mg/Ca.

# Summary

Echinoderms have a skeleton of mesodermal origin, consisting of many plates with a distinct trabecular structure (the so-called stereom). Their skeleton is made of high-magnesium calcite with a small admixture of organic compounds, amorphous calcium carbonate (ACC) and water, and is produced through biologically controlled mineralization.

Until recently it was believed that calcium and magnesium ions required for the formation of the echinoderm skeleton come exclusively from seawater, and that the skeletal Mg/Ca ratio constitutes a proxy for the secular variation in the concentration of these two elements in the environment. Thanks to geochemical data (more precisely, the Mg/Ca ratio) derived from the skeletons of echinoderms, it is possible to calculate the molar ratio of $Mg^{2+}/Ca^{2+}$ of the seawater in which these echinoderms grew. The potential of such reconstructions was recognized by the researchers who used well-preserved fossil echinoderms to reconstruct the chemical composition of the ancient oceans. Nevertheless, in recent years, several published studies suggested that the skeletal Mg/Ca ratio can be also influenced by environmental (temperature and salinity) and biological factors (resulting from the organism's physiology; the so-called vital effect), which means that the degree of biomineralization controlled by echinoderms is larger than previously thought. Moreover, there is no reliable experimental data from Recent echinoderms suggesting a relationship between Mg/Ca in their skeleton and the seawater $Mg^{2+}/Ca^{2+}$ ratio. The aim of the PhD thesis was to conduct a series of biomineralization experiments to verify the effect of the seawater $Mg^{2+}/Ca^{2+}$ ratio and diet on the chemical composition of the echinoderm skeleton.

As part of the PhD thesis, three biomineralization experiments on various unrelated species of echinoderms were planned. The results of these experiments are summarized in the three chapters/articles listed below.

1) Short-term (14 days) experiment testing the effect of increased $Ca^{2+}$ concentration in the seawater and $MgCO_3$-enriched diet on the chemical composition of regenerating spines in adult specimens of an euechinoid *Paracentrotus lividus*;
2) Extended (21 days) experiment testing the effect of a lowered $Mg^{2+}/Ca^{2+}$ ratio in the seawater (achieved through increasing $Ca^{2+}$ and lowering $Mg^{2+}$ concentration) and MgO-enriched diet on the growth rate, respiration rate, and chemical composition of newly formed test plates, teeth, demipyramids, and spines of two echinoid specimens (cidaroid *Prionocidaris baculosa* and euechinoid *Psammechinus miliaris*);

3) Extended (21 days) experiment testing the effect of a lowered $Mg^{2+}/Ca^{2+}$ ratio in the seawater (achieved through increasing $Ca^{2+}$ and lowering $Mg^{2+}$ concentration) on the chemical composition of newly formed plates in asteroids (*Asterias rubens*) and ophiuroids (*Ophiocomina nigra*).

At the beginning of the first experiment, tips of the echinoid spines were cut to initiate regeneration. After that the echinoderms were kept in a sea water with a control (~ 5.2 mol/mol) or lowered (~ 1.9 mol/mol) $Mg^{2+}/Ca^{2+}$ molar ratio and fed with a diet containing a standard (~0.3 wt%) or increased (~ 11 wt%) magnesium content. At the end of the experiment, the spines were removed and the chemical composition (Mg/Ca) of the regenerated tips was investigated. Spines grown under reduced $Mg^{2+}/Ca^{2+}$ ratio conditions displayed lower Mg/Ca ratio in the regenerated tips, which confirmed the hypothesis about the significant effect of seawater on the chemical composition of the echinoderm skeleton. However, echinoids which fed a magnesium-enriched diet had a higher Mg/Ca ratio in the skeleton. This suggests that seawater is not the only source of ions in the biomineralization process, i.e., some of the magnesium can also originate from the diet. In addition, the results also suggest that the transport pathway of magnesium ions in the biomineralization of regenerating sea urchin spines is more complex than previously thought. More specifically, until now, it was believed that the transport of magnesium ions from seawater to sclerocytes (skeleton-forming cells) is mediated solely by the spine-covering epidermis. The results of the experiment suggest that the magnesium originating from the diet could be transported to calcification sites in the spines with the aid of phagocytes or spherulocytes (the only types of cells capable of migrating from coelom to spines). Overal, this has implications in the context of the use of fossil echinoderms in palaeoenvironmental reconstructions. In particular, it seems that the type of diet can influence the chemical composition of echinoderm skeleton, which in turn may induce reconstruction errors of seawater $Mg^{2+}/Ca^{2+}$ ratio inferred from echinoderm material.

In the experiment described above, the decrease of seawater $Mg^{2+}/Ca^{2+}$ molar ratio was achieved through the addition of $Ca^{2+}$-containing salt ($CaCl_2$), however in the geological history, the seawater $Mg^{2+}/Ca^{2+}$ variations were related to changes in the concentration of both ions ($Mg^{2+}$ and $Ca^{2+}$). For this reason, in the next experiment the seawater $Mg^{2+}/Ca^{2+}$ ratio was decreased through the addition of calcium chloride and Mg-free water (obtained by dissolution of NaCl, $Na_2SO_4$, KCl, KBr, $SrCl_2$, NaF, $H_3BO_3$, and $NaHCO_3$ in ultrapure water). This time two species of sea urchins with different environmental preferences were used for the study: temperate *Psammechinus miliaris* and tropical *Prionocidaris baculosa*. In *P. miliaris* tips of the spines were cut off in order to induce regeneration (in cidaroid *P. baculosa* spine regeneration does not occur). Additionally, both species were labeled with manganese (1 mg/L) and imaged with a cathodoluminescence microscope. The advantage of Mn-labeling, apart from easy, low-cost preparation and lack of negative effects (at low Mn concentrations) on animals' physiology, is the high resolution enabling precise determination of new growth. After labeling, sea urchins were kept in water with a molar ratio of $Mg^{2+}/Ca^{2+}$: ~5.2, ~2.5, ~1.5 (mol/mol) and fed with a standard (~0.3 wt%) or magnesium-enriched (~20 wt%) diet. At the end of the experiment, different parts ot the skeleton (i.e. spines, teeth, demipyramids and ambital plates) of each specimen were collected. The prepared material was observed under a cathodoluminescence microscope in order to distinguish the newly formed zones of the skeleton to calibrate the growth rate and determine chemical composition (Mg/Ca). The results showed that sea urchins cultured in seawater with a lowered $Mg^{2+}/Ca^{2+}$ molar ratio grew slower and produced a skeleton with a lowered Mg/Ca ratio. However, the skeletons of individuals which fed the magnesium-enriched diet had a higher Mg/Ca molar ratio than the skeletons of individuals which fed the magnesium-depleted diet. These data support the conclusions of the first experiment suggesting that some of the ions in the biomineralization process can originate from the diet, which may have an impact on the resulting skeletal Mg/Ca ratio. Importantly, the Mg/Ca ratio in the calcite that builds the skeleton of sea urchins can be heterogenous within a single specimen (depending on the ossicle type), or even within a single ossicle (depending on the type of stereom). This means that the reconstruction of the seawater $Mg^{2+}/Ca^{2+}$ ratio based on the geochemical data (Mg/Ca) obtained from the echinoderm skeleton may be affected by errors resulting not only from the diet effect, but also from the intraspecimen variation stemming from vital effects. The chapter discusses errors resulting from such reconstructions, calculated on the basis of experimental data. The results of geochemical studies (Mg/Ca) of well-preserved Jurassic and Miocene sea urchins, which were used to reconstruct past seawater $Mg^{2+}/Ca^{2+}$ ratios, were also discussed. Jurassic echinoids usually display lower Mg/Ca ratios than the Miocene ones, which is consistent with the seawater chemistry at the time ("calcite" Jurassic seas and "aragonite" Miocene seas), however a large geochemical variation r complicates accurate reconstruction of the seawater $Mg^{2+}/Ca^{2+}$ ratio changes in the Phanerozoic based on echinoderm material.

The third part of the dissertation discusses the impact of changes in the chemical composition of seawater on the skeletal Mg/Ca ratio in two less frequently studied groups of echinoderms, i.e., asteroids and ophiuroids. As part of the experiment, individuals belonging to two species (sea star *Asterias rubens* and brittle star *Ophiocomina nigra*) were first tagged with manganese and then placed in aquariums containing seawater with a molar ratio of ~5.2, ~2.5 and ~1.5 (mol/mol). In the case of brittle stars, within the first week most of the specimens cultured under reduced $Mg^{2+}/Ca^{2+}$ conditions experienced high mortality, autotomy, and growth inhibition, which made it impossible to obtain data from most individuals (although in few cases we obtained data indicating lowered Mg/Ca in the skeleton). Sea stars which were cultured for 21 days under lowered $Mg^{2+}/Ca^{2+}$ molar ratio, produced skeleton with a lowered Mg/Ca ratio. The $Mg^{2+}/Ca^{2+}$ ratios applied in the experiment on modern asteroids were compared with the seawater $Mg^{2+}/Ca^{2+}$ ratios reconstructed from fossil asteroids. Reconstructions based on well-preserved Jurassic and Miocene fossil sea stars are consistent with geological data showing a low $Mg^{2+}/Ca^{2+}$ ratio in the Jurassic seas and high in the Miocene seas. However, the accuracy of the reconstruction is strongly limited by a different degree of magnesium fractionation in different species of echinoderms, as well as local environmental conditions, which may additionally affect the skeletal Mg/Ca ratio.

# Introduction

Echinoderms are a very diverse phylum of marine invertebrates, whose origins date back to the Cambrian Series 2 (ca. 520 Ma; Bottjer et al. 2006, Zamora et al., 2013). Five classes of echinoderms have survived to the present day: sea lilies (Crinoidea), sea stars (Asteroidea), brittle stars (Ophiuroidea), sea cucumbers (Holothuroidea), and sea urchins (Echinoidea). The most characteristic features of this phylum include pentaradial symmetry as adults, water vascular system, and a calcite endoskeleton, made of numerous ossicles, with a characteristic meshwork-like microstructure (stereom), that is filled with connective tissue (stroma).

## General morphology of the echinoderm skeleton

Due to their widespread accessibility and easy maintenance, representatives of three classes: echinoids, asteroids, and ophiuroids were chosen for the biomineralization experiments detailed in the following chapters. Herein a brief overview of the skeletal morphology of these classes will be given; for more specific anatomical description see e.g., Hickman et al. (1997).

Echinoid skeleton consists of a test, composed of ossicles immersed in dermis, and spines (Fig. 1). Just like in the other echinoderm classes, the echinoid skeleton is covered by epidermis. Their body plan (in regular echinoids) can be easily recognized as pentaradial due to alternating sections of ambulacral and interambulacral ossicles. Test plates bear small tubercles on which the spines articulate. Sea urchins additionally possess other appendages such as pedicellariae which are small, jaw-bearing structures manipulated by muscles. Inside the test is a complex masticatory apparatus termed Aristotle's lantern, which is composed of several calcitic ossicles including demipyramids, to which the teeth are attached.

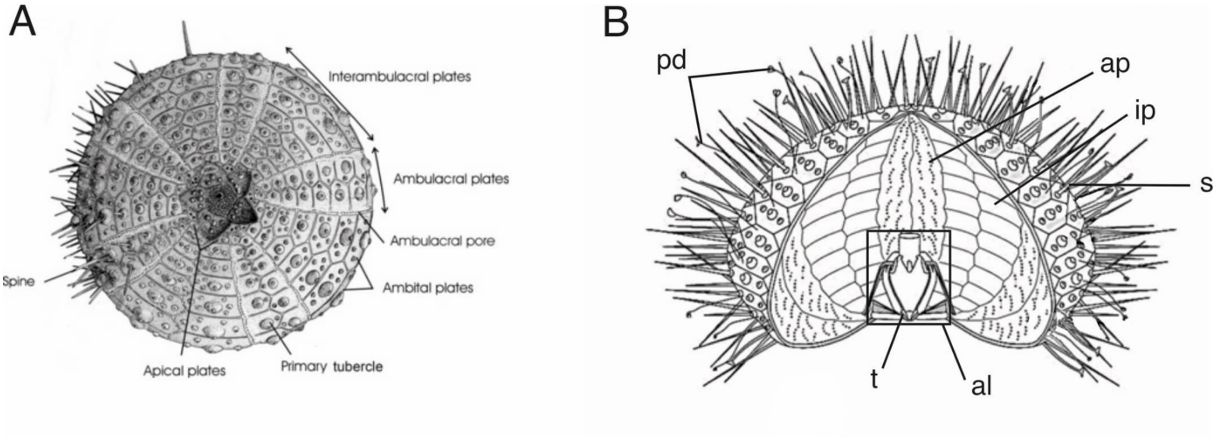

**Figure 1.** (A) Aboral view of the test of an euechinoid (after Trousset in: Collard et al., 2016). (B) Schematic reconstruction of regular echinoid test showing its overall external and internal anatomy including the lantern system. al = Aristotle's lantern, ap = ambulacral plate, ip =

interambulacral plate, pd = pedicellariae, s = spine, t = tooth (modified after Perricone et al., 2020).

Asteroids (Fig. 2A) consist of a central disc which merges gradually with the converging five (or more) arms with their respective ambulacral grooves and rows of minute spines; other appendages include pedicellariae. The endoskeleton, composed of ossicles (Fig. 2B), is bound together by a connective tissue.

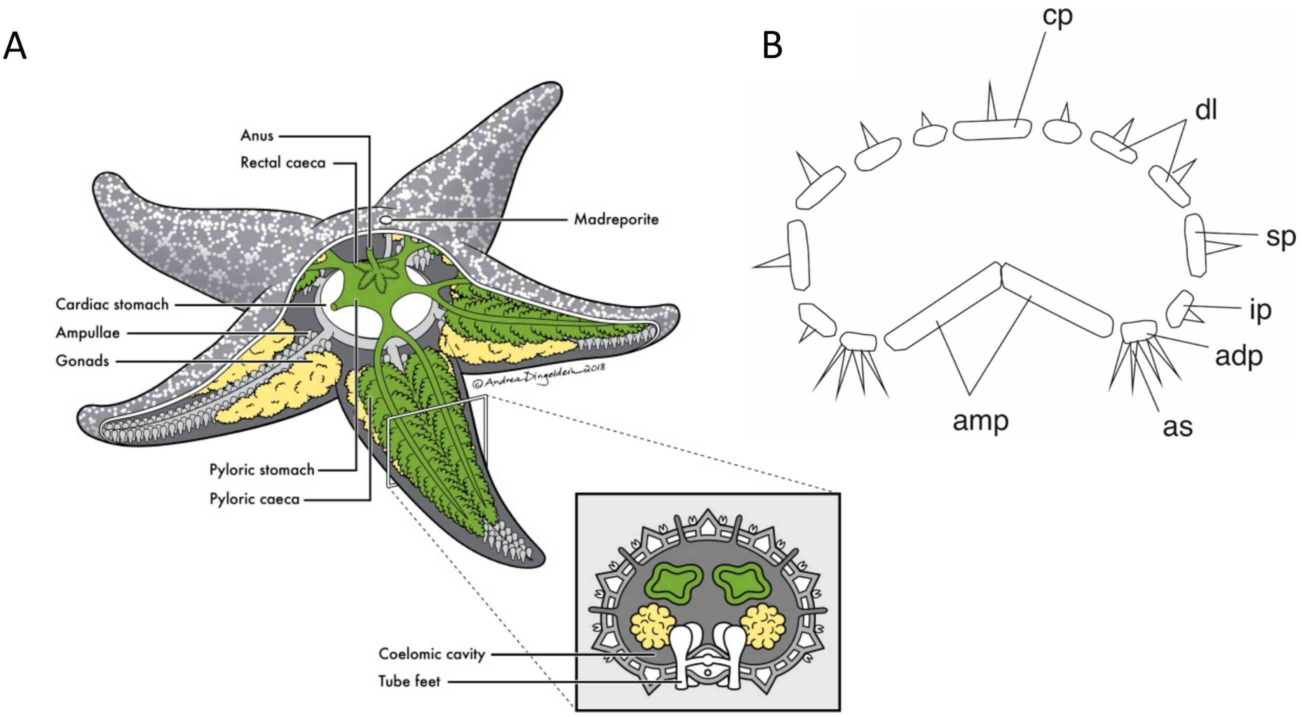

**Figure 2.** (A) Basic anatomy of a sea star with cross section of a ray (Jackson et al., 2018). (B) Generalised cross section of asteroid arm with identification of major skeletal components. adp = adambulacral plate, amp = ambulacral plate, as = adambulacral spine, cp = carinal plate, dl = dorso-lateral ossicles, ip = inframarginal plate, sp = supramarginal plate (modified after Weber, 1968).

Ophiuroids also typically possess five arms, but they are usually thinner and more slender than in asteroids (Fig. 3A). The arms are also sharply separated from the central disc which contains the visceral organs. Each arm is made of a column of articulated ossicles termed vertebrae, which are joined by muscles and covered by other calcareous plates (Fig. 3B).

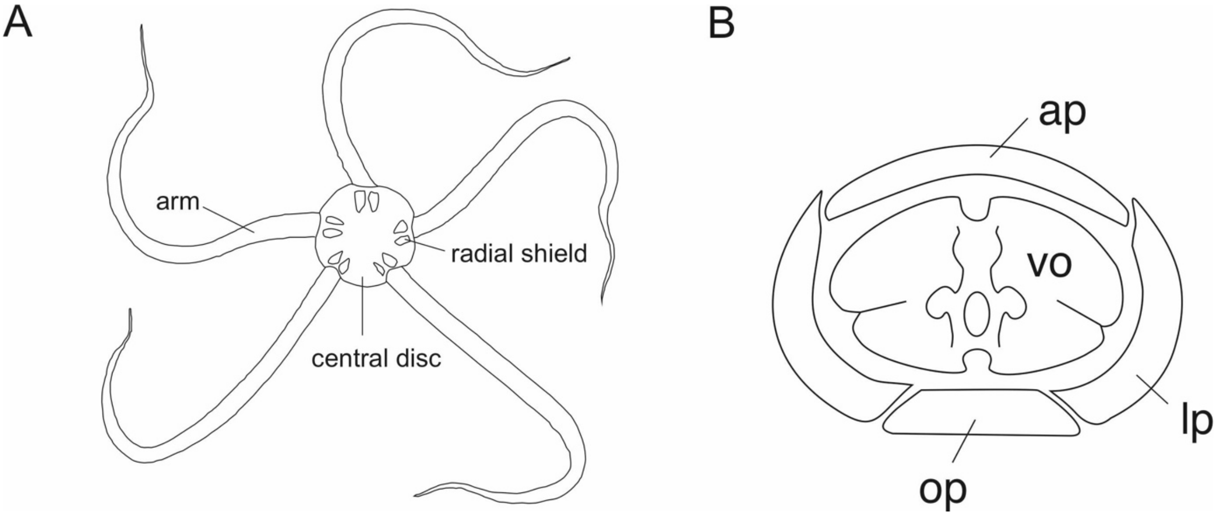

**Figure 3.** (A) Schematic drawing of aboral view of a brittle star. (B) Generalised cross section of ophiuroid arm with identification of major skeletal components. ap = aboral plate, lp = lateral plate, op = oral plate, vo = vertebral ossicle (modified after Weber, 1968).

### Stereom microstructure

Based on the differences in the distribution and thickness of the trabeculae (i.e., meshwork-forming bars) and porosity, the following stereom fabrics have been distinguished (Smith, 1980; Fig. 4):

- Rectilinear stereom – a regular system of trabeculae organized in a cubic or orthorhombic lattice, with pores perpendicular to each other. A type common in echinoid and asteroid plates, it is also found in crinoids.
- Laminar stereom – thin, porous layers separated by vertical pillars. It has a significant constructional importance and occurs, among others, in the plates and spines of some echinoids, ophiuroid discs and the body wall ossicles of some holothurians.
- Galleried stereom – a system of trabeculae and large pores termed galleries arranged in parallel in one plane (galleries are larger than the pores in the perpendicular plane). This type of stereom is associated with collagen fibers and is present in areas that require additional reinforcement, e.g., sutures faces in echinoid and asteroid plates.
- Labyrinthic stereom – irregular meshwork of trabeculae; pores of different shapes and sizes. Fine labyrinthic stereom is usually associated with the sites of muscle insertions (e.g., the attachment of the spines to the test in sea urchins) whereas the coarse one has a structural importance (surfaces of plates in all echinoderm classes).

- Microperforate stereom – low-porosity type with fine, cylindrical perforations. Present, for example, in test plates of some sea urchins.
- Fascicular stereom – a system of branched, parallel or almost parallel trabeculae with irregular and often narrowing pores formed during growth in one direction. Appears for instance in the spines of some echinoids and ambulacral plates of asteroids.
- Retiform layer – a single layer of a thickness smaller than the maximum diameter of its pores; present at the sites of muscle attachment in various echinoderm classes.
- Perforate layer – a layer thicker than the maximum pore diameter; depending on the pore arrangement can be simple or irregular; common on the external surfaces of plates of all echinoderm classes.
- Imperforate layer – a pore-free layer present on the external surfaces and articulation surfaces of plates in all echinoderm classes (e.g., spine septa and tubercles of echinoids, teeth of some ophiuroids).

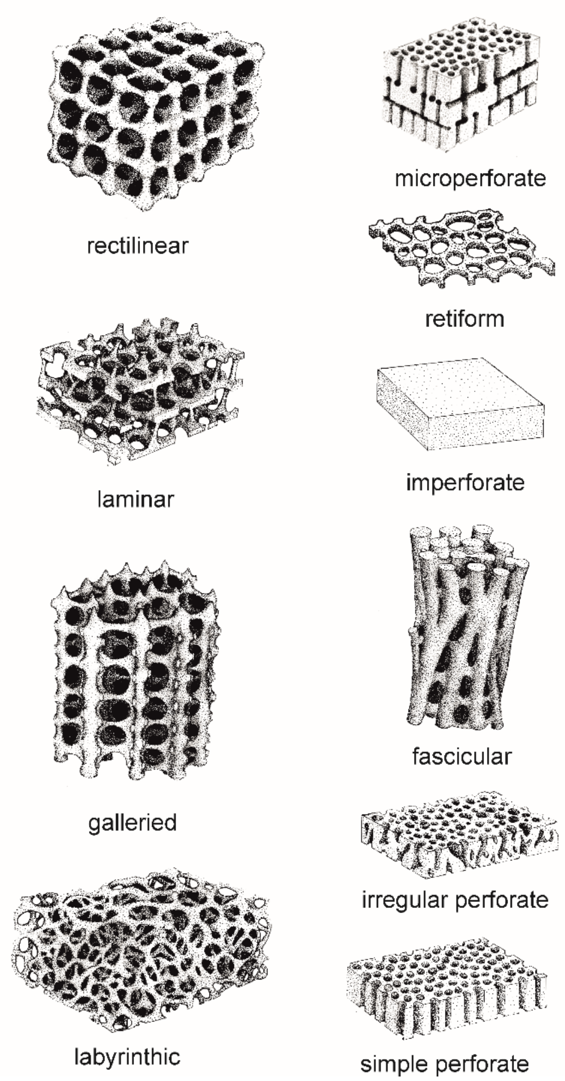

**Figure 4.** Composite block diagrams of stereom fabrics (slightly modified after Smith, 1980).

The development of all types of stereom fabrics is similar: small, conical projections emerge and connect via lateral bridges to form a fine mesh. The resulting stereom is gradually thickened and its pores may be eventually filled with secondary calcite (Dubois and Jangoux, 1990; Gorzelak et al., 2011; Gorzelak et al., 2014; Gorzelak et al., 2017).

## Biomineralization of the echinoderm skeleton

The echinoderm endoskeleton is of a mesodermal origin. The skeleton formation typically starts intracellularly within calcification sites delimited by a plasma membrane; however it becomes extracellular once the cell membrane is degraded (Märkel et al., 1986). Biomineralization of regenerates (e.g., fractured spines) is fully extracellular. Mature skeleton consists of magnesium-rich calcite (or even protodolomite in the case of echinoid teeth tips; e.g., Schroeder et al., 1969), and small admixture of organic matter (1.2-1.6 wt%), anhydrous amorphous calcium carbonate (ACC, 10 wt%) and water (up to 0.2 wt%) (Albéric et al., 2018). The $MgCO_3$ content in skeletal calcite varies from 3 to 43.5 mol% (Schroeder et al., 1969; Weber, 1969; McClintock et al., 2011).

Until recently, it was thought that only sclerocytes, or skeleton forming cells (SFCs), and – in the case of teeth – odontoblasts (Ameye, 1999), were responsible for biomineralization in echinoderms. However, according to recent studies, non-specialized epithelial cells may also be involved in this process (Vidavsky et al., 2014). Seawater is considered the main source of ions in the biomineralization, and the ion transport system involves a complex system of pumps, channels, exchargers, and cotransporters (Dubois and Chen, 1989).

The general model of biomineralization of the echinoderm skeleton assumes that ions from seawater are transported into vesicles, which gather in the syncytial pseudopodium formed by sclerocytes. More specifically, in larvae it has been shown that seawater is endocytosed into vesicles within primary mesenchyme cells (PMCs), epithelial and endothelial cells (Vidavsky et al., 2016). In larval PMCs, intracellular ion concentration occurs within individual vesicles to the point where a disordered mineral phase, the so-called amorphous calcium carbonate (ACC), is formed (Kahil et al., 2020). Vesicles containing ACC and scattered biomolecules are transported to the syncytium, where the aggregation of ACC grains and secondary crystallization to “monocrystalline” calcite occurs on the organic matrix (Weiner and Addadi, 2011; Seto et al., 2012; Fig. 5).

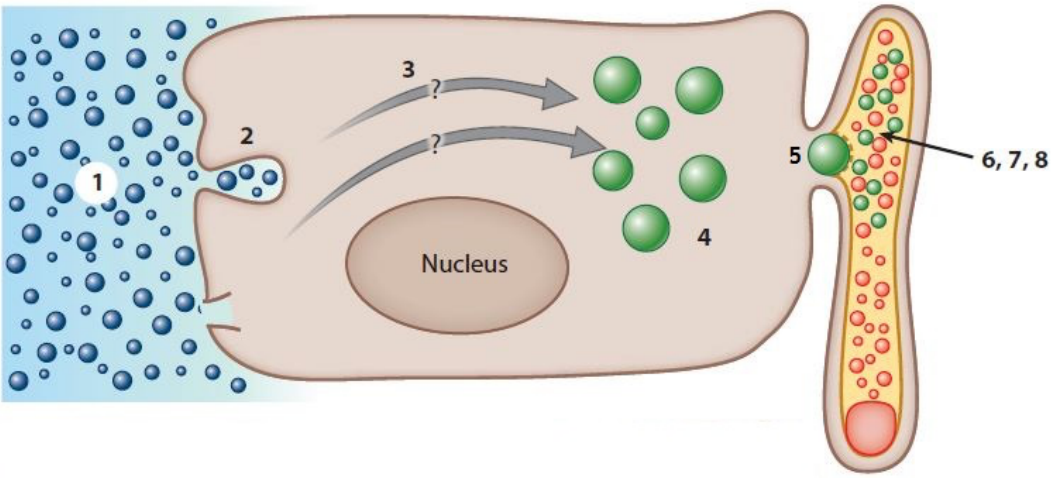

**Figure 5.** Biomineralization pathway in echinoderms (slightly modified after Weiner and Addadi, 2011). (1) The medium from which the ions are derived (seawater or body fluids). (2) The ion-sequestering process: endocytosis of seawater droplets and / or ion channels and / or transporters. (3) Transport within the cell to specialized vesicles. (4) Specialized vesicles in which the formation of the first disordered mineral phase occurs. (5) Transport of the mineral-bearing vesicles and their contents into the extracellular environment or into the syncytium. (6) The translocation of the disordered phase to the crystallization front. (7) Transformation of the initial disordered phase into more ordered phases. (8) The mature mineralized tissue.

In echinoderms, ACC, the precursor metastable phase, was first observed in the spicules of sea urchin larvae (Beniash et al., 1997, Beniash et al., 1999, Raz et al., 2003). It has been subsequently reported in regenerating sea urchin spines (Politi et al., 2004) and in the forming end of the sea urchin teeth (Killian et al., 2009). Two forms of ACC were distinguished: type I (hydrated) and type II (anhydrous). The hydrated form transforms very quickly into the anhydrous form, which in turn recrystallizes into calcite (Albéric et al., 2019). Both types of ACC are found in adult sea urchin spines, but the rate of dehydration within the spine is highly structure-dependent and is usually faster in open stereom than in septa, which may indicate biological control of the organism over ACC stabilization (Albéric et al., 2019).

The biological aspect of skeletal mineralization is also strongly related to the presence of an intrastereomic organic matrix (IOM). In addition to stabilizing ACC, IOM influences biomineralization by controlling magnesium content and regulating crystal growth (e.g., Lowenstam and Weiner, 1989; Hermans et al., 2011). The organic component in individual trabeculae of the stereom is usually organized in the form of thin, concentric layers (Dubois, 1991; Ameye et al., 1998) which at the nanoscale exhibit a structure sometimes termed composite, due to the presence of fine mineral grains (20-100 nm in diameter) and intermingled with organic material. Composite is a material with a heterogeneous structure, made of phases with different physical, chemical, and mechanical properties (Perricone et al., 2020). The combination of various components in a specific proportion produces a new material with properties that differ significantly from those of the individual components. From the material engineering point of view, the calcite that builds the skeleton of echinoderms should contain more organic compounds to be called a true mineral-organic composite (Berman et al., 1988). Interestingly, high ACC content in calcite (8-10 wt%) could make the echinoderm skeleton a mineral composite (Seto et al., 2012; Perricone et al., 2020). Regardless of the terminology, organic compounds (including proteins and glycoproteins) present in the skeletal calcite significantly affect hardness and stiffness of the echinoderm skeleton (Weiner, 1985). The characteristic conchoidal fracture of the skeleton, associated with the presence of organic substances (Berman et al., 1988, 1990), indicates increased flexibility and fracture resistance.

An important trace element of the echinoderm skeleton is magnesium. It is involved in stabilizing the transient ACC phase (Loste et al., 2003). Moreover, it is believed that the presence of magnesium in calcite increases the hardness and resistance to deformation of the skeleton by a strong distortion of the crystal lattice (Wang et al., 1997). For example, sea urchins are able to grind a hard (even basaltic) substrate thanks to their teeth, composed of numerous plates and needles surrounded by a magnesium-rich polycrystalline matrix (Ma et al., 2008; 2009). Kanold et al. (2015) showed that the spicules of sea urchin larvae cultured in water with an increased $Mg^{2+}/Ca^{2+}$ molar ratio (11.4 mol/mol), and thus enriched with $Mg^{2+}$ ions, displayed greater hardness (H) and Young's modulus (E) than the control individuals. In the opposite situation, i.e., under the conditions of lowered $Mg^{2+}/Ca^{2+}$ (0.71 mol/mol), deterioration of the mechanical properties of spicules was observed (Lemloh et al., 2013). Magnesium deficiency in the environment causes serious development disorders and deformations of the skeleton of sea urchin larvae (Martino et al., 2019).

The final chemical composition and properties of the stereom strongly depend on the relationship between the magnesium-enriched calcite, ACC, and organic compounds. The resulting material is therefore the result of the action of both environmental and physiological factors. Due to its chemical composition, structure and mechanical properties, the skeleton of echinoderms is an inspiration to many different fields of technology, including robotics, biomedical engineering and materials science (review in Perricone et al., 2020). Some researchers are particularly interested in the microstructure of the calcite skeleton and the possibility of using it in the production of new materials for prosthetics (e.g., Weber et al., 1971; Vecchio et al., 2007).

## Application of echinoderms in palaeoenvironmental studies

Since isolated ossicles of echinoderms are common in the fossil record, they have been long used in palaeoenvironmental research. For instance, echinoderm remnants are primarily an indicator of the marine environment and can provide important palaeoecological information (e.g. Benton and Harper, 2009; Belaústegui et al., 2017; Gorzelak, 2021). With the development of microscopic and analytical techniques, research on the chemical composition of fossil organisms, including echinoderms (e.g., Chave, 1954; Weber, 1969) has significantly progressed. In particular, fossil echinoderms were considered as a reliable proxy in the reconstruction of changes in chemical composition (mainly the $Mg^{2+}/Ca^{2+}$ molar ratio) of the seawater in the past (Dickson, 2002, 2004; Ries, 2004; Kroh and Nebelsick, 2009; Hasiuk and Lohmann, 2010; Evans and Muller, 2012), despite a potential diagenetic imprint on their skeletal mineralogy (Gorzelak et al., 2016).

It is believed that the $Mg^{2+}/Ca^{2+}$ ratio oscillated in the Phanerozoic between ~1 and ~5.2 (mol/mol; Wilkinson and Algeo, 1989; Hardie, 1996; Stanley and Hardie, 1998; Horita et al., 2002; Fig.7) and that these changes influenced the dominance of a given calcium carbonate polymorph (aragonite or calcite) in the fossil record (Sandberg, 1983, 1985). The nucleation of a certain $CaCO_3$ polymorph can be also influenced by temperature and, to some extent, several carbonic acid system parameters (see Balthasar and Cusack, 2015, and literature cited therein). Additionally, the concentration of $SO_4^{2-}$ (a level of which covaried with seawater $Mg^{2+}/Ca^{2+}$ in the Phanerozoic; Hardie, 1996) may also affect $CaCO_3$ polymorph precipitation. For instance, it has been shown that when concentration of $SO_4^{2-}$ decreases (i.e., below <10mM; Bots et al., 2011), the Mg/Ca threshold for preferential aragonite precipitation increases, which results in an overall increase of precipitated calcite. However, during biomineralization, the concentration of sulphates in the calcifying fluids is usually much lower than that of the surrounding seawater (e.g., Shumway, 1977). Thus, despite some fluctuations in $SO_4^{2-}$ in the Phanerozoic, its effect on the boundary between nucleation fields for biogenic $CaCO_3$ polymorphs is thought to be similar through time (e.g., van Dijk et al. 2016).

The geochemical composition of the seawater that may favor precipitation of different calcium carbonate polymorphs (low magnesium calcite vs. aragonite (or/and high magnesium calcite) is affected by rapid or slow formation of the oceanic crust (Hardie, 1996). During the periods of active rifting and transformation of basalts to greenstones, calcium ions are released into the water while magnesium is removed. In general, $Mg^{2+}/Ca^{2+}$ seawater molar ratio lower than 2 (mol/mol) ("calcite sea conditions") leads to the precipitation of calcite with a low Mg content, while $Mg^{2+}/Ca^{2+}$ ratio higher than 2 (mol/mol) (”aragonite sea conditions”) favors the precipitation of aragonite and/or Mg-rich calcite. Secular changes in the seawater $Mg^{2+}/Ca^{2+}$ ratio in the Phanerozoic are supported by the presence of mineralogically related evaporites (Hardie, 1996) and inclusions in halites (Lowenstein et al., 2001). It is worth emphasizing, however, that the molar ratio of $Mg^{2+}/Ca^{2+}$ seawater, contrary to widespread assumptions, is not a uniform value that characterizes all seawater at a given point in time. New data from the modern global ocean show that the $Mg^{2+}/Ca^{2+}$ ratio in seawater is strongly dependent on location, ecosystem, and depth (Lebrato et al., 2020). For the modern ocean, the constant molar ratio of $Mg^{2+}/Ca^{2+}$ ~5.2 (mol/mol) is usually assumed, however in the upwelling regions, polar zones, shelves or areas strongly dependent on river activity, the ratio in seawater varies between ~4.4 and 6.4 (mol/mol), while in the open ocean it ranges from ~4.9 to ~5.3 (mol/mol).

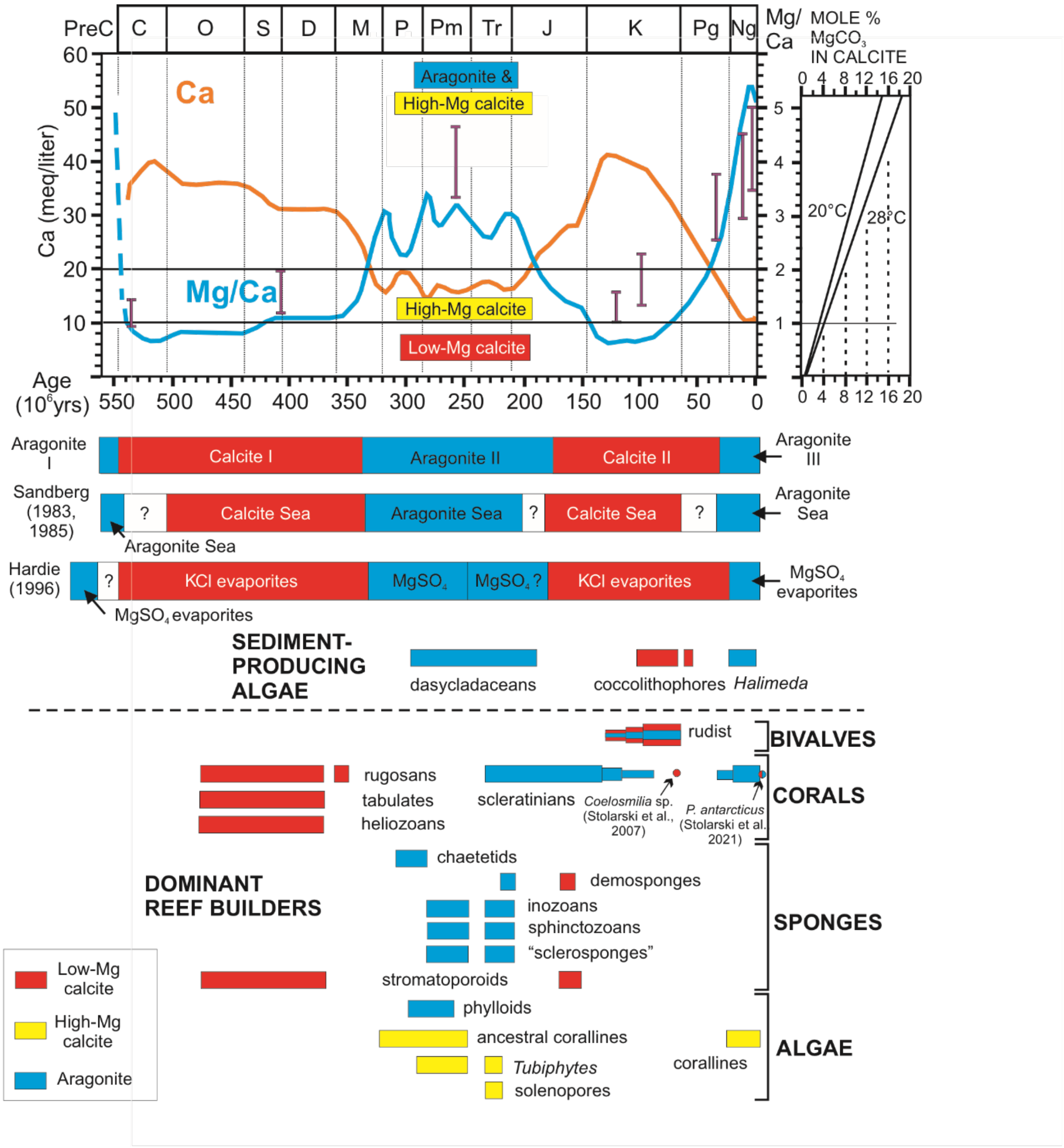

**Figure 6.** Global trends in seawater $Mg^{2+}/Ca^{2+}$ ratio with reconstruction of calcite (Calcite I and II) and aragonite sea (Aragonite I, II, and III) intervals based on modeled seawater Mg/Ca reconstructions after Sandberg, 1983, 1985; Hardie, 1996, supported by Mg/Ca from fluid inclusions (violet bars after Lowenstein et al., 2001). Below distribution of major carbonate-producing taxa (modified after Stanley, 2008). Fluctuations of other ions (such as $Sr^{2+}$ and $SO_4^{2-}$) were not presented herein because their estimates are subject to high uncertainties.

From a geological perspective, changes of the seawater chemistry in time can affect biomineralization in various ways. For instance, changes in the dominant calcium carbonate polymorph explain the abundance of individual groups of organisms in the fossil record (Stanley and Hardie, 1998; see also Kiessling et al., 2008). Moreover, it is believed that the skeletal polymorph and/or Mg/Ca ratio in the skeletons of some (i.e., with low biological control over biomineralization) organisms reflects the changes in the ambient seawater chemistry, i.e., $Mg^{2+}/Ca^{2+}$ molar ratio (Stanley, 2008). Calcifying organisms could switch from low- to high-Mg calcite or aragonite according to the seawater chemistry at that time (e.g., Stolarski et al., 2007; Ries, 2010). Although well-preserved fossil echinoderms have been commonly used to reconstruct the $Mg^{2+}/Ca^{2+}$ molar ratio of the Phanerozoic seawater, reliable experimental data that could confirm the validity of using them in such reconstructions are almost lacking. The available data concerned only one species of sea urchin (*Eucidaris tribuloides*; Ries, 2004), the skeleton of which changed the Mg/Ca ratio depending on the chemical composition of the seawater. However, during this experiment, individuals of this species from each treatment were kept in one tank, posing the risk of pseudo-replication.

Moreover, the Mg/Ca ratio in the echinoderm skeleton can be influenced by other environmental parameters such as temperature and salinity (e.g., Chave, 1954; Weber, 1969, 1973; Smith et al. 2016). For instance, Hermans et al. (2010) showed that with increasing surrounding seawater temperature, an increase in the Mg/Ca ratio is observed in the newly formed skeleton in the juveniles of the sea urchin *Paracentrotus lividus*. However, juveniles of the sea urchin *Lytechinus variegatus* exposed to increased ambient temperature (30 °C) displayed lower skeletal Mg/Ca ratios than the individuals cultivated under 26 °C (Duquette et al., 2018). Another study showed that increased salinity also affects the Mg/Ca ratio in the starfish *Asterias rubens* and is responsible for 25% of the Mg/Ca variation in the skeleton (Borremans et al., 2009). Moreover, in the skeletons of Recent echinoderms, high chemical variability was observed (e.g., within the same population, e.g., McClintock et al., 2011; Smith et al., 2016; Iglikowska et al., 2017; 2018; 2020), which suggests that biological factors (the so-called vital effect) can affect the fractionation of basic elements during biomineralization. Asnaghi et al. (2014) also observed that the skeletons of juveniles of the sea urchin *Paracentrotus lividus* fed with different types of diet (i.e., calcifying algae *Ellisolandia* (formerly *Corallina*) and non-calcifying *Dictyota* and *Cystoseira*) have a different Mg/Ca ratio in the skeleton. However, the latter authors did not provide information on the chemical composition of these algae.

The aim of this PhD thesis was to determine the effect of changes in the seawater $Mg^{2+}/Ca^{2+}$ molar ratio and diet on the biomineralization (i.e., the skeletal Mg/Ca ratio and growth rate) of the echinoderm skeleton. The results of this research allowed to answer the question of whether seawater is the only source of ions in the biomineralization of echinoderms, and whether well-preserved fossil echinoderms can be reliably used in paleoenvironmental reconstructions.

## References

Albéric, M., Caspi, E. N., Bennet, M., Ajili, W., Nassif, N., Azaïs, T., Berner, A., Fratzl, P., Zolotoyabko, E., Bertinetti, L., & Politi, Y. (2018). Interplay between calcite, amorphous calcium carbonate, and intracrystalline organics in sea urchin skeletal elements. *Crystal Growth & Design*, 18(4), 2189-2201.

Albéric, M., Stifler, C. A., Zou, Z., Sun, C. Y., Killian, C. E., Valencia, S., Mawass, M.-A., Bertinetti, L., Gilbert, P.U.P.A., & Politi, Y. (2019). Growth and regrowth of adult sea urchin spines involve hydrated and anhydrous amorphous calcium carbonate precursors. *Journal of Structural Biology*: *X*, 1, 100004.

Ameye, L., (1999). Control of biomineralization in echinoderms: Ultrastructure and cytochemistry of the organic matrix. PhD thesis, Université Libre Bruxelles, Faculté des Sciences, Laboratorie de Biologie Marine.

Ameye, L, Compère Ph., Dille, J., and Dubois, Ph. (1998). Ultrastructure and cytochemistry of the early calcification site and of its mineralization organic matrix in *Paracentrotus lividus* (Echinodermata: Echinoidea). *Histochemistry and Cell Biology*, 110, 285–294.

Asnaghi, V., Mangialajo, L., Gattuso, J. P., Francour, P., Privitera, D., & Chiantore, M. (2014). Effects of ocean acidification and diet on thickness and carbonate elemental composition of the test of juvenile sea urchins. *Marine Environmental Research*, 93, 78–84.

Balthasar, U., & Cusack, M. (2015). Aragonite-calcite seas—Quantifying the gray area. *Geology*, 43(2), 99-102.

Belaústegui, Z., Muñiz, F., Nebelsick, J. H., Domènech, R., & Martinell, J. (2017). Echinoderm ichnology: bioturbation, bioerosion and related processes. *Journal of Paleontology*, 91(4), 643-661.

Beniash, E., Addadi, L., & Weiner, S. (1999). Cellular control over spicule formation in sea urchin embryos: a structural approach. *Journal of Structural Biology*, 125, 50–62.

Beniash, E., Aizenberg, J., Addadi, L., & Weiner, S. (1997). Amorphous calcium carbonate transforms into calcite during sea urchin larval spicule growth. *Proceedings of the Royal Society of London. Series B: Biological Sciences*, 264(1380), 461-465.

Benton, M. J., & Harper, D. A. T. (2009). Introduction to paleobiology and the fossil record. Chichester, West Sussex, UK: Wiley-Blackwell.

Berman, A., Addadi, L., Kvick, Å., Leiserowitz, L., Nelson, M., & Weiner, S. (1990). Intercalation of sea urchin proteins in calcite: study of a crystalline composite material. *Science*, 250(4981), 664-667.

Berman, A., Addadi, L., & Weiner, S. (1988). Interactions of sea-urchin skeleton macromolecules with growing calcite crystals—a study of intracrystalline proteins. *Nature*, 331(6156), 546-548.

Borremans, C., Hermans, J., Baillon, S., André, L., & Dubois, P. (2009). Salinity effects on the Mg/Ca and Sr/Ca in starfish skeletons and the echinoderm relevance for paleoenvironmental reconstructions. *Geology*, 37(4), 351–354.

Bots, P., Benning, L. G., Rickaby, R., & Shaw, S. (2011). The role of $SO_4$ in the switch from calcite to aragonite seas. *Geology*, 39(4), 331-334.

Bottjer, D. J., Davidson, E. H., Peterson, K. J., & Cameron, R. A. (2006). Paleogenomics of echinoderms. *Science*, 314(5801), 956-960.

Chave, K. (1954). Aspects of the biogeochemistry of magnesium. 1- Calcareous marine organisms. *Journal of Geology*, *62*(3), 266–283.

Chao, S. M. (1999). A revision of the family Astropectinidae (Echinodermata: Asteroidea) from Taiwan, with description of five new records. *Zoological Studies - Taipei*, 38(3), 257-267.

Collard, M., Rastrick, S. P., Calosi, P., Demolder, Y., Dille, J., Findlay, H. S., Hall-Spencer, J. M. Milazzo, M., Moulin, L., Widdicombe, S., Dehairs, F., & Dubois, P. (2016). The impact of ocean acidification and warming on the skeletal mechanical properties of the sea urchin *Paracentrotus lividus* from laboratory and field observations. *ICES Journal of Marine Science*, 73(3), 727-738.

Dickson, J. A. D. (2002). Fossil Echinoderms As Monitor of the Mg/Ca Ratio of Phanerozoic Oceans. *Science*, 298(5596), 1222–1224.

Dickson, J. A. D. (2004). Echinoderm skeletal preservation: calcite-aragonite seas and the Mg/Ca ratio of Phanerozoic oceans. *Journal of Sedimentary Research*, 74(3), 355-365.

Dubois, P. (1991). Morphological evidence of coherent organic material within the stereom of postmetamorphic echinoderms. In Suga, S., Nakahara, H. (eds.), Mechanisms and phylogeny of mineralization in biological systems, 41-45. Springer-Verlag, Tokyo.

Dubois, P., & Chen, C. P. (1989). Calcification in echinoderms. *Echinoderm Studies* 3, 109-178.

Dubois, P., & Jangoux, M. (1990). Stereom morphogenesis and differentiation during regeneration of adambulacral spines of *Asterias rubens* (Echinodermata, Asteroida). *Zoomorphology*, 109(5), 263-272.

Duquette, A., Vohra, Y. K., McClintock, J. B., & Angus, R. A. (2018). Near-future temperature reduces Mg/Ca ratios in the major skeletal components of the common subtropical sea urchin *Lytechinus variegatus*. *Journal of Experimental Marine Biology and Ecology*, 509, 1-7.

Evans, D., & Müller, W. (2012). Deep time foraminifera Mg/Ca paleothermometry: Nonlinear correction for secular change in seawater Mg/Ca. *Paleoceanography*, 27(4).

Gorzelak, P. (2021). Functional Micromorphology of the Echinoderm Skeleton (Elements of Paleontology). Cambridge: Cambridge University Press.

Gorzelak, P., Dery, A., Dubois, P., & Stolarski, J. (2017). Sea urchin growth dynamics at microstructural length scale revealed by Mn-labeling and cathodoluminescence imaging. *Frontiers in Zoology*, 14(1), 1-17.

Gorzelak, P., Krzykawski, T., & Stolarski, J. (2016). Diagenesis of echinoderm skeletons: constraints on paleoseawater Mg/Ca reconstructions. *Global and Planetary Change*, 144, 142-157.

Gorzelak, P., Stolarski, J., Dery, A., Dubois, P., Escrig, S., & Meibom, A. (2014). Ultrascale and microscale growth dynamics of the cidaroid spine of *Phyllacanthus imperialis* revealed by 26Mg labeling and NanoSIMS isotopic imaging. *Journal of Morphology*, 275(7), 788-796.

Gorzelak, P., Stolarski, J., Dubois, P., Kopp, C., & Meibom, A. (2011). $^{26}$Mg labeling of the sea urchin regenerating spine: Insights into echinoderm biomineralization process. *Journal of Structural Biology,* 176(1), 119-126.

Hardie, L. A. (1996). Secular variation in seawater chemistry: An explanation for the coupled secular variation in the mineralogies of marine limestones and potash evaporites over the past 600 m.y. *Geology*, 24(3), 279–283.

Hasiuk, F. J., & Lohmann, K. C. (2010). Application of calcite Mg partitioning functions to the reconstruction of paleocean Mg/Ca. *Geochimica et Cosmochimica Acta*, 74(23), 6751-6763.

Hermans, J., André, L., Navez, J., Pernet, P., & Dubois, P. (2011). Relative influences of solution composition and presence of intracrystalline proteins on magnesium incorporation in calcium carbonate minerals: Insight into vital effects. *Journal of Geophysical Research: Biogeosciences*, 116(1), 1–10.

Hermans, J., Borremans, C., Willenz, P., André, L., & Dubois, P. (2010). Temperature, salinity and growth rate dependences of Mg/Ca and Sr/Ca ratios of the skeleton of the sea urchin *Paracentrotus lividus* (Lamarck): An experimental approach. *Marine Biology*, 157(6), 1293–1300.

Hickman, C. P., Roberts, L. S., & Larson, A. (1997). Integrated Principles of Zoology. Boston, Mass: WCB/McGraw-Hill.

Horita, J., Zimmermann, H., & Holland, H. D. (2002). Chemical evolution of seawater during the Phanerozoic: Implications from the record of marine evaporites. *Geochimica et Cosmochimica Acta*, 66(21), 3733-3756.

Iglikowska, A., Borszcz, T., Drewnik, A., Grabowska, M., Humphreys-Williams, E., Kędra, M., Krzemińska, M., Piwoni-Piórewicz, A., & Kukliński, P. (2018). Mg and Sr in Arctic echinoderm calcite: Nature or nurture? *Journal of Marine Systems*, 180, 279-288.

Iglikowska, A., Najorka, J., Voronkov, A., Chełchowski, M., & Kukliński, P. (2017). Variability in magnesium content in Arctic echinoderm skeletons. *Marine environmental research*, 129, 207-218.

Iglikowska, A., Humphreys-Williams, E., Przytarska, J., Chełchowski, M., & Kukliński, P. (2020). Minor and trace elements in skeletons of Arctic echinoderms. *Marine Pollution Bulletin*, 158, 111377.

Jackson, E. W., Pepe-Ranney, C., Debenport, S. J., Buckley, D. H., & Hewson, I. (2018). The microbial landscape of sea stars and the anatomical and interspecies variability of their microbiome. *Frontiers in Microbiology*, 9, 1829.

Kahil, K., Varsano, N., Sorrentino, A., Pereiro, E., Rez, P., Weiner, S., & Addadi, L. (2020). Cellular pathways of calcium transport and concentration toward mineral formation in sea urchin larvae. *Proceedings of the National Academy of Sciences*, 117(49), 30957-30965.

Kanold, J. M., Lemloh, M. L., Schwendt, P., Burghard, Z., Baier, J., Herbst, F., Bill, J., Marin, F., & Brümmer, F. (2015). In vivo enrichment of magnesium ions modifies sea urchin spicule properties. *Bioinspired, Biomimetic and Nanobiomaterials*, 4(2), 111-120.

Kiessling, W., Aberhan, M., & Villier, L. (2008). Phanerozoic trends in skeletal mineralogy driven by mass extinctions. *Nature Geoscience*, 1(8), 527-530.

Killian, C. E., Metzler, R. A., Gong, Y. U. T., Olson, I. C., Aizenberg, J., Politi, Y., Wilt, F.H., Scholl, A., Young, A., Doran, A., Kunz, M., Tamura, N., Coppersmith, S. N., & Gilbert, P. U. P. A. (2009). Mechanism of calcite co-orientation in the sea urchin tooth. *Journal of the American Chemical Society*, 131(51), 18404-18409.

Kroh, A., & Nebelsick, J. H. (2009). Echinoderms and Oligo-Miocene carbonate systems: Potential applications in sedimentology and environmental reconstruction: *International Association of Sedimentologists Special Publication* 42.

Lebrato, M., Garbe-Schönberg, D., Müller, M. N., Blanco-Ameijeiras, S., Feely, R. A., Lorenzoni, L., Molinero, J.-C., Bremer, K., Jones, D. O. B., Iglesias-Rodriguez, D., Greeley, D., Lamare, M. D., Paulmier, A., Graco, M., Cartes, J., Barcelos e Ramos, J., de Lara, A., Sanchez-Leal, R., Jimenez, P., Paparazzo, F. E., Hartman, S. E., Westernströer, U., Küter, M., Benavides, R., da Silva, A. F., Bell, S., Payne, C., Olafsdottir, S., Robinson, K., Jantunen, L. M., Korablev, A., Webster, R. J., Jones, E. M., Gilg, O., Bailly du Bois, P., Beldowski, J., Ashjian, C., Yahia, N. D., Twining, B., Chen, X. G., Tseng, L. C., Hwang, J. S., Dahms, H. U. & Oschlies, A. (2020). Global variability in seawater Mg: Ca and Sr: Ca ratios in the modern ocean. *Proceedings of the National Academy of Sciences*, 117(36), 22281-22292.

LeClair, E. E. (1996). Arm joint articulations in the ophiuran brittlestars (Echinodermata: Ophiuroidea): a morphometric analysis of ontogenetic, serial, and interspecific variation. *Journal of Zoology*, 240(2), 245-275.

Lemloh, M. L., Burghard, Z., Forien, J. B., Bill, J., & Brümmer, F. (2013). Low Mg/Ca ratio alters material properties in sea urchin larvae skeleton. *Bioinspired, Biomimetic and Nanobiomaterials*, 2(1), 28-34.

Loste, E., Wilson, R. M., Seshadri, R., & Meldrum, F. C. (2003). The role of magnesium in stabilising amorphous calcium carbonate and controlling calcite morphologies. *Journal of Crystal Growth*, 254(1-2), 206-218.

Lowenstam, H. A., & Weiner, S. (1989). On biomineralization. Oxford University Press, New York.

Lowenstein, T. K., Timofeeff, M. N., Brennan, S. T., Hardie, L. A., & Demicco, R. V. (2001). Oscillations in Phanerozoic seawater chemistry: Evidence from fluid inclusions. *Science*, 294(5544), 1086-1088.

Ma, Y., Cohen, S. R., Addadi, L., & Weiner, S. (2008). Sea Urchin Tooth Design: An "All-

Calcite" Polycrystalline Reinforced Fiber Composite for Grinding Rocks. *Advanced Materials*, 20(8), 1555-1559.

Ma, Y., Aichmayer, B., Paris, O., Fratzl, P., Meibom, A., Metzler, R. A., Politi, Y., Addadi, L., Gilbert, P.U.P.A., & Weiner, S. (2009). The grinding tip of the sea urchin tooth exhibits exquisite control over calcite crystal orientation and Mg distribution. *Proceedings of the National Academy of Sciences*, 106(15), 6048-6053.

Martino, C., Chiarelli, R., Roccheri, M. C., Matranga, V., & Byrne, M. (2019). Effects of magnesium deprivation on development and biomineralization in the sea urchin *Arbacia lixula*. *Invertebrate Reproduction and Development*, 00(00), 1–12.

Märkel, K., Röser, U., Mackenstedt, U., & Klostermann, M. (1986). Ultrastructural investigation of matrix-mediated biomineralization in echinoids (Echinodermata, Echinoida). *Zoomorphology*, 106(4), 232-243.

McClintock, J. B., Amsler, M. O., Angus, R. A., Challener, R. C., Schram, J. B., Amsler, C. D., Mah, C. L., Cuce, J., & Baker, B. J. (2011). The Mg-Calcite Composition of Antarctic Echinoderms: Important Implications for Predicting the Impacts of Ocean Acidification. *The Journal of Geology*, 119(5), 457–466.

Perricone, V., Grun, T., Marmo, F., Langella, C., & Carnevali, M. D. C. (2020). Constructional design of echinoid endoskeleton: main structural components and their potential for biomimetic applications. *Bioinspiration & Biomimetics*, 16, 011001.

Politi, Y., Arad, T., Klein, E., Weiner, S., & Addadi, L. (2004). Sea urchin spine calcite forms via a transient amorphous calcium carbonate phase. *Science*, 306(5699), 1161-1164.

Raz, S., Hamilton, P. C., Wilt, F. H., Weiner, S., & Addadi, L. (2003). The transient phase of amorphous calcium carbonate in sea urchin larval spicules: the involvement of proteins and magnesium ions in its formation and stabilization. *Advanced Functional Materials*, 13(6), 480-486.

Ries, J. B. (2004). Effect of ambient Mg/Ca ratio on Mg fractionation in calcareous marine invertebrates: A record of the oceanic Mg/Ca ratio over the Phanerozoic. *Geology*, 32(11), 981-984.

Ries, J. B. (2010). Geological and experimental evidence for secular variation in seawater Mg/Ca (calcite-aragonite seas) and its effects on marine biological calcification. *Biogeosciences*, 7(9), 2795-2849. ISO 690

Sandberg, P. A. (1983). An oscillating trend in Phanerozoic non-skeletal carbonate mineralogy. *Nature*, 305(5929), 19-22.

Sandberg, P. A. (1985). Nonskeletal aragonite and $pCO_2$ in the Phanerozoic and Proterozoic.

*The carbon cycle and atmospheric $CO_2$: Natural variations Archean to present*, 32, 585-594.

Schroeder, J. H., Dwornik, E. J., & Papike, J. J. (1969). Primary protodolomite in echinoid skeletons. *Geological Society of America Bulletin*, 80(8), 1613-1616.

Seto, J., Ma, Y., Davis, S. A., Meldrum, F., Gourrier, A., Kim, Y. Y., Schilde, U., Sztucki, M., Burghammer, M., Maltsev, S., Jäger, C., & Cölfen, H. (2012). Structure-property relationships of a biological mesocrystal in the adult sea urchin spine. *Proceedings of the National Academy of Sciences*, 109(10), 3699-3704.

Shumway, S. E. (1977). The effects of fluctuating salinities on four species of asteroid echinoderms. *Comparative Biochemistry and Physiology Part A: Physiology*, 58(2), 177-179.

Smith, A. B. (1980). Stereom microstructure of the echinoid test. *Special Paper in Palaeontology* 25: 1-81.

Smith, A. M., Clark, D. E., Lamare, M. D., Winter, D. J., & Byrne, M. (2016). Risk and resilience: variations in magnesium in echinoid skeletal calcite. *Marine Ecology Progress Series*, *561*, 1–16.

Stanley, S. M. (2008). Effects of global seawater chemistry on biomineralization: past, present, and future. *Chemical Reviews*, 108(11), 4483-4498.

Stanley, S. M., & Hardie, L. A. (1998). Secular oscillations in the carbonate mineralogy of reef-building and sediment-producing organisms driven by tectonically forced shifts in seawater chemistry. *Palaeogeography, Palaeoclimatology, Palaeoecology*, 144(1-2), 3-19.

Stolarski, J., Meibom, A., Przeniosło, R., & Mazur, M. (2007). A Cretaceous scleractinian coral with a calcitic skeleton. *Science*, 318(5847), 92-94.

Stolarski, J., Coronado, I., Murphy, J. G., Kitahara, M. V., Janiszewska, K., Mazur, M., Gothmann, A. M., Bouvier, A.-S., Marin-Carbonne, J., Taylor, M. L., Quattrini, A. M., McFadden, C. S., Higgins, J. A., Robinson, L. F., & Meibom, A. (2021). A modern scleractinian coral with a two-component calcite–aragonite skeleton. *Proceedings of the National Academy of Sciences*, 118(3).

van Dijk, I., de Nooijer, L. J., Hart, M. B., & Reichart, G. J. (2016). The long-term impact of magnesium in seawater on foraminiferal mineralogy: Mechanism and consequences. *Global Biogeochemical Cycles*, 30(3), 438-446.

Vecchio, K. S., Zhang, X., Massie, J. B., Wang, M., & Kim, C. W. (2007). Conversion of sea urchin spines to Mg-substituted tricalcium phosphate for bone implants. *Acta Biomaterialia*, 3(5), 785-793.

Vidavsky, N., Addadi, S., Mahamid, J., Shimoni, E., Ben-Ezra, D., Shpigel, M., Weiner, S., & Addadi, L. (2014). Initial stages of calcium uptake and mineral deposition in sea urchin embryos. *Proceedings of the National Academy of Sciences*, 111(1), 39-44.

Vidavsky, N., Addadi, S., Schertel, A., Ben-Ezra, D., Shpigel, M., Addadi, L., & Weiner, S. (2016). Calcium transport into the cells of the sea urchin larva in relation to spicule formation. *Proceedings of the National Academy of Sciences*, 113(45), 12637-12642.

Wang, R. Z., Addadi, L., & Weiner, S. (1997). Design strategies of sea urchin teeth: structure, composition and micromechanical relations to function. *Philosophical Transactions of the Royal Society of London. Series B: Biological Sciences*, 352(1352), 469-480.

Weber, J. N. (1968). Fractionation of the stable isotopes of carbon and oxygen in calcareous marine invertebrates—the Asteroidea, Ophiuroidea and Crinoidea. *Geochimica et Cosmochimica Acta,* 32(1), 33-70.

Weber, J. N. (1969). The incorporation of magnesium into the skeletal calcites of echinoderms. *American Journal of Science*, *267*(5), 537–566.

Weber, J. N. (1973). Temperature dependence of magnesium in echinoid and asteroid skeletal calcite: a reinterpretation of its significance. *The Journal of Geology*, *81*(5), 543–556.

Weber, J. N., White, E. W., & Lebiedzik, J. (1971). New porous biomaterials by replication of echinoderm skeletal microstructures. *Nature*, 233(5318), 337-339.

Weiner, S. (1985). Organic matrix-like macromolecules associated with the mineral phase of sea urchin skeletal plates and teeth. *Journal of Experimental Zoology*, 234, 7–15.

Weiner, S., & Addadi, L. (2011). Crystallization pathways in biomineralization. *Annual Review of Materials Research*, 41, 21-40.

Wilkinson, B. H., & Algeo, T. J. (1989). Sedimentary carbonate record of calcium-magnesium cycling. *American Journal of Science*, 289(10), 1158-1194.

Zamora, S., Lefebvre, B., Álvaro, J. J., Clausen, S., Elicki, O., Fatka, O., Jell, P., Kouchinski, A., Lin, J.-P., Nardin, E., Parsley, R., Rozhnov, S., Sprinkle, J., Sumrall, C. D., Vizcaïno, D., & Smith, A. B. (2013). Cambrian echinoderm diversity and palaeobiogeography. *Geological Society, London, Memoirs*, 38(1), 157-171.

# Chapter I

## Effects of seawater chemistry ($Mg^{2+}/Ca^{2+}$ ratio) and diet on the skeletal Mg/Ca ratio in the common sea urchin *Paracentrotus lividus*[1]

Dorota Kołbuk[a], Philippe Dubois[b], Jarosław Stolarski[a], Przemysław Gorzelak[a]*

[a] Institute of Paleobiology, Polish Academy of Sciences, Twarda 51/55, PL-00-818 Warsaw, Poland; *pgorzelak@twarda.pan.pl

[b] Université Libre de Bruxelles, Faculté des Sciences, Laboratoire de Biologie Marine, CP 160/15, av. F.D. Roosevelt, 50 B-1050, Bruxelles, Belgium

### Abstract

It has been argued that concentration of major metallic ions such as $Mg^{2+}$ and $Ca^{2+}$ plays a role in determining the composition of the echinoderm skeleton. Consequently, in several studies Mg/Ca ratio from modern and fossil echinoderm ossicles was used as a proxy of secular $Mg^{2+}/Ca^{2+}$ changes of Phanerozoic seawater. However, although significant progress has been made in understanding biomineralization of echinoderms, it is still largely unknown what are the sources and physiological pathways of major ions that contribute to skeleton formation. Herein we tested the effects of modifications of ambient seawater $Mg^{2+}/Ca^{2+}$ ratio (which is typically ~5) and Mg-enrichment of the diet on the Mg/Ca ratio in regenerating spines of sea urchin *Paracentrotus lividus* under experimental conditions. We found that sea urchins cultured in seawater with $Mg^{2+}/Ca^{2+}$ ratio decreased to ~1.9 produced a skeleton with also decreased Mg/Ca ratio. However, the skeleton of specimens fed on a Mg-enriched diet showed significantly higher Mg/Ca ratio. This suggests that the seawater is an important but not the only source of ions that contributes to the Mg/Ca ratio of the skeleton. Consequently, the reliability of geochemical models that link directly seawater chemistry with the Mg/Ca ratio of the skeleton should be re-evaluated.

### Keywords

Echinoderms, magnesium, growth, geochemistry, mineralization, palaeontology

---

[1] Postprint version of an article: Kołbuk, D., Dubois, Ph., Stolarski, J. & Gorzelak, P. 2019. Effects of seawater chemistry ($Mg^{2+}/Ca^{2+}$ ratio) and diet on the skeletal Mg/Ca ratio in the common sea urchin *Paracentrotus lividus*. Marine Environmental Research 145: 22-26, doi:10.1016/j.marenvres.2019.02.006

## 1. Introduction

Seawater has been widely considered the only source of $Mg^{2+}$ and $Ca^{2+}$ ions in echinoderm biomineralization (e.g., Weiner and Addadi, 2011). This is supported by a number of experiments, which showed that labeling seawater with fluorescent markers, radioactive or stable isotopes, results in staining of the newly grown skeleton (Nakano et al., 1963; Lewis et al., 1990; Ebert, 2007; Gorzelak et al., 2011, 2014). However, the mechanisms involved in the fractionation of the major ions during biomineralization are poorly understood. It has been only suggested that $Ca^{2+}$ ions are specifically transported by pumps, channels and exchangers (Dubois and Chen, 1989; Stumpp et al., 2012) and that their concentration in the coelomic fluid is controlled by the organism (Stickle and Diehl, 1987; Santos et al., 2013). A recent study on echinoid embryos showed that seawater with its ions can be also directly incorporated into the cells by endocytosis (Vidavsky et al., 2016).

The Mg/Ca ratio in echinoderm skeleton can be also controlled by a number of environmental parameters other than seawater chemistry. As pointed out by Weber (1969), there is a strong positive correlation of ambient temperature with Mg concentration in echinoderm skeletons. An experimental study, however, demonstrated that skeletal Mg/Ca ratios in the euechinoid species *Paracentrotus lividus* increased with increasing temperature until reaching a plateau at high temperature (~24 °C), which is explained by the properties of the intrastereomic organic matrix (Hermans et al., 2010). In another experimental study, Borremans et al. (2009) found that there is a positive correlation between salinity and skeletal Mg/Ca ratio in the starfish *Asterias rubens*.

Apart from environmental parameters, physiological effects are also important in controlling Mg/Ca ratio in echinoderm skeleton (Weber, 1973). Notably, echinoderms from the same locations are known to display a wide range of skeletal Mg contents (e.g., Chave, 1954; Weber, 1969; Gorzelak et al., 2013; Iglikowska et al., 2017), which may vary at different length scales (among ossicles within a single individual, intra- and interspecies, and higher taxonomic levels). Hermans et al. (2011) experimentally showed that Mg/Ca ratios in echinoderm skeleton can be modulated by intrastereomic organic matrix composition and/or its concentration.

Diet is another factor which affects cell physiology, and may be also important in modulating chemical composition of echinoderm skeleton. It has been recently shown that the skeletal Mg/Ca ratio in the euechinoid species *Paracentrotus lividus* may vary according to the type of consumed macroalgal diet (Asnaghi et al., 2014). More specifically, it was found that sea urchins which fed non-calcifying algae *Cystoseira* displayed low Mg/Ca ratios in their skeletons comparing with those feeding on non-calcifying *Dictyota* and calcifying *Corallina*, that are generally thought to have higher Mg level (Wahbeh et al., 1985).

As the physiological mechanisms involved in the biomineralization process are poorly known, the skeletal Mg/Ca ratios have been usually attributed to the changes in the concentration of $Mg^{2+}$ and $Ca^{2+}$ ions in the seawater. Accordingly, it has been argued that the Mg/Ca ratio of well-preserved fossil echinoderms can be used as a reliable proxy for interpreting secular changes in the $Mg^{2+}/Ca^{2+}$ ratio of ancient seawater (Dickson, 2002, 2004; Hasiuk and Lohmann, 2010; Ries, 2004), which has varied significantly (1.0–5.2) throughout the Phanerozoic (Sandberg, 1983; Hardie, 1996; Lowenstein et al., 2001). These variations are thought to have been mainly caused by changes in $Ca^{2+}$ that are driven by variations in the rate of ocean crust production, affecting mixing rates of $Ca^{2+}$-rich hydrothermal brines and river waters (Hardie, 1996).

Experimental studies testing the effect of ambient $Mg^{2+}/Ca^{2+}$ ratio on echinoderms and justifying the use of well-preserved fossil echinoderms in the reconstruction of seawater $Mg^{2+}/Ca^{2+}$ ratio throughout the Phanerozoic are limited. Notably, there has been only one experimental study which investigated the effect of ambient $Mg^{2+}/Ca^{2+}$ ratio on skeletal Mg/Ca ratio in Recent echinoderms. Ries (2004) found that Mg/Ca ratios in spines and coronal plates of tropical cidaroid *Eucidaris tribuloides* decreased proportionally with decreasing $Mg^{2+}/Ca^{2+}$ ratio of seawater, in which they were growing. Although these data clearly revealed ambient $Mg^{2+}/Ca^{2+}$ effect, this was tested for only one species of sea urchin belonging to the clade Cidaroidea, which differs by numerous skeletal (e.g., presence of primary spines with external cortex) and physiological (e.g., low buffering capacity of the coelomic fluid) characteristics from other echinoids (Euechinoidea) (Lawrence and Jangoux, 2013; Collard et al., 2014; Dery et al., 2014).

The aim of this study is to determine the effect of changing $Mg^{2+}/ Ca^{2+}$ ratio in seawater and diet on the chemical composition of the skeleton of the euechinoid species *Paracentrotus lividus*. By exposing sea urchins to different $Mg^{2+}/Ca^{2+}$ ratios (current and decreased levels) and different types of diets (standard and Mg-enriched), we verified the previously proposed hypotheses which consider: (i) seawater as the only source of ions in echinoderm biomineralization, and (ii) echinoderms as a reliable proxy of $Mg^{2+}/Ca^{2+}$ ratios in seawater.

## 2. Material and methods

*Paracentrotus lividus* (~3 cm in diameter) was collected from the aquaculture facility in Luc-sur-Mer (English Channel, Normandy, France) and transported to Laboratoire de Biologie Marine (Université Libre de Bruxelles, Belgium) for acclimatization. The specimens were starved one week before the beginning of the experiment. Additionally, two days before the experiment, three tips of primary spines from each individual were cut off at mid-height to initiate regeneration.

Twelve specimens were incubated in two different chemical compositions of seawater, i.e., $Mg^{2+}/Ca^{2+}$ ratio = 5.02 (~present-day value) and 1.91 [mol/mol]. Natural seawater from the English Channel slightly adjusted with seasalts to increase salinity was used. Decreased molar $Mg^{2+}/Ca^{2+}$ ratio in seawater was obtained by addition of $CaCl_2{\cdot}2H_2O$ (SIGMA), which increased the absolute concentration of $Ca^{2+}$ (from ~9.8 to ~25.5mmol), a level that is believed to have occurred in the geological history (e.g., Hardie, 1996; Lowenstein et al., 2001). Twelve sea urchins were fed on a diet (one pellet per day) containing different amounts of magnesium: ~0.3 wt% Mg (Zeigler Bros pellets) or ~11 wt% Mg (Zeigler Bros pellets mixed with carrageenan and enriched by magnesium by the addition of $MgCO_3$ $x2H_2O$ (SIGMA)). Dissolution of magnesium from pellets into the seawater, potentially increasing ambient $Mg^{2+}/Ca^{2+}$ ratio, was excluded as inferred from the chemical analyses of control seawater samples. Furthermore, the amount of magnesium (~1.2 g/l) in 1 L seawater (the volume of each aquarium) is more than 100 times higher than in a single pellet (~0.011 g); which means that even if all the magnesium from diet dissolved into the seawater, it would have no effect on $Mg^{2+}/ Ca^{2+}_{sw}$ ratio.

Twelve specimens (two $Mg^{2+}/Ca^{2+}$ ratios/x/two different diet types/x/three replicates per treatment = 12) were incubated in separate 1 L aquaria for 14 days under constant temperature (mean range: 17.2–17.4 °C; SD: 0.5–0.8); salinity (mean range: 33.4–33.6 psu; SD: 0.3–0.5) and pH (in total scale) (mean range: 8.07–8.12; SD: 0.06–0.08) conditions. The parameters were measured three times per day by WTW Multi 340i multimeter equipped with a conductivity cell, pH electrode, and integrated temperature sensor. The pH electrode was calibrated with Merck CertiPUR buffer solutions pH 4.00 and 7.00. pH measurements were converted to total scale according to DelValls and Dickson's method using TRIS/AMP buffers (provided by Prof. Lei Chou from the laboratory of Biogéochimie et Modélisation du Système Terre: Océanographie Chimique et Géochimie des Eaux, Université Libre de Bruxelles). In order to minimize variations in physico-chemical parameters within aquaria, seawater was renewed every day. $Mg^{2+}/Ca^{2+}$ ratio in seawater in two treatments was additionally verified with inductively coupled plasma-optical emission spectrometry (ICP-OES) at the Bureau Veritas Minerals Laboratory in Canada. Variations in $Mg^{2+}/ Ca^{2+}$ ratios remained within less than 5% (SD: 0.04).

After 14 days of experiment, the spines with regenerated tips were removed from the urchins and treated with 2.5% sodium hypochlorite (NaOCl) solution and rinsed in ultrapure water to remove soft tissues, which is a standard cleaning procedure. Spines with regenerated tips were embedded in epoxy resin[2]. They were cut along the shaft length, polished through a series of diamond suspensions, and carbon-coated. An advantage of analysing regenerated tips is that the newly formed skeleton, without necessity of staining, can be easily distinguished from the older one. Regenerative process, which initiates not earlier than 3 days after spine breakage (e.g. Heatfield, 1971; Gorzelak et al., 2011, 2017), can be recognized by an abrupt change in spine diameter above the cutting fracture.

Mg/Ca ratios of the so-called open stereom (excluding septa and the distalmost parts of the spine) in regenerated tips of spines were determined with the aid of Wavelength Dispersive Spectroscopy (WDS) performed on CAMECA SX100 electron microprobe at the Micro-Area Analysis Laboratory, Polish Geological Institute - National Research Institute in Warsaw (accelerating voltage 15 kV, beam current 5 nA for calcium and 20 nA for magnesium, beam diameter ~5 μm). Mean Mg/ Ca ratios for each of the 12 specimens were calculated from 5 to 15 spot measurements (pooled from 1 to 3 regenerated spines from the same individual). The number of spot geochemical analyses depended on the size of the newly grown regenerated tip. The area of each spot analysis was smaller than stereom bar. The range of observed intra-individual skeletal Mg/Ca variation was not considerable (SD within and amongst specimens were small and comparable to each other (~0.005)). Few spot analyses were also performed on the stereom in the shaft below the cutting fracture.

Statistical analyses (two-way ANOVA, fully crossed design, followed by a post-hoc Tukey's HSD test) were performed in the Statistica software, with significance levels set at 0.05. Statistical analyses did not include geochemical data collected from the spine stereom below cutting fracture as it was formed prior to exposure to experimental conditions.

---

[2] Sections of investigated material are housed at the Institute of Paleobiology, Polish Academy of Sciences, Warsaw (ZPALV.42 PhD).

## 3. Results

Due to pre-experimental period of starvation, all sea urchins were intensely feeding on provided pellets (frequency of eaten pellets was very high and comparable to each other, i.e., 86–93%). Regeneration was observed in at least one spine in each specimen. Results from the same specimen were pooled. Mean Mg/Ca skeletal ratios of sea urchins from each treatment are shown in Fig. 1.

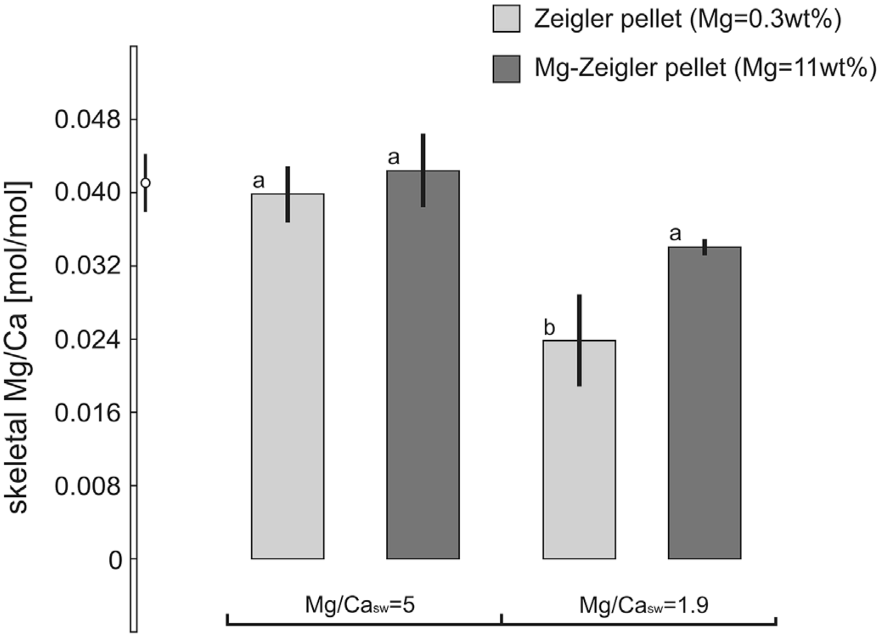

**Figure 1.** Mean skeletal Mg/Ca ratios (± SD) in four treatments. Means sharing the same superscript are not significantly different ($p \geq 0.05$, post-hoc Tukey's HSD test). Open circle indicates mean skeletal Mg/Ca ratio (± SD) obtained from the measurements of spine stereom below cutting fracture in 12 individuals.

**Table 1.** Results of two-way ANOVA for independent samples. Variables are seawater $Mg^{2+}/Ca^{2+}$ ratio and type of diet, $Mg^{2+}/Ca^{2+}_{sw}$*Diet - interaction of these two factors. Bold p-values are statistically significant at $p < 0.05$.

| | SS | df | MS | F | P |
|---|---|---|---|---|---|
| MgCa$_{sw}$ | 0.000445 | 1 | 0.000445 | 36.09816 | **0.0003** |
| Diet | 0.000122 | 1 | 0.000122 | 9.90941 | **0.014** |
| MgCa$_{sw}$*Diet | 0.000044 | 1 | 0.000044 | 3.54259 | 0.097 |
| Standard error | 0.000099 | 8 | 0.000012 | | |

Results of two-way ANOVA (Table 1) show that both effects i.e., the seawater $Mg^{2+}/Ca^{2+}$ ($p = 0.0003$) and the diet ($p = 0.014$) are significant. However, the interaction between these two factors is not significant ($p = 0.09$). Mean skeletal Mg/Ca ratio for sea urchins fed on Zeigler pellets and cultured under high $Mg^{2+}/Ca^{2+}$ sw (~5) is 0.0397 mol/mol ($SD_{Mg/Ca}$: 0.003; mean Mg wt%: 0.9; mean Ca wt%: 37.28). The specimens kept in the same seawater type but which were fed on Mg-enriched diet are characterized by a slightly higher Mg/Ca ratio (0.0423 mol/mol; $SD_{Mg/Ca}$: 0.004; mean Mg wt%: 0.96; mean Ca wt%: 37.41). The specimens incubated in a low $Mg^{2+}/Ca^{2+}$ sw ratio (~1.9) display lower mean Mg/Ca ratio in their regenerated tips. Under these conditions, however, mean skeletal Mg/Ca ratio in the specimens fed on Mg-enriched diet is much higher (0.0339 mol/mol, $SD_{Mg/Ca}$: 0.001; mean Mg wt%: 0.78; mean Ca wt%: 37.78) than in the specimens fed on "standard" Zeigler pellets (0.0237 mol/mol; $SD_{Mg/Ca}$: 0.005; mean Mg wt%: 0.54; mean Ca wt%: 37.46). Tukey's post hoc tests show that only the mean skeletal Mg/Ca ratio of specimens incubated under low $Mg^{2+}/Ca^{2+}$ and fed on Zeigler pellets is significantly different from that of other treatments (Fig. 1). Mean skeletal Mg/Ca ratios of echinoids from the other treatments do not differ from each other.

Using Mg fractionation algorithm (Ries, 2004), which is used to calculate paleoceanic $Mg^{2+}/Ca^{2+}$ ratios from unaltered fossils echinoderms, we reconstructed theoretical seawater $Mg^{2+}/Ca^{2+}$ in our treatments based on skeletal Mg/Ca ratios obtained from our specimens, and then estimated the error induced by the diet effect on the $Mg^{2+}/Ca^{2+}$ seawater reconstructions (Table 2).

We found that the error introduced by diet may reach up to about 8.7% for the specimens incubated under normal $Mg^{2+}/Ca^{2+}$ ratio and 91.2% for the specimens cultured under low $Mg^{2+}/Ca^{2+}$ ratio.

**Table 2**. Comparisons between measured seawater $Mg^{2+}/Ca^{2+}$ ratios and those reconstructed from skeletal Mg/Ca ratios following Ries' (2004) algorithm $Mg/\ Ca_C = S(0.000837T + 0.0155)Mg/Ca_{SW}^{0.538}$. SW – seawater, C – calcite, T – temperature, S – species coefficient.

| | Sea urchins fed on Zeigler pellets | | Sea urchins fed on Mg-enriched pellets | |
|---|---|---|---|---|
| Measured $Mg^{2+}/Ca^{2+}_{sw}$ ratio | 5.02 | 1.91 | 5.02 | 1.91 |
| Calculated $Mg^{2+}/Ca^{2+}_{sw}$ ratio | 4.90 | 1.89 | 5.46 | 3.65 |
| Calculated error in reconstruction | 2.5% | 0.9% | 8.7% | 91.2% |

## 4. Discussion

As expected, under low ambient $Mg^{2+}/Ca^{2+}$ ratio, echinoderms produced a skeleton with decreased Mg/Ca ratio. Interestingly, however, the skeletal Mg/Ca ratios in the specimens fed on Mg-enriched diet, notwithstanding chemical composition of seawater, were higher than in the specimens fed on “normal” low-Mg diet. The magnitude of this increase, however, appears to be higher in the specimens cultured in seawater with decreased $Mg^{2+}/Ca^{2+}$ ratio (Fig. 1). Notably, only the mean skeletal Mg/Ca ratio of sea urchins incubated under low $Mg^{2+}/ Ca^{2+}$ ratio and fed on Zeigler pellets is significantly different from the other treatments (Fig. 1).

Overall these results strongly suggest that seawater may not be the only source of ions in echinoderm biomineralization, consistent with previous hypothesis by Asnaghi et al. (2014). Notably, in the case of other ions, a clear relationship between the contents of Fe in echinoderm skeletons and consumed algae was found, suggesting that skeletal Fe derives from food (e.g., Stevenson and Ufret, 1966).

Our results suggest that the effect of the Mg-enriched diet should be taken into account when reconstructing $Mg^{2+}/Ca^{2+}$ ratio of not only modern, but also ancient seawater. Indeed, the error introduced by diet may be significant, especially for the specimens cultured under low $Mg^{2+}/Ca^{2+}$ ratio (Table 2). However, the bias introduced by diet in the natural environments is expected to be lower because natural diet of sea urchins typically contains lower contents of magnesium. Notwithstanding, the skeletons of some living coralline algae and scleractinian corals, which represent an important component of the diet of some sea urchins, may be significantly enriched with magnesium due to association of microbially-induced Mg-minerals (such as brucite $Mg(OH)_2$ or magnesite $MgCO_3$) (Nothdurft et al., 2005; Buster et al., 2006; Nash et al., 2011; Nash et al., 2015). Furthermore, sea urchins are known to graze and ingest different types of sedimentary and metamorphic rocks (Russell et al., 2018), some of which may be particularly enriched in Mg.

Interpretation of Mg content in fossil samples may be even more complicated. Mg/Ca ratio may be significantly enriched or depleted due to various diagenetic factors (e.g. Dickson, 1995; Stolarski et al., 2009; Gorzelak et al., 2016). High-magnesium calcite of echinoderm biomineral is metastable and tends to transform into low-magnesium polymorph during diagenesis. Only the samples that meet all structural and geochemical criteria of good preservation can be used in further interpretation but even then, a precise assessment of the extent of diagenetic alteration is often difficult to evaluate (Gorzelak et al., 2016). For instance, sub-microscale removal of intrastereom organic matrix and internal dissolution-precipitation with some transfer of ions may occur without change of stereom architecture (Gorzelak and Zamora, 2013; Gorzelak et al., 2016).

Our observations also shed light on some not well elucidated physiological mechanism of biomineralization of regenerating echinoid spines. The spines are connected with the body wall only with connective tissues (muscles and ligaments) and a thin layer of epidermis with no coelomic extensions (Heatfield and Travis, 1975). It has been thus widely assumed that biomineralization of spine is only mediated by the covering epidermis (e.g., Gorzelak et al., 2014). Our data, however, suggest that magnesium from diet (either in the form of ions or already formed Mg-enriched nanograins), which may contribute to Mg-enrichment of the spine, may be transported directly from the coelom to the spines. Nevertheless, pathway of dietary magnesium transport to spine tip remains puzzling. The only cell types with capability of migration from the body wall to spines, which might have been possibly involved in this transport, are phagocytes and/or spherule-bearing cells, the so-called spherulocytes. Both cell types are known to enclose a variety of granular material (Heatfield and Travis, 1975). Notably, based on ultrastructural evidence, Dubois et al. (1995) suggested that most connective tissue cells are of mesothelial origin and proposed that skeleton-forming cells are part of a mesothelial component pervading the whole dermis. Interestingly, recent study demonstrated that micrometer-size vesicles composed of solid calcium carbonate can be formed elsewhere, even within non-specialized epithelial cells (Vidavsky et al., 2014). These granules are thought to be transferred into the spicule compartment, where they likely disaggregate into nanoparticles, which subsequently undergo secondary crystallization.

Spines are the most outward part of the sea urchin bodies, providing protection from predators. It has been shown that spine regeneration induces changes in resource allocation leading to growth inhibition of test (e.g., Ebert, 1968; Edwards and Ebert, 1991). It can be speculated that, especially under stressful conditions of low ambient $Mg^{2+}/Ca^{2+}$ ratio, additional sources of magnesium from diet (if available) contribute to $Mg^{2+}$ incorporation into the skeleton as an impurity.

## 5. Conclusions

Our data demonstrate that under low $Mg^{2+}/Ca^{2+}$ seawater ratio sea urchins produce a skeleton with decreased Mg/Ca ratio. Nevertheless, sea urchins fed on Mg-enriched diet show significantly higher Mg content in their skeletons. These results, although based on a limited number of specimens, suggest that seawater may not necessarily be the only source of ions in echinoderm biomineralization. To fully substantiate these conclusions, however, more experiments testing the impact of different $Mg^{2+}/Ca^{2+}$ ratios (formulated not only with addition of $Ca^{2+}$) and diet on biomineralogy of different echinoderms species are needed. Such experimental studies are currently being developed (Gorzelak and Kołbuk, in progress).

**Acknowledgments**. We thank three anonymous reviewers for their many insightful comments and suggestions. This research was funded by the National Science Centre (NCN) grant no. 2016/23/B/ST10/00990 and was performed in the NanoFun laboratory co-financed by the European Regional Development Fund within the Innovation Economy Operational Programme POIG.02.02.00–00-025/09. Ph. Dubois is a Research Director of the National Fund for Scientific Research (FRS- FNRS; Belgium).

The experiments on live echinoids were performed in Brussels (Belgium), where no ethics approval is required for the maintenance and handling of this particular species. Nevertheless, our research conformed to the ethical principles of replacement, reduction, refinement and minimization of animal suffering following the guidelines reported in the European Directive 86/609/EEC.

## References

Asnaghi, V., Mangialajo, L., Gattuso, J. P., Francour, P., Privitera, D., & Chiantore, M. (2014). Effects of ocean acidification and diet on thickness and carbonate elemental composition of the test of juvenile sea urchins. *Marine Environmental Research*, *93*, 78–84.

Borremans, C., Hermans, J., Baillon, S., André, L., & Dubois, P. (2009). Salinity effects on the Mg/Ca and Sr/Ca in starfish skeletons and the echinoderm relevance for paleoenvironmental reconstructions. *Geology*, *37*(4), 351–354.

Buster, N. A., Holmes, C. W., Goreau, T. J., & Hilbertz, W. (2006). Crystal Habits of the Magnesium Hydroxide Mineral Brucite Within Coral Skeletons. In *American Geophysical Union Annual Meeting* (p. Abstract and Poster).

Chave, K. (1954). Aspects of the biogeochemistry of magnesium.1- Calcareous marine organisms. *Journal of Geology*, *62*(3), 266–283.

Collard, M., Dery, A., Dehairs, F., & Dubois, P. (2014). Euechinoidea and Cidaroidea respond differently to ocean acidification. *Comparative Biochemistry and Physiology Part A: Molecular & Integrative Physiology*, *174*, 45–55.

Dery, A., Guibourt, V., Catarino, A. I., Compère, P., & Dubois, P. (2014). Properties, morphogenesis, and effect of acidification on spines of the cidaroid sea urchin

*Phyllacanthus imperialis*. *Invertebrate Biology*, *133*(2), 188–199.Dickson, J. A. D. (1995). Paleozoic Mg calcite preserved: Implications for the Carboniferous ocean. Geology, 23(6), 535-538.

Dickson, J. A. D. (2002). Fossil Echinoderms As Monitor of the Mg/Ca Ratio of Phanerozoic Oceans. *Science*, *298*(5596), 1222–1224.

Dickson, J. A. D. (2004). Echinoderm skeletal preservation; calcite-aragonite seas and the Mg/Ca ratio of Phanerozoic oceans. *Journal of Sedimentary Research*, *74*(3), 355–365.

Dubois, P., & Chen, C. P. (1989). Calcification in echinoderms. Echinoderm studies, 3, 109-178.

Dubois, P., Ghyoot, M., & Jangoux, M. (1995). Are most mesenchymatous cells of echinoderms from mesothelial origin? A review of the evidence. *Echinoderm Research*, 259–262.

Ebert, T. A. (1968). Growth Rates of the Sea Urchin *Strongylocentrotus Purpuratus* Related to Food Availability and Spine Abrasion. *Ecological Society of America*, *49*(6), 1075–1091.

Ebert, T. A. (2007). Growth and survival of postsettlement sea urchins. In Developments in Aquaculture and Fisheries Science. 37, 95-134. Elsevier.

Edwards, P. B., & Ebert, T. A. (1991). Plastic responses to limited food availability and spine damage in the sea urchin *Strongylocentrotus purpuratus*, *145*, 205–220.

Gorzelak, P., Dery, A., Dubois, P., & Stolarski, J. (2017). Sea urchin growth dynamics at microstructural length scale revealed by Mn-labeling and cathodoluminescence imaging. *Frontiers in Zoology*, 14(1), 42.

Gorzelak, P., Krzykawski, T., & Stolarski, J. (2016). Diagenesis of echinoderm skeletons: Constraints on paleoseawater Mg/Ca reconstructions. *Global and Planetary Change*, *144*, 142–157.

Gorzelak, P., Stolarski, J., Dery, A., Dubois, P., Escrig, S., & Meibom, A. (2014). Ultrascale and microscale growth dynamics of the cidaroid spine of *Phyllacanthus imperialis* revealed by $^{26}$Mg labeling and NanoSIMS isotopic imaging. *Journal of Morphology*, *275*(7), 788–796.

Gorzelak, P., Stolarski, J., Dubois, P., Kopp, C., & Meibom, A. (2011). $^{26}$Mg labeling of the sea urchin regenerating spine: Insights into echinoderm biomineralization process. *Journal of structural biology*, *176*(1), 119-126.

Gorzelak, P., Stolarski, J., Mazur, M., & Meibom, A. (2013). Micro- to nanostructure and geochemistry of extant crinoidal echinoderm skeletons. *Geobiology*, *11*(1), 29–43.

Gorzelak, P., & Zamora, S. (2013). Stereom microstructures of Cambrian echinoderms revealed by cathodoluminescence (CL). *Palaeontologia Electronica*, *16*(3), 1–17.

Hardie, L. A. (1996). Secular variation in seawater chemistry: An explanation for the coupled secular variation in the mineralogies of marine limestones and potash evaporites over the past 600 my. Geology, 24(3), 279-283.Hasiuk, F. J., & Lohmann, K. C. (2010). Application of calcite Mg partitioning functions to the reconstruction of paleocean Mg/Ca. *Geochimica et Cosmochimica Acta*, *74*(23), 6751–6763.

Heatfield, B. M. (1971). Growth of the calcareous skeleton during regeneration of spines of the sea urchin, Strongylocentrotus purpuratus (Stimpson): a light and scanning electron microscopic study. *Journal of Morphology*, *134*(1), 57-89.

Heatfield, B. M., & Travis, D. F. (1975). Ultrastructural Studies of Regenerating Spines of the Sea Urchin *Strongylocentrotus purpuratus*. *Journal of Morphology*, *145*(1), 51–71.

Hermans, J., André, L., Navez, J., Pernet, P., & Dubois, P. (2011). Relative influences of solution composition and presence of intracrystalline proteins on magnesium incorporation in calcium carbonate minerals: Insight into vital effects. *Journal of Geophysical Research: Biogeosciences*, *116*(1), 1–10.

Hermans, J., Borremans, C., Willenz, P., André, L., & Dubois, P. (2010). Temperature, salinity and growth rate dependences of Mg/Ca and Sr/Ca ratios of the skeleton of the sea urchin *Paracentrotus lividus* (Lamarck): An experimental approach. *Marine Biology*, *157*(6), 1293–1300.

Iglikowska, A., Najorka, J., Voronkov, A., Chełchowski, M., & Kukliński, P. (2017). Variability in magnesium content in Arctic echinoderm skeletons. *Marine Environmental Research*, *129*, 207–218.

Lawrence, J. M., & Jangoux, M. (2013). Cidaroids. In *Developments in Aquaculture and Fisheries Science* (Vol. 38, pp. 225–242). Elsevier.

Lewis, C. A., Ebert, T. A., & Boren, M. E. (1990). Allocation of $^{45}$ calcium to body components of starved and fed purple sea urchins (*Strongylocentrotus purpuratus*).

Lowenstein, T. K., Timofeeff, M. N., Brennan, S. T., Hardie, L. A., & Demicco, R. V. (2001). Oscillations in Phanerozoic seawater chemistry: Evidence from fluid inclusions. *Science*, *294*(5544), 1086-1088.

Nakano, E., Okazaki, K., & Iwamatsu, T. (1963). Accumulation of radioactive calcium the larvae of the sea urchin *Pseudocentrotus depressus*. *The Biological Bulletin*, *125*(1), 125-132.

Nash, M. C., Russell, B. D., Dixon, K. R., Liu, M., & Xu, H. (2015). Discovery of the mineral brucite (magnesium hydroxide) in the tropical calcifying alga *Polystrata dura* (Peyssonneliales, Rhodophyta). *Journal of Phycology*, *51*(3), 403–407.

https://doi.org/10.1111/jpy.12299

Nash, M. C., Troitzsch, U., Opdyke, B. N., Trafford, J. M., Russell, B. D., & Kline, D. I. (2011). First discovery of dolomite and magnesite in living coralline algae and its geobiological implications. *Biogeosciences*, *8*(11), 3331–3340.

Nothdurft, L. D., Webb, G. E., Buster, N. A., Holmes, C. W., Sorauf, J. E., & Kloprogge, J. T. (2005). Brucite microbialites in living coral skeletons: Indicators of extreme microenvironments in shallow-marine settings. *Geology*, *33*(3), 169–172.

Ries, J. B. (2004). Effect of ambient Mg/Ca ratio on Mg fractionation in calcareous marine invertebrates: A record of the oceanic Mg/Ca ratio over the Phanerozoic. *Geology*, *32*(11), 981–984.

Russell, M. P., Gibbs, V. K., & Duwan, E. (2018). Bioerosion by pit-forming, temperate-reef sea urchins: History, rates and broader implications. *PloS One*, *13*(2), e0191278.

Sandberg, P. A. (1983). An oscillating trend in Phanerozoic non-skeletal carbonate mineralogy. *Nature*, *305*(5929), 19.

Santos, I. A., Castellano, G. C., & Freire, C. A. (2013). Direct relationship between osmotic and ionic conforming behavior and tissue water regulatory capacity in echinoids. *Comparative Biochemistry and Physiology Part A: Molecular & Integrative Physiology*, *164*(3), 466–476.

Stevenson, R. A., & Ufret, S. L. (1966). Iron, Manganese, and Nickel in Skeletons and Food of the Sea Urchins *Tripneustes esculentus* and *Echinometra lucunter*. *Limnology and Oceanography*, *11*(1), 11–17. https://doi.org/10.4319/lo.1966.11.1.0011

Stickle, W. B., & Diehl, W. J. (1987). Effects of salinity on echinoderms. *Echinoderm Studies*, *2*, 235–285.

Stumpp, M., Hu, M. Y., Melzner, F., Gutowska, M. A., Dorey, N., Himmerkus, N., Holtmann, W. C., Dupont, S. T., Thorndyke, M. C., & Bleich, M. (2012). Acidified seawater impacts sea urchin larvae pH regulatory systems relevant for calcification. *Proceedings of the National Academy of Sciences*, *109*(44), 18192-18197.

Vidavsky, N., Addadi, S., Mahamid, J., Shimoni, E., Ben-Ezra, D., Shpigel, M., Weiner, S., Addadi, L. (2014). Initial stages of calcium uptake and mineral deposition in sea urchin embryos. *Proceedings of the National Academy of Sciences of the United States of America*, *111*(1), 39–44.

Vidavsky, N., Addadi, S., Schertel, A., Ben-Ezra, D., Shpigel, M., Addadi, L., & Weiner, S. (2016). Calcium transport into the cells of the sea urchin larva in relation to spicule formation. *Proceedings of the National Academy of Sciences*, *113*(45), 12637-12642.

Wahbeh, M. I., Mahasneh, D. M., & Mahasneh, I. (1985). Concentrations of zinc, manganese, copper, cadmium, magnesium and iron in ten species of algae and sea water from Aqaba, Jordan. *Marine Environmental Research*, *16*(2), 95-102.

Weber, J. N. (1969). The incorporation of magnesium into the skeletal calcites of echinoderms. *American Journal of Science*, *267*(5), 537–566.

Weber, J. N. (1973). Temperature dependence of magnesium in echinoid and asteroid skeletal calcite: a reinterpretation of its significance. *The Journal of Geology*, *81*(5), 543–556.

Weiner, S., & Addadi, L. (2011). Crystallization Pathways in Biomineralization. *Annual Review of Materials Research*, *41*(1), 21–40.

# Chapter II

## Effects of seawater $Mg^{2+}/Ca^{2+}$ ratio and diet on the biomineralization and growth of sea urchins and the relevance of fossil echinoderms to paleoenvironmental reconstructions[3]

Dorota Kołbuk[a,] Sarah Di Giglio[b], Saloua M'Zoudi[b], Philippe Dubois[b], Jarosław Stolarski[a], Przemysław Gorzelak[a*]

[a] Institute of Paleobiology, Polish Academy of Sciences, Twarda 51/55, PL-00-818 Warsaw, Poland; *pgorzelak@twarda.pan.pl
[b] Université Libre de Bruxelles, Faculté des Sciences, Laboratoire de Biologie Marine, CP 160/15, av. F.D. Roosevelt, 50 B-1050, Bruxelles, Belgium

### Abstract

It has been argued that skeletal Mg/Ca ratio in echinoderms is mostly governed by $Mg^{2+}$ and $Ca^{2+}$ concentrations in the ambient seawater. Accordingly, well-preserved fossil echinoderms were used to reconstruct Phanerozoic seawater $Mg^{2+}/Ca^{2+}$ ratio. However, Mg/Ca ratio in echinoderm skeleton can be affected by a number of environmental and physiological factors, the effects of which are still poorly understood. Notably, experimental data supporting the applicability of echinoderms in paleoenvironmental reconstructions remain limited. Here, we investigated the effect of ambient $Mg^{2+}/Ca^{2+}$seawater ratio and diet on skeletal Mg/Ca ratio and growth rate in two echinoid species (*Psammechinus miliaris* and *Prionocidaris baculosa*). Sea urchins were tagged with manganese and then cultured in different $Mg^{2+}/Ca^{2+}$ conditions to simulate fluctuations in the $Mg^{2+}/Ca^{2+}$seawater ratios in the Phanerozoic. Simultaneously, they were fed on a diet containing different amounts of magnesium. Our results show that the skeletal Mg/Ca ratio in both species varied not only between ossicle types but also between different types of stereom within a single ossicle. Importantly, the skeletal Mg/Ca ratio in both species decreased proportionally with decreasing seawater $Mg^{2+}/Ca^{2+}$ratio. However, sea urchins feeding on Mg-enriched diet produced a skeleton with a higher Mg/Ca ratio. We also found that although incubation in lower ambient $Mg^{2+}/Ca^{2+}$ratio did not affect echinoid respiration rates,

---

[3] Postprint version of an article: Kołbuk, D., Di Giglio, S., M'Zoudi, S., Dubois, P., Stolarski, J., & Gorzelak, P. (2020). Effects of seawater $Mg^{2+}/Ca^{2+}$ ratio and diet on the biomineralization and growth of sea urchins and the relevance of fossil echinoderms to paleoenvironmental reconstructions. Geobiology, 18(6), 710-724, doi: 10.1111/gbi.12409

it led to a decrease or inhibition of their growth. Overall, these results demonstrate that although skeletal Mg/Ca ratios in echinoderms can be largely determined by seawater chemistry, the type of diet may also influence skeletal geochemistry, which imposes constraints on the application of fossil echinoderms as a reliable proxy. The accuracy of paleoseawater $Mg^{2+}/Ca^{2+}$ calculations is further limited by the fact that Mg partition coefficients vary significantly at different scales (between species, specimens feeding on different types of food, different ossicle types, and stereom types within a single ossicle).

**Keywords**

Echinodermata, Mg-calcite, skeletal chemistry, stereo, vital effects

## 1. Introduction

The Mg-calcite skeleton of echinoderms consists of numerous ossicles with a distinct tridimensional porous microstructure termed stereom that is formed through the initial deposition of amorphous calcium carbonate (ACC) with different hydration levels (e.g., Alberic et al., 2019). Despite a highly controlled intracellular biomineralization process, environmental controls on the elemental composition of the echinoderm skeleton have been evidenced. For instance, the skeletal Mg/Ca ratio is linked to the ambient seawater $Mg^{2+}/Ca^{2+}$ ratio (Dickson, 2002; Ries, 2004). As a consequence, well-preserved fossil echinoderms have been used as a proxy for the ancient seawater $Mg^{2+}/Ca^{2+}$ ratio (Dickson, 2002; 2004; Ries, 2004; Hasiuk and Lohmann, 2010), which has varied (from ~1 to 5.2 [mol/mol]) throughout the Phanerozoic (e.g., Wilkinson and Algeo, 1989; Hardie, 1996; Stanley and Hardie, 1998).

The Mg/Ca ratio in echinoderm skeletons, however, can be also affected by a number of other environmental parameters, such as temperature and salinity (e.g., Chave, 1954; Weber, 1969, 1973; Richter and Bruckschen, 1998; Smith et al., 2016). For instance, an experimental study on the echinoid *Paracentrotus lividus* demonstrated that its skeletal Mg/Ca ratio increased with increasing seawater temperature until it reached a plateau (at ~24°C; Hermans et al., 2010). On the other hand, the skeletal Mg/Ca in the Aristotle's lantern of the sea urchin *Lytechinus variegatus* was found to be higher for the specimens cultured at 26°C rather than at 30°C (Duquette et al., 2018b). In another experimental study, Borremans et al. (2009) showed that salinity significantly affects the skeletal Mg/Ca ratio in the starfish *Asterias rubens*.

Remarkably, magnesium content may vary between different echinoderm taxa and also between and within ossicles of specimens from the same population (Chave, 1954; Weber, 1969, 1973; McClintock et al., 2011; Smith et al., 2016), suggesting that biological factors ("vital effects") may be also important in modulating their skeletal Mg/Ca ratios. Hermans et al.(2011) suggested that variations in skeletal Mg/Ca ratio in echinoderms may be related to the variations in content of intra-crystalline organic molecules, such as aspartic-rich proteins, possessing a domain binding $Mg^{2+}$, which are known to stabilize ACC (Raz et al., 2003).

Interestingly, it has been recently shown that diet can also modify the skeletal Mg/Ca ratio in both juveniles and adults of the echinoid *Paracentrotus lividus* (Asnaghi et al., 2014; Kołbuk et al., 2019). More specifically, these studies demonstrated that sea urchins fed on magnesium-enriched artificial or natural diet displayed higher Mg/Ca ratios in their skeletons, which suggests that seawater is not the only source of $Mg^{2+}$ in echinoderm biomineralization.

Experimental data to verify the applicability of fossil echinoderms to ancient seawater $Mg^{2+}/Ca^{2+}$ ratio reconstructions are limited and involved only two species of echinoids (*Eucidaris tribuloides* in Ries, 2004; *Paracentrotus lividus* in Kołbuk et al., 2019). Furthermore, in these experiments, the specimens from each treatment were either maintained in the same tank (Ries, 2004) inducing a problem of confounding effects or were incubated in artificial seawater in which only concentration of $Ca^{2+}$ was adjusted (Kołbuk et al., 2019), hindering interpretation of these results in the context of ancient marine conditions (where $Ca^{2+}$ concentration is believed to changed concomitantly with $Mg^{2+}$ level (Wilkinson and Algeo, 1989; Hardie, 1996)).

To test the effect of changing $Mg^{2+}/Ca^{2+}$ ratio in seawater and diet on the chemical composition and growth dynamics of the echinoderm skeleton, we incubated two phylogenetically distant echinoid species in artificial seawater with decreased $Mg^{2+}/Ca^{2+}$ ratios that existed throughout the Phanerozoic and fed them with two types of diet containing different amount of magnesium. We also examined several well-preserved fossil echinoids from the so-called “calcite” and “aragonite” seas to further explore whether echinoderm skeletons are indeed a reliable monitor of ambient seawater $Mg^{2+}/Ca^{2+}$ ratio.

## 2. Materials and methods

### 2.1. Collection, handling, and tagging

The specimens of a temperate euechinoid *Psammechinus miliaris* (~3 cm in ambital test diameter) and a tropical cidaroid *Prionocidaris baculosa* (~2 cm in ambital test diameter) were collected from the North Sea (near Nieuwpoort town; coordinates: 51°11.10N, 2°42.07E) and the coastal regions of Cebu in the Philippines (coordinates: ~10°14′08″N 123°53′59″E), respectively. All sea urchins were transported for acclimatization to the Laboratoire de Biologie Marine (Université Libre de Bruxelles, Belgium), where they were fed intensively on Zeigler Bros pellets for about 10 days. Subsequently, they were starved for two weeks before the experiment. Three days before the beginning of the experiment, three spines from each of 18 individuals of *Psammechinus miliaris* were cut in the mid-height in order to initiate their regeneration. These specimens along with 18 individuals of *Prionocidaris baculosa* were labeled with manganese (1 mg/L) following the method described by Gorzelakand et al. (2017). More specifically, sea urchins were incubated for two days in separate 1 L beakers, each containing 1 L of natural seawater from the English Channel (slightly adjusted with sea salts to increase salinity) mixed with dissolved $MnCl_2*4H_2O$ (Sigma-Aldrich) resulting in nominal $Mn^{2+}$ concentration 1 mg/L.

## 2.2. Experimental setup and seawater parameters

Following Mn labeling, 18 specimens of each species were incubated for 21 days in seawater with three different $Mg^{2+}/Ca^{2+}$ ratios [mol/mol]: ~5.2 [=modern value], ~2.5 [a level that existed for example during the late Mississippian, Pennsylvanian, early Permian, Middle Triassic, Early Jurassic, and late Paleogene; see Hardie, 1996; Demiccoand et al., 2005], and ~1.5 [a ratio which characterized middle Mississippian, Middle Jurassic and early Paleogene seas; see Hardie, 1996; Demicco et al. 2005]. Decreased $Mg^{2+}/Ca^{2+}$ molar ratios were obtained through lowering $Mg^{2+}$ and increasing $Ca^{2+}$ concentration prepared by mixing natural seawater from the English Channel with artificial $Ca^{2+}$-enriched seawater without $Mg^{2+}$ (prepared by dissolving NaCl, $Na_2SO_4$, $CaCl_2$, KCl, KBr, $SrCl_2$, NaF, $H_3BO_3$, and $NaHCO_3$ (SIGMA) in ultrapure water).

Sea urchins were fed on a diet with different amounts of magnesium: ~0.3 wt% (Zeigler Bros pellets) or ~20 wt% (Zeigler Bros pellets mixed with carrageenan and MgO (SIGMA)). One pellet (~100 mg) per day was introduced to each individual. Mg pellets did not dissolve nor affected the seawater $Mg^{2+}/Ca^{2+}$ ratio, which was confirmed by the chemical analysis of seawater samples (see below). Notwithstanding, even if all the magnesium from the pellet dissolved into the seawater, this would have marginal effect on $Mg^{2+}/Ca^{2+}$sw ratio given the much higher quantity of $Mg^{2+}$ in seawater (~920 mg/L, ~1,100 mg/L, ~1,260 mg/L depending on the treatment) than in a single pellet (~20 mg).

Eighteen specimens (three $Mg^{2+}/Ca^{2+}$ seawater ratios*two diet types*three replicates per treatment) of each species were kept in separate 1 L aquaria for 21 days under constant temperature (~13.7°C for *Psammechinus miliaris*, ~25.5°C for *Prionocidaris baculosa*), salinity (~32.8 psu) and pH (~8.0) in two thermostatic chambers. The specimens were cultured under 12 hr–light/12 hr–dark period. Water parameters were measured three times per day using a WTW Multi 340i multimeter with a conductivity cell and an integrated temperature sensor, and a Metrohm pH-meter (826 pH mobile) equipped with a combined glass electrode Metrohm 6.0228.010. The electrode was daily calibrated with Merck CertiPUR buffer solutions pH 4.00 and 7.00. Measured electromotive force values were converted to total scale following Del Valls and Dickson's (1998) method with TRIS/AMP buffers (provided by the laboratory of Biogéochimie et Modélisation du Système Terre: Océanographie Chimique et Géochimie des Eaux, Université Libre de Bruxelles, Belgium). Seawater in each beaker was renewed every day. $Mg^{2+}$ and $Ca^{2+}$ concentrations of seawater samples taken twice a day (at the beginning of incubation and before seawater replacement) from each aquarium from each treatment were analyzed with inductively coupled plasma-optical emission spectrometry (ICP-OES) at the Bureau Veritas Minerals Laboratory in Canada.

Differences between seawater parameters (temperature, salinity, pH, $Mg^{2+}/Ca^{2+}$ ratio) were assessed using one-way ANOVA and Tukey's HSD test (the latter being a post hoc pairwise comparison test used to identify the means that are significantly different from each other), which confirmed that temperature, salinity and pH, and targeted three levels of $Mg^{2+}/Ca^{2+}$ ratio remained constant throughout the experiment (Table S1 in supplementary files).

### 2.3. Respiration rate

Measurements of respiration rate, considered as a proxy for metabolism (and indirectly of stress), were performed on days 3, 10 and 19 on all 18 specimens of *Psammechinus miliaris* and 15 out of 18 specimens of *Prionocidaris baculosa*. Sea urchins were randomly placed in Plexiglas respiratory chambers (diameter: 5.5 cm) with an optode oxygen sensor (PreSens, Regensburg, Germany), and which were filled with seawater from each respective aquarium. Subsequently, all chambers with urchins and one control chamber filled only with seawater were put on magnetic stirrers in order to mix and homogenize the oxygen content. The oxygen saturation was measured for one hour in five-minute intervals with the aid of Fibox 3 PC-controlled fiber-optic oxygen meter and registered via Fibox 3 software v602 (PreSens). After the measurements, the animals were weighted. The uptake rate was corrected with reference to seawater volume (seawater density calculations based on Millero and Poisson, 1981; Millero and Huang, 2009) and each individual's wet weight.

### 2.4. Termination of the experiment, geochemical analyses, and data handling

After 21 days of incubation, the sea urchins were dissected and dried at 50°C for 48 hr. Selected ossicles (test plates [mostly ambitals], spines, teeth [primary plates], and demipyramids) were cleaned with 2.5% sodium hypochlorite (Merck), rinsed with ultrapure water and air-dried. Standard thin sections from selected ossicles embedded in epoxy resin were prepared through a series of diamond suspensions, and carbon-coated[4]. To detect the presence of the skeletal Mn-enriched tag in thin sections they were observed under cathodoluminescence (CL) microscope at the Institute of Paleobiology of the Polish Academy of Sciences in Warsaw (hot cathode; electron energy 14 keV, beam currents 0.1-0.15 mA, exposure time 7-8 s). Mean

---

[4] Sections of investigated material are housed at the Institute of Paleobiology, Polish Academy of Sciences, Warsaw (ZPALV.42 PhD).

skeletal Mg/Ca ratios in the newly grown stereom for each ossicle type from each individual were determined using CAMECA SX100 electron microprobe at the Micro-Area Analysis Laboratory, Polish Geological Institute – National Research Institute in Warsaw (accelerating voltage 15 kV, beam current 5 nA for calcium, 20 nA for magnesium, beam diameter ~ 5 μm; details in Kołbuk et al. 2019). Growth rate of the skeletal elements was determined from cathodoluminescence photomicrographs (Figure 1) via measurements in the ImageJ software (Abràmoff et al., 2004). Measurements are given only for sufficiently preserved and properly oriented ossicles, such as demipiramids and ambital test plates (in meridional direction only); estimations of extension rates of teeth and spines were not possible commonly due to oblique orientation of the cut surface and loss of the plumula or distalmost tips of spines.

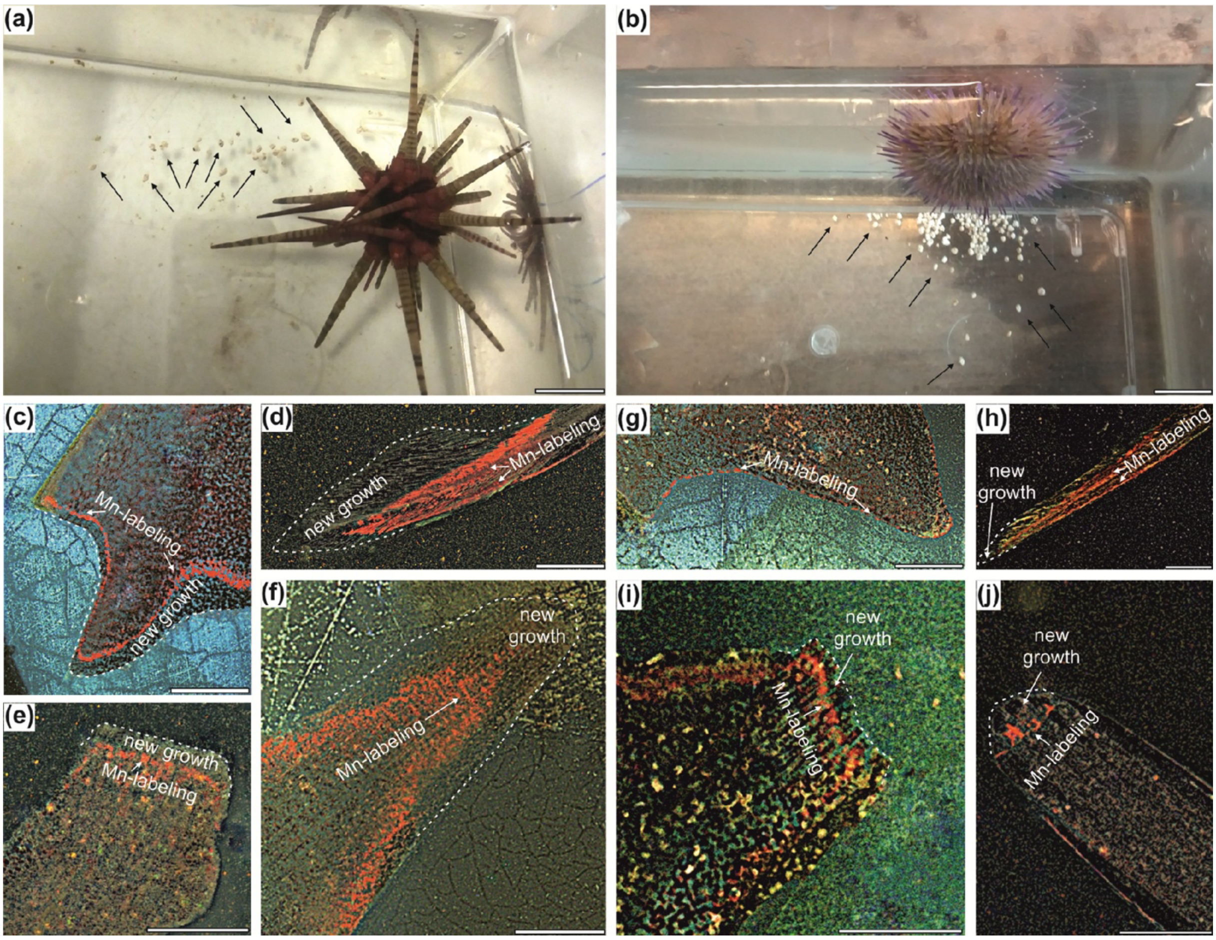

**Figure 1.** Sea urchins (a) *Prinocidaris baculosa* and (b) *Psammechinus miliaris* actively feeding on Mg-enriched pellets and producing large amounts of fecal material (arrows) (scale bar 1 cm). Examples of CL images of polished ossicles of *Prinocidaris baculosa* (c-f) and *Psammechinus miliaris* (g-j) labeled with $Mn^{2+}$ at 1 mg/L: (c) demipyramid, (d) tooth, (e)

ambital test plate, (f) spine, (g) demipyramid with post-tagged growth inhibition, (h) tooth, (i) ambital test plate, (j) spine. Scale bar 500 μm.

Statistical analyses were performed in the Statistica 13 software (TIBCO Software Inc. (2017)). Skeletal Mg/Ca ratios and growth rates were analyzed by two-factor ANOVA, fully crossed design, with seawater $Mg^{2+}/Ca^{2+}$ ratio level and diet type as fixed factors. Repeated measures design was used for test plates because of the additional factor—stereom type. The relationships between skeletal Mg/Ca ratio and $Mg^{2+}/Ca^{2+}$ seawater ratio and growth rate were analyzed with linear regression. Respiration rate as a function of time was analyzed with repeated measures nested ANOVA (with $Mg^{2+}/Ca^{2+}$ and diet as fixed crossed factors, time as repeated crossed factor, and specimen as random factor nested in the interaction term between $Mg^{2+}/Ca^{2+}$ and diet). Analyses were followed by a post hoc Tukey's HSD test. The significance level was fixed at 0.05. The Mg/Ca ratios of echinoid test plates from each treatment were used for the reconstruction of the seawater $Mg^{2+}/Ca^{2+}$ ratios, based on the algorithm provided by Ries (2004): $Mg/Ca_{C} = S(0.000719T + 0.0292)Mg/Ca_{SW}0.668$, where $_{SW}$—seawater, $_{C}$—calcite (skeleton), T—temperature, S—species coefficient (which is defined as "skeletal Mg/Ca ratio of that species in the wild divided by the skeletal Mg/Ca ratio predicted by the algorithm, given the temperature and seawater Mg/Ca ratio (~5.2) in which the wild specimen lived"). In this way species coefficients calculated for the plates (more specifically, galleried stereom) equaled S = 0.122 for *Psammechinus miliaris*, and S = 0.155 for *Prionocidaris baculosa*. The reconstructed seawater $Mg^{2+}/Ca^{2+}$ ratios from echinoid skeletons were compared with the actual seawater $Mg^{2+}/Ca^{2+}$ ratios applied during the experiment to assess the reconstruction error.

### 2.5. Fossil specimens

For comparison, Mg/Ca ratios in several well-preserved fossil echinoid ossicles were determined with the aid of CAMECA SX100 electron microprobe (following the parameters outlined above). These echinoid ossicles came from three museum collections (Faculty of Natural Sciences, University of Silesia in Katowice [GIUS 8-3442]; Institute of Paleobiology, Polish Academy of Sciences, Warsaw [ZPAL E.I]; and Museum of the Earth, Polish Academy of Sciences, Warsaw [MZ VIII Ee]), and were collected from the Middle Jurassic ($Mg^{2+}/Ca^{2+}$sw ~1.5 [calcite sea conditions]) and Miocene ($Mg^{2+}/ Ca^{2+}$sw ~ 3.5 [aragonite sea conditions]). They are not significantly altered by diagenesis as suggested by structural features (presence of stereom trabeculae revealing relicts of growth layering after formic acid etching) and non-luminescent behavior or blotchy dark color in cathodoluminescence (Figure 2), which are identical to those observed in present-day echinoderms (see Gorzelak et al., 2013).

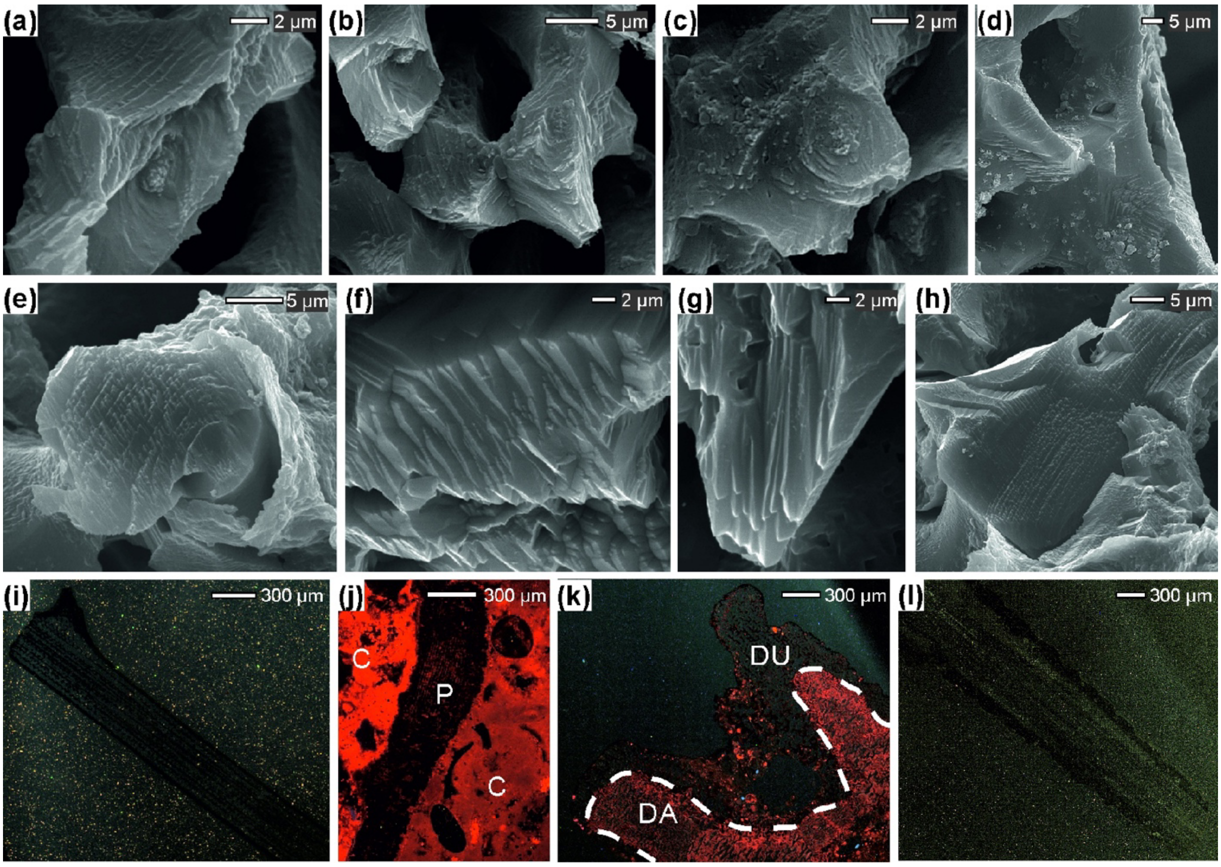

**Figure 2.** Preserved relicts of within-stereom laminated microstructure in fossil specimens observable after slight etching under SEM in (a-c) *Rhabdocidaris* sp. spines (Middle Jurassic (Bathonian), Gnaszyn) [GIUS 8-3442/AK8, AK4, AK7], (d) *Rhabdocidaris* sp. test plate (Middle Jurassic (Bathonian)), [GIUS 8-3442/AP] (e) spatangoid test plate (middle Miocene (Badenian), Korytnica), [MZ VIII Ee-1585], (f) cassiduloid test plate (middle Miocene (Badenian), Korytnica) [MZ VIII Ee-1583], (g) spatangoid spine (middle Miocene (Badenian), Korytnica) [MZ VIII Ee-1584], (h) spatangoid test plate (middle Miocene (Badenian), Korytnica) [MZ VIII Ee-1585]. Examples of CL images showing (i) non-luminescent *Rhabdocidaris* sp. spine (Middle Jurassic (Bathonian), Gnaszyn), [GIUS 8-3442/AK2], (j) Mn-activated intense orange luminescent diagenetic cement (C) and unaltered non-luminescent test plate (P) microregion in *Pygomalus ovalis* (Middle Jurassic (Bathonian), Rudniki), [ZPAL E.I/201], (k) diagenetically unaltered (DU) dark stereom with some Mn-activated orange spots shifting into diagenetically altered (DA) stereom with intense luminescence in the test plate of *Echinocyamus* sp. (middle Miocene (Badenian), Korytnica), [MZ VIII Ee-1580], (l) non-

luminescent *Eucidaris zeamays* spine (middle Miocene (Badenian), Korytnica), [MZ VIII Ee-1578].

The Mg/Ca ratios in these fossil ossicles were further used for the reconstruction of ancient seawater $Mg^{2+}/Ca^{2+}$ ratios employing different algorithms: (a) partition coefficient: $Mg/Ca_C = 0.03182(Mg/Ca_{SW})$ (Dickson, 2004), (b) power partition function: $Mg/Ca_C = 0.0516(Mg/Ca_{SW})^{0.668}$ for test plates and $Mg/Ca_C = 0.0213(Mg/Ca_{SW})^{0.538}$ for spines (Ries, 2004), (c) species-normalized Mg partition algorithm as a function of seawater $Mg^{2+}/Ca^{2+}$ ratio and temperature: $Mg/Ca_C = S(0.000719T + 0.0292)Mg/Ca_{SW}{}^{0.668}$ for test plates and $Mg/Ca_C = S(0.000837T + 0.0155)Mg/Ca_{SW}{}^{0.538}$ for spines (Ries, 2004; where $_{SW}$—seawater, $_C$—calcite (skeleton), T—temperature, S—species coefficient. Temperature data for these calculations were taken from Wierzbowski and Joachimski (2007), and Scheiner et al. (2018) for the Bathonian and Miocene respectively; species coefficients (as defined by Ries, 2004) were calculated from the available literature data on the skeletal Mg/Ca ratios (converted from $\%MgCO_3$, if needed) of extant relatives of the fossil taxa, along with the temperature and the seawater $Mg^{2+}/Ca^{2+}$ ratio (~5.2 mol/mol) in which these recent taxa lived (see Table 4). Skeletal Mg/Ca ratio for the test plates were collected from galleried/rectilinear stereom, except for one specimen, where geochemical data were also collected from the labyrinthic-like/perforate layer.

## 3. Results

No mortality occurred during the experiment. Most sea urchins were actively feeding on provided pellets and produced large amounts of fecal pellets (Figure 1a-b), with the exception of one specimen of *Prionocidaris baculosa* incubated in ~1.5 [mol/mol] seawater $Mg^{2+}/Ca^{2+}$ ratio, which did not eat any pellet throughout the entire experimental period. This specimen was thus excluded from further analyses.

Distinct orange-red luminescent growth fronts overgrown by non-luminescent increments corresponding to a single two-day manganese labeling event and subsequent 21-days of post-tagging period, respectively, were detectable in all types of ossicles (Figure 1c-j) except in some spines of *Prionocidaris baculosa*, which suggests they were not growing during tagging and consequently they were excluded from the geochemical analyses. Likewise, in some ossicles, in particular from the specimens that were incubated under the lowest seawater $Mg^{2+}/Ca^{2+}$ ratio, Mn-label was distributed along the ossicle margin only (e.g., Figure 1g), which indicates that their growth was inhibited during the post-tagging period.

### 3.1. Skeletal Mg/Ca ratio

Skeletal Mg/Ca ratio in both species varied systematically not only between ossicle types (test plates, spines, teeth, and demipyramids) but also between different types of stereom within a single ossicle. There were significant differences between ossicles, more specifically, demipyramids and test plates which usually exhibited higher magnesium concentrations, whereas teeth and in particular spines were depleted in magnesium (Figure 3). The skeletal Mg/Ca in test plates varied according to the stereom type: the galleried and rectilinear stereom typically exhibited higher Mg/Ca ratio than labyrinthic-like stereom or the irregularly perforate coarse stereom layer distributed along the inner test plate margin ($p_{\mathrm{ANOVA}} << .05$ in both species). The differences were also observable at the interspecies level as skeletal elements of *Prionocidaris baculosa* typically displayed higher Mg/Ca ratios than their counterparts in *Psammechinus miliaris* (note, however, that both species were incubated in different temperature conditions).

Echinoids cultured under lower $Mg^{2+}/Ca^{2+}$ seawater ratios exhibited lower mean skeletal Mg/Ca ratios than the controls (Figure 3; Table 1). The effect of seawater $Mg^{2+}/Ca^{2+}$ on skeletal Mg/Ca was significant for spines, demipyramids and teeth in both species ($p_{\mathrm{ANOVA}}$ << .05; Table 1). Interestingly, the ossicles of sea urchins that were fed Mg-enriched pellets tended to have higher skeletal Mg/Ca ratios than the urchins fed on low-Mg (Zeigler) pellets (Figure 3). This effect was observable in spines of *Psammechinus miliaris* ($p_{\mathrm{ANOVA}} = .018$; data for *Prionocidaris baculosa* spines were insufficient; Table 1), although p-values computed by the multiple pairwise comparisons test were usually higher than the alpha significance level ($p_{\mathrm{Tukey}} > .05$; see Figure 3), probably due to a small sample size. Similarly, the diet effect was detected in demipyramids of *Psammechinus* ($p_{\mathrm{ANOVA}} = .0014$) and *Prionocidaris* ($p_{\mathrm{ANOVA}} = .0294$; Table 1), though post hoc comparisons showed a statistically significant difference only in the case of *Psammechinus* incubated under high $Mg^{2+}/Ca^{2+}$sw, where sea urchins, which fed on Mg-enriched diet, displayed higher Mg/Ca ratios than the control group ($p_{\mathrm{Tukey}} = .004$). In the case of teeth, the diet effect was not statistically significant in *Psammechinus* ($p_{\mathrm{ANOVA}} = .19$), but was significant in *Prionocidaris* ($p_{\mathrm{ANOVA}} = .0018$; Table 1, but $p_{\mathrm{Tukey}} > .05$).

The effect of seawater $Mg^{2+}/Ca^{2+}$ ratio was also detected in test plates ($p_{\mathrm{ANOVA}} << .05$; Table 1). The diet effect, however, was only observed in the test plates of *Prionocidaris* ($p_{\mathrm{ANOVA}} = 0.0036$), although multiple comparisons test detected a statistically significant difference between two diet types only in the case of galleried stereom in the test plates of *Prionocidaris* kept under low $Mg^{2+}/Ca^{2+}$ sw ($p_{\mathrm{Tukey}} = .0357$). The diet effect in *Psammechinus* did not reach the significance level ($p_{ANOVA}$ = .0627). The interaction between seawater $Mg^{2+}/Ca^{2+}$ and diet (notwithstanding the ossicle/stereom type in both species) was usually not significant (Table 1).

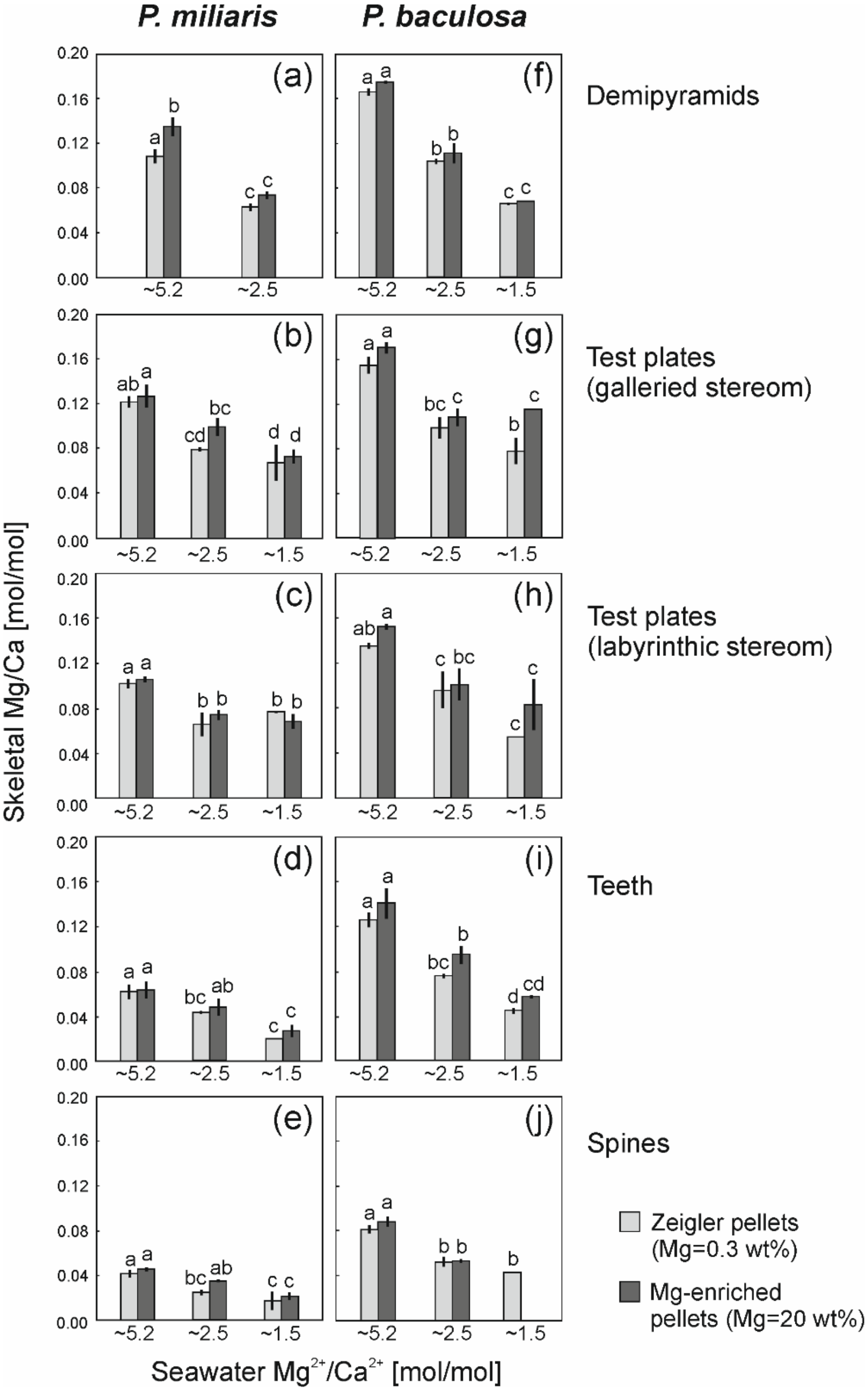

**Figure 3.** Mean skeletal Mg/Ca ratio (± SD) in different ossicles of (a-e) *Psammechinus miliaris* and (f-j) *Prionocidaris baculosa*, cultured under different $Mg^{2+}/ Ca^{2+}$ seawater ratios ($MgCa_{sw;}$ high ~5.2, medium ~2.5, low ~1.5 [mol/mol]). Light gray and dark gray bars represent sea urchins fed on Zeigler and Mg-enriched pellets, respectively. Means sharing the same superscript are not significantly different (p ≥ .05, post hoc Tukey's HSD test.

The relationship between seawater $Mg^{2+}/Ca^{2+}$ and skeletal Mg/ Ca ratio can be described by a linear function. Each ossicle type (or stereom type within the test plates) exhibits a different magnesium fractionation curve. Partition coefficients ($D_C$Mg; calculated as skeletal Mg/Ca divided by seawater $Mg^{2+}/Ca^{2+}$) vary with the ambient $Mg^{2+}/Ca^{2+}$, diet, and ossicle or stereom type. Fractionation curves with linear regression equations and corresponding partition coefficients are presented in Figure 4.

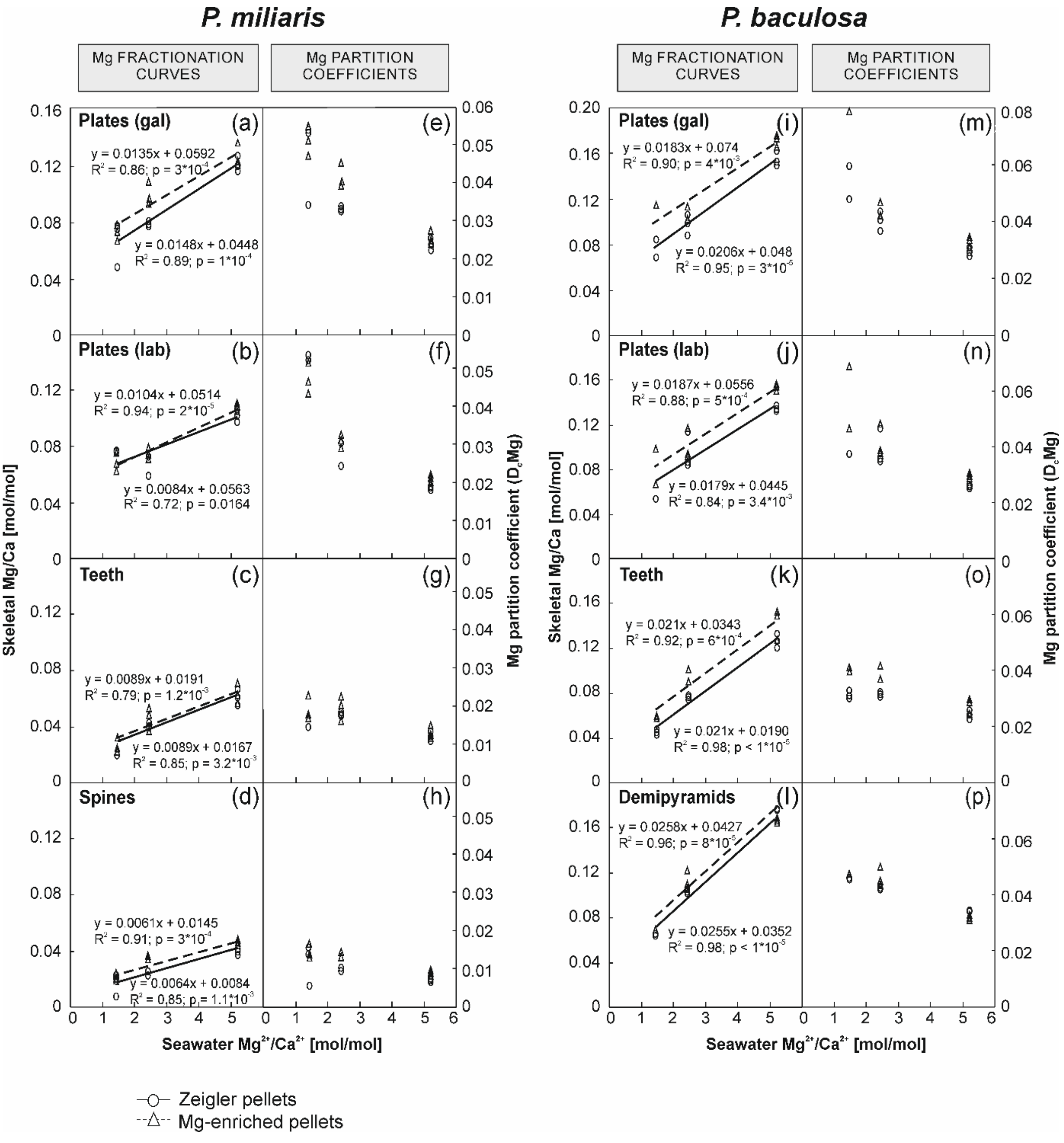

**Figure 4.** Magnesium fractionation curves and partition coefficients for test plates (considering different stereom types), teeth, and spines and/or demipyramids in (a-h) *Psammechinus*

*miliaris* and (i-p) *Prionocidaris baculosa*. Mg partition coefficients (DcMg) were calculated as skeletal Mg/Ca divided by seawater $Mg^{2+}/Ca^{2+}$.

## 3.2. Growth rate

The effect of ambient $Mg^{2+}/Ca^{2+}$ ratio on growth rate is presented in Figure 5. Growth rate of test plates in the meridional direction in both species was reduced or inhibited under lower ambient $Mg^{2+}/ Ca^{2+}$ ratio. The effect of seawater $Mg^{2+}/Ca^{2+}$ ratio was statistically significant both for *Psammechinus miliaris* ($p_{ANOVA}$ = .008, Table 2) and *Prionocidaris baculosa* ($p_{ANOVA}$ = .003). A similar effect was observed in demipyramids which showed decreased growth rates under incubation in low seawater $Mg^{2+}/Ca^{2+}$ ratio ($p_{ANOVA}$ = .0112 in *P. miliaris* and $p_{ANOVA}$ = .0007 in *P. baculosa*; Table 2). Diet and its interaction with $Mg^{2+}/Ca^{2+}$ treatment had no significant effect on the growth rate in any type of ossicle (Table 2).

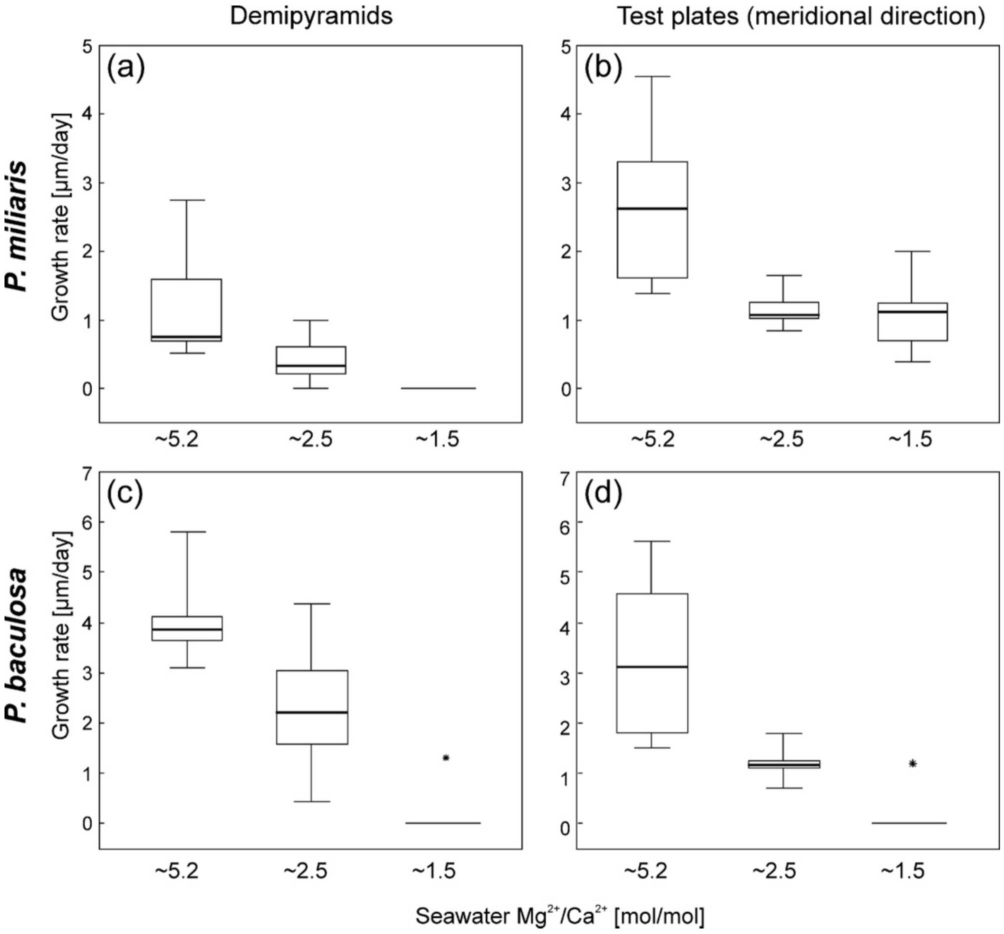

**Figure 5.** Box and whiskers plot on the growth rate of demipyramids and test plates in meridional direction in sea urchins (a-b) *Psammechinus miliaris* and (c-d) *Prionocidaris baculosa*, cultured under different $Mg^{2+}/Ca^{2+}$ seawater ratios ($MgCa_{sw}$; high ~5.2, medium ~2.5, low ~1.5 [mol/mol]). Medians highlighted in bold; bars represent the 25% and 75%

quartiles; whiskers represent the lowest and highest data points. Asterisks in low $Mg^{2+}/Ca^{2+}$ seawater ratio represent single outliers.

### 3.3. Respiration rate

No significant effect of seawater $Mg^{2+}/Ca^{2+}$ ratio on respiration rate of both species was detected. On the other hand, sea urchins feeding on Zeigler pellets exhibited higher respiration rates than those which consumed Mg-enriched pellets (Figure 6; *Psammechinus miliaris*: $p_{ANOVA} = .019$, *Prionocidaris baculosa*: $p_{ANOVA} = .003$); this can be probably attributed to the lower nutritional value of Mg-enriched pellets with high mineral content as compared to algal-rich Zeigler pellets.

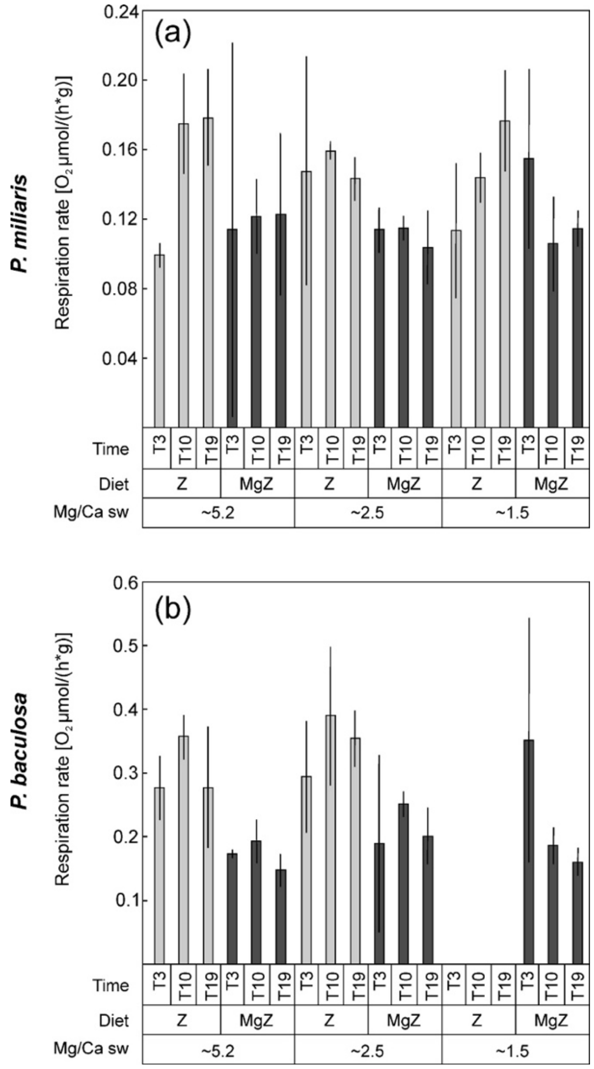

**Figure 6.** Mean respirations rates (± SD) at different time (days: 3, 10, 19), diet (Z—Zeigler pellets, MgZ—Mg-enriched pellets) and ambient $Mg^{2+}/Ca^{2+}$ (MgCa sw; high ~5.2, medium ~2.5, low ~1.5 [mol/mol]) treatments in (a) *Psammechinus miliaris* and (b) *Prionocidaris baculosa.*

3.4. Reconstruction error

For both species, the error in the reconstructed ambient seawater $Mg^{2+}/Ca^{2+}$ ratio induced by magnesium-enriched diet is relatively low for the specimens cultured under control conditions (up to 15.6% for *Prionocidaris baculosa*). However, it is much more pronounced for the specimens incubated under decreased $Mg^{2+}/Ca^{2+}$ ratios (*P. miliaris*: 57.7% and 64.5% in Mg-diet groups vs. 11.1% and 49.8% in Zeigler-diet groups; *P. baculosa*: 23.8% and 59.2% in Mg-diet groups vs. 9.6% and 28.5% in Zeigler-diet groups; (Figure 7; Table 3)).

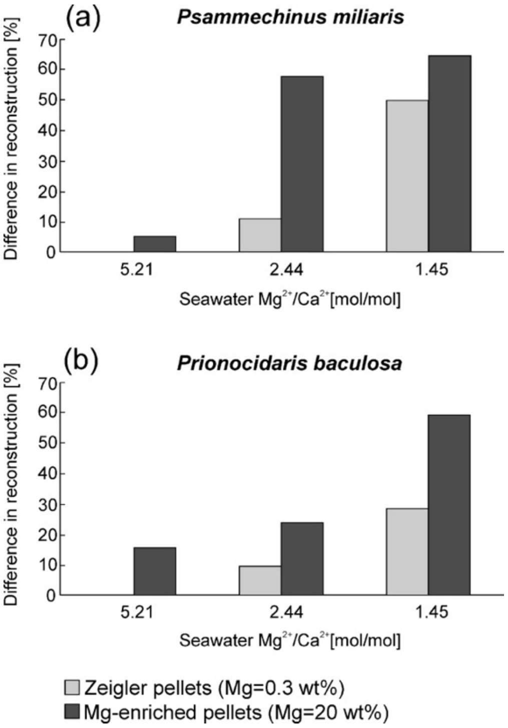

**Figure 7.** Difference in seawater $Mg^{2+}/Ca^{2+}$ reconstruction for different treatments in (a) *Psammechinus miliaris* and (b) *Prionocidaris baculosa*, calculated from skeletal Mg/Ca ratios using Ries' (2004) algorithm for test plates.

3.5. Fossil specimens

Jurassic specimens have much lower Mg/Ca ratios than that displayed by Miocene specimens (Table 4), which is consistent with low $Mg^{2+}/Ca^{2+}$ ratio of the Jurassic “calcite sea” and high $Mg^{2+}/Ca^{2+}$ ratio of the Miocene “aragonite sea”. However, a range of observed variation (intra- and interspecies, and between different ossicles of the same taxon) is very high. Not surprisingly, the calculated paleoceanic $Mg^{2+}/Ca^{2+}$ ratios from these fossil echinoids vary greatly (Table 4).

**Table 1.** Two-way ANOVA results table for skeletal Mg/Ca under factors MgCa_sw (seawater $Mg^{2+}/Ca^{2+}$), diet and their interaction, and additional factor stereom (type of stereom) for test plates. Note: Values statistically significant ($p<0.05$) are marked in bold and with an asterisk. Raw data available in the supplementary files (Table S2). Abbreviations: SS – sum of squares, df – degrees of freedom, MS – mean squares, F – F ratio.

| | | *PSAMMECHINUS* | | | | | *PRIONOCIDARIS* | | | | |
|---|---|---|---|---|---|---|---|---|---|---|---|
| Ossicle | | *SS* | *df* | *MS* | *F* | *p* | *SS* | *df* | *MS* | *F* | *p* |
| Spine | MgCa_sw | 0.001786 | 2 | 0.000893 | 51.0405 | **0.000006*** | 0.002528 | 1 | 0.002528 | 201.8534 | **0.000008*** |
| | Diet | 0.000139 | 1 | 0.000139 | 7.9347 | **0.018259*** | | 0 | | | |
| | MgCa_sw*Diet | 0.000027 | 2 | 0.000014 | 0.7810 | 0.484009 | 0.000022 | 1 | 0.000022 | 1.7374 | 0.235547 |
| | Error | 0.000175 | 10 | 0.000018 | | | 0.000075 | 6 | 0.000013 | | |
| Demipyramid | MgCa_sw | 0.007582 | 1 | 0.007582 | 219.058 | 0.**000002*** | 0.023386 | 2 | 0.011693 | 583.020 | **0.000000*** |
| | Diet | 0.000909 | 1 | 0.000909 | 26.263 | **0.001362*** | 0.000134 | 1 | 0.000134 | 6.692 | **0.029366*** |
| | MgCa_sw*Diet | 0.000168 | 1 | 0.000168 | 4.864 | 0.063221 | 0.000022 | 2 | 0.000011 | 0.541 | 0.599711 |
| | Error | 0.000242 | 7 | 0.000035 | | | 0.000181 | 9 | 0.000020 | | |
| Tooth | MgCa_sw | 0.003145 | 2 | 0.001572 | 46.5178 | **0.000009*** | 0.018734 | 2 | 0.009367 | 179.845 | **0.000000*** |
| | Diet | 0.000067 | 1 | 0.000067 | 1.9724 | 0.190485 | 0.000918 | 1 | 0.000918 | 17.621 | **0.001835*** |
| | MgCa_sw*Diet | 0.000017 | 2 | 0.000008 | 0.2456 | 0.786846 | 0.000029 | 2 | 0.000015 | 0.282 | 0.760133 |
| | Error | 0.000338 | 10 | 0.000034 | | | 0.000521 | 10 | 0.000052 | | |
| Test plate | MgCa_sw | 0.010625 | 2 | 0.005312 | 156.949 | **0.000000*** | 0.021581 | 2 | 0.010791 | 105.913 | **0.000006*** |
| | Diet | 0.000148 | 1 | 0.000148 | 4.387 | 0.062656 | 0.001876 | 1 | 0.001876 | 18.411 | **0.003607*** |
| | MgCa_sw*Diet | 0.000503 | 2 | 0.000252 | 7.436 | **0.010508*** | 0.000836 | 2 | 0.000418 | 4.103 | 0.066201 |
| | Error | 0.000338 | 10 | 0.000034 | | | 0.000713 | 7 | 0.000102 | | |
| | Stereom type | 0.001580 | 1 | 0.001580 | 42.581 | **0.000067*** | 0.001583 | 1 | 0.001583 | 63.050 | **0.000096*** |
| | Stereom type*MgCa_sw | 0.000520 | 2 | 0.000260 | 7.005 | **0.012534*** | 0.000213 | 2 | 0.000106 | 4.238 | 0.062243 |
| | Stereom type*Diet | 0.000061 | 1 | 0.000061 | 1.647 | 0.228371 | 0.000002 | 1 | 0.000002 | 0.076 | 0.790135 |
| | Stereom type*MgCa_sw*Diet | 0.000039 | 2 | 0.000020 | 0.532 | 0.603290 | 0.000149 | 2 | 0.000075 | 2.971 | 0.116374 |
| | Error | 0.000371 | 10 | 0.000037 | | | 0.000176 | 7 | 0.000025 | | |

**Table 2.** Two-way ANOVA results table for growth rate for demipyramids and test plates (meridional direction) under factors MgCa_sw (seawater $Mg^{2+}/Ca^{2+}$), diet and their interaction. Note: Values statistically significant ($p<0.05$) are marked in bold and with an asterisk. Abbreviations: SS – sum of squares, df – degrees of freedom, MS – mean squares, F – F ratio.

| | | *PSAMMECHINUS* | | | | | *PRIONOCIDARIS* | | | | |
|---|---|---|---|---|---|---|---|---|---|---|---|
| Ossicle | | *SS* | *df* | *MS* | *F* | *p* | *SS* | *df* | *MS* | *F* | *p* |
| Demipyramid | MgCa | 4.233368 | 2 | 2.11668 | 6.67552 | **0.011249*** | 39.46664 | 2 | 19.73332 | 15.16470 | **0.000689*** |
| | Diet | 0.011577 | 1 | 0.01157 | 0.03651 | 0.851660 | 0.00625 | 1 | 0.00625 | 0.00481 | 0.945976 |
| | MgCa*Diet | 0.437366 | 2 | 0.21868 | 0.68967 | 0.520568 | 0.92413 | 2 | 0.46206 | 0.35509 | 0.708861 |
| | Error | 3.804978 | 12 | 0.31708 | | | 14.31393 | 11 | 1.30127 | | |
| Test plate (meridional direction) | MgCa_sw | 9.74055 | 2 | 4.8702 | 7.40228 | **0.008051*** | 26.01304 | 2 | 13.00652 | 10.32301 | **0.002992*** |
| | Diet | 0.15432 | 1 | 0.1543 | 0.23455 | 0.636889 | 0.11218 | 1 | 0.11218 | 0.08904 | 0.770965 |
| | MgCa_sw*Diet | 1.49439 | 2 | 0.7472 | 1.13566 | 0.353430 | 1.21653 | 2 | 0.60826 | 0.48277 | 0.629555 |
| | Error | 7.89531 | 12 | 0.6579 | | | 13.85949 | 11 | 1.25995 | | |

**Table 3.** Comparison of $Mg^{2+}/Ca^{2+}$ seawater ratios used in the experiment and $Mg^{2+}/Ca^{2+}$ seawater ratios calculated from skeletal Mg/Ca ratios using Ries' (2004) algorithm for test plates: $Mg/Ca_C = S(0.000719T + 0.0292)Mg/Ca_{SW}^{0.668}$. SW - seawater, C - calcite, T - temperature, S - species coefficient.

| | | Sea urchins fed on Zeigler pellets | | | Sea urchins fed on Mg-enriched pellets | | |
|---|---|---|---|---|---|---|---|
| | Measured $Mg^{2+}/Ca^{2+}{}_{SW}$ ratio [mol/mol] | 5.21 | 2.44 | 1.45 | 5.21 | 2.44 | 1.45 |
| *Psammechinus miliaris* | Calculated $Mg^{2+}/Ca^{2+}{}_{SW}$ ratio [mol/mol] | 5.21 | 2.71 | 2.17 | 5.50 | 3.85 | 2.40 |
| | Error in reconstruction | 0% | 11.1% | 49.8% | 5.4% | 57.7% | 64.5% |
| *Prionocidaris baculosa* | Calculated $Mg^{2+}/Ca^{2+}{}_{SW}$ ratio [mol/mol] | 5.21 | 2.66 | 1.86 | 6.02 | 3.03 | 2.31 |
| | Error in reconstruction | 0% | 9.6% | 28.5% | 15.6% | 23.8% | 59.2% |

**Table 4.** Reconstructed seawater $Mg^{2+}/Ca^{2+}$ ratios for fossil specimens (n=13). $Mg/Ca_C$ data from the test plates were collected from galleried/rectilinear stereom, unless indicated otherwise (* - labyrinthic-like or perforate layer).

| Taxon | Sampling site | Age | Ossicle type | Skeletal Mg/Ca [mol/mol] | Seawater $Mg^{2+}/Ca^{2+}$ [mol/mol] (Dickson, 2004) | Seawater $Mg^{2+}/Ca^{2+}$ [mol/mol] (Ries, 2004) | Seawater $Mg^{2+}/Ca^{2+}$ [mol/mol] including T and S data (Ries, 2004) | Source of data for species coefficient calculation |
|---|---|---|---|---|---|---|---|---|
| *Rhabdocidaris* sp. | Gnaszyn, Poland | Bathonian, Middle Jurassic | spine | 0.0375 | 1.18 | 2.86 | 3.55 | Chave, 1954 |
| *Rhabdocidaris* sp. | Gnaszyn, Poland | Bathonian, Middle Jurassic | spine | 0.0418 | 1.31 | 3.5 | 4.34 | Chave, 1954 |
| *Rhabdocidaris* sp. | Gnaszyn, Poland | Bathonian, Middle Jurassic | spine | 0.0436 | 1.37 | 3.79 | 4.71 | Chave, 1954 |
| *Rhabdocidaris* sp. | Gnaszyn, Poland | Bathonian, Middle Jurassic | plate | 0.0577 | 1.81 | 1.18 | 1.24 | Chave, 1954 |
| *Rhabdocidaris* sp. | Gnaszyn, Poland | Bathonian, Middle Jurassic | plate | 0.0534 | 1.68 | 1.05 | 1.1 | Chave, 1954 |
| *Nucleolites (Echinobrissus) terquemi* | Rudniki, Poland | Bathonian, Middle Jurassic | plate | 0.0604 | 1.9 | 1.27 | -- | no extant relatives |
| *Pygomalus ovalis* | Rudniki, Poland | Bathonian, Middle Jurassic | plate | 0.0779 | 2.45 | 1.85 | -- | no extant relatives |
| *Pygorhytis ringens* | Rudniki, Poland | Bathonian, Middle Jurassic | plate | 0.0662 | 2.08 | 1.45 | -- | no extant relatives |
| *Eucidaris zeamays* | Korytnica, Poland | Miocene, Neogene | spine | 0.0568 | 1.79 | 6.19 | 4.45 | Müller et al., 2017 |

| | | | | | | | | |
|---|---|---|---|---|---|---|---|---|
| Cidaroid | Korytnica, Poland | Miocene, Neogene | plate | 0.1072 | 3.37 | 2.99 | 3.09 | Herein study (wild *P. baculosa*) |
| *Genocidaris (Arbacina) monilis* | Korytnica, Poland | Miocene, Neogene | plate | 0.117 | 3.68 | 3.41 | 3.34 | Weber, 1969 |
| Spatangoid | Korytnica, Poland | Miocene, Neogene | plate | 0.1144 | 3.6 | 3.29 | 1.61 | Weber, 1969 |
| *Echinocyamus* sp. | Korytnica, Poland | Miocene, Neogene | plate | 0.1361 | 4.28 | 4.27 | 3.39 | Richter and Bruckschen, 1998 |
| | | | | *0.1187 | *3.73 | *3.48 | *2.76 | |

## 4. Discussion

Decreased $Mg^{2+}/Ca^{2+}$ ratio in seawater did not appear to affect the respiration rate of sea urchins, which suggests a normal metabolic level and lack of significant stress during the experiment. It did, however, affect their calcification rates. In particular, growth rates of demipyramids and test plates decreased during incubation in low $Mg^{2+}/Ca^{2+}$ seawater ratio. Similar effect was found in aragonite-producing scleractinian corals and bryopsidales algae (Ries et al.; Ries, 2006), which exhibited slower growth rates in the seawater that favors precipitation of low-Mg calcite over aragonite and high-Mg calcite. The latter authors attributed this decrease in the rate of calcification to the difficulties in the production of largely aragonitic skeletons in chemically unfavorable seawater ($Mg^{2+}/Ca^{2+} < 2$). However, magnesium is critically involved in regulation of physiological functions (including biomineralization processes) of all organisms. In echinoderms, magnesium is stabilizing transient amorphous calcium carbonate (e.g., Addadi et al., 2003). A recent experimental study on echinoderm embryos of *Arbacia lixula* showed that development of their skeleton, expression of skeletogenic genes, and production of echinochrome by the pigment cells were all significantly impaired in Mg-deprived seawater (Martino et al., 2019). Another study on this species demonstrated that a lowered $Mg^{2+}/Ca^{2+}$ seawater ratio induced morphological defects of larval spicule and altered its mechanical properties (Lemloh et al., 2013). Decrease in calcification rate and/or growth inhibition reported herein in sea urchins are thus not surprising.

Given that growth rates appeared to be affected by the $Mg^{2+}/ Ca^{2+}$ seawater ratio, one may argue that $Mg^{2+}/Ca^{2+}$ seawater ratio only indirectly controls the skeletal Mg/Ca ratio in echinoids, that is, the observed differences in the skeletal Mg/Ca ratio may be attributed to kinetic factors (i.e., decrease in growth rate due to incubation in low $Mg^{2+}/Ca^{2+}$ seawater ratio). Interestingly, Weber (1973) argued that calcification rate may be an important factor controlling magnesium levels in echinoderms. Subsequent experimental studies, however, demonstrated that skeletal Mg in echinoderms is not clearly related to the growth rate (Borremans et al., 2009; Hermans et al., 2010). Accordingly, our results show that skeletal Mg/Ca ratio rather poorly correlates with their growth rate (Figure F1 in supplementary files). It does, however, correlate well with $Mg^{2+}/Ca^{2+}$ ratio of the ambient seawater (Figure 4). This indicates that the skeletal chemistry in echinoderms is predominantly controlled by seawater chemistry, consistent with previous studies by Ries (2004). Interestingly, however, our results show that sea urchins fed on Mg-enriched diet tend to have higher skeletal Mg/Ca ratios in various types of ossicles (Figure 3), which confirms previous suggestions (Asnaghi et al. 2014; Kołbuk et al. 2019) that seawater may not be the only source of ions in echinoderm biomineralization. The interaction between seawater $Mg^{2+}/Ca^{2+}$ ratio and diet is mostly not significant (Table 1), which suggests that additional sources of magnesium from diet (if available) may be passively incorporated into the skeleton as an impurity. Kołbuk et al. (2019) recently hypothesized that phagocytes and/or spherule-bearing cells may be involved in the transport of dietary magnesium (either in the form of ions or already formed Mg-enriched nanograins) to the skeleton, however, this biomineralization pathway remains to be determined.

The diet effect has potential implications for the use of echinoderms in paleoenvironmental (ancient seawater $Mg^{2+}/Ca^{2+}$ ratio) reconstructions. A number of authors provided Mg partition algorithms, which can be used to calculate (paleo)oceanic $Mg^{2+}/Ca^{2+}$ ratios from unaltered echinoderm skeletons (Dickson, 2004; Ries, 2004; Hasiuk and Lohmann, 2010). However, the accuracy of these algorithms is usually low as they omit some environmental and physiological variables (such as salinity, metabolic processes, and diet) which may influence Mg distribution in echinoderms (Borremans et al., 2009; Kołbuk et al. 2019). For instance, for the specimens fed on magnesium-enriched diet and cultured under low $Mg^{2+}/Ca^{2+}$ ratio (~1.5 mol/mol), the reconstruction error introduced by diet can reach up to 64.5% (Figure 7; Table 3). Admittedly, however, in our experiments, we used pellets with very high magnesium content (~20 wt%), which is usually higher than that in the natural diet of echinoids in the wild. Thus, the potential bias introduced by diet is expected to be lower. However, some coralline algae and scleractinian corals, which constitute an important component of the diet of some sea urchins, can be associated with microbially induced Mg minerals (such as brucite $Mg(OH)_2$ or magnesite $MgCO_3$; see Discussion in Kołbuk et al., 2019). Noteworthy, sea urchins can also actively graze and ingest different types of rock substrates that may be significantly enriched in Mg (Russell et al., 2018).

Another potential problem in the use of algorithms in paleoenvironmental reconstructions is the high range of Mg/Ca variation observed both in the fossil and extant echinoderms (Table 4). Mg/Ca ratio in the stereom of recent echinoderms can differ on a number of organizational levels, starting with the class (e.g., Chave 1954; Weber, 1969; Duquette et al., 2018a). Significant variation is also observable within lower taxonomic ranks, that is, orders and families (Weber, 1969; Smith et al., 2016). Phylogenetically distant species can yield different Mg fractionation curves (Figure 4). Additionally, the ossicles within specimens of the same species also vary in terms of Mg concentration (e.g., Weber, 1973; Smith et al., 2016; Duquette et al., 2018a). Interestingly, magnesium concentrations can vary even within the same ossicle (e.g., Gorzelak et al., 2013). In echinoids, significant differences in magnesium content were observed between dense (septa or cortex) and open stereom within a single spine (Magdans and Gies, 2004; Moureaux et al., 2010; Dery et al., 2018) and teeth (Robach et al., 2006; Stock, 2014). As we demonstrated in this study, within test plates skeletal Mg/Ca ratio was systematically higher in galleried/rectilinear rather than in labyrinthic-like or microperforate inner stereom. The reason behind this within-ossicle systematic variation is unknown. This variation can be hypothetically linked (at least partly) to kinetic factors given the well-known differences in the growth rates between galleried/rectilinear and inner coarse stereom (e.g., Gorzelak et al. 2017) or to the involvement of different type and/or concentration of organic matrix in biomineralization (Hermans et al., 2011). Noteworthy, increased contents of magnesium impurities in calcite biominerals generally enhance their hardness and toughness by increasing sliding resistance of dislocations and the deformation resistance of the crystals (Wang et al. 1997; Ma et al., 2008; Ma et al., 2009), thus elevated contents of Mg within functionally important galleried/rectilinear stereom (that is associated with collagenous fibers joining adjacent test plates) may be desirable. However, the importance of elevated Mg content in the skeletal hardness and toughness in echinoderms has been so far only well established in echinoid tooth (Ma et al., 2008, 2009) and larval skeleton (Lemloh et al., 2013; Kanold et al., 2015).

## 5. Conclusions

Our results show that the skeletal Mg/Ca ratio in echinoids is affected by seawater $Mg^{2+}/Ca^{2+}$ ratio. Under incubation in low ambient $Mg^{2+}/Ca^{2+}$ seawater ratio, sea urchins grow more slowly and produce a skeleton with decreased Mg/Ca ratio. Nonetheless, their skeletal Mg/Ca ratio can be also modified by a specific diet, which suggests that the effect of diet should be considered while reconstructing ancient seawater $Mg^{2+}/Ca^{2+}$ ratio. Magnesium partition coefficients in echinoids vary on different organizational levels (between species, specimens feeding on different types of diet, different ossicle types and even among different types of the stereom within a single ossicle), which additionally complicates the use of a single algorithm in ancient seawater $Mg^{2+}/Ca^{2+}$ reconstructions.

**Acknowledgements.** We thank Thierry Dupont (Université Libre de Bruxelles) for technical support with experimental setup, Andreas Kroh (Natural History Museum, Vienna) for help with identifying fossil specimens and two anonymous reviewers for useful comments. We also thank the Museum of the Earth, Polish Academy of Sciences, Warsaw and Faculty of Natural Sciences, University of Silesia in Katowice for providing the fossil specimens. This research was funded by the National Science Centre (NCN) grant no. 2016/23/B/ST10/00990 and was performed in part in the NanoFun laboratory co-financed by the European Regional Development Fund within the Innovation Economy Operational Programme POIG.02.02.00–00-025/09, and at the Micro-Area Analysis Laboratory, Polish Geological Institute— National Research Institute in Warsaw. Ph. Dubois is a Research Director and S. Di Giglio was holder of a FRIA grant, both of the National Fund for Scientific Research (FRS-FNRS; Belgium). All experiments on live echinoids were performed in Brussels (Belgium), where no ethics approval is required for the maintenance and handling of these species. Nevertheless, our research conformed to the ethical principles of replacement, reduction, refinement and minimization of animal suffering following the guidelines reported in the European Directive 2010/63/EU.

## References

Abràmoff, M. D., Magalhães, P. J., & Ram, S. J. (2004). Image processing with ImageJ. *Biophotonics international*, 11(7), 36-42.

Addadi, L., Raz, S., & Weiner, S. (2003). Taking advantage of disorder: amorphous calcium carbonate and its roles in biomineralization. *Advanced Materials*, 15(12), 959-970.

Alberic, M., Stifler, C. A., Zou, Z., Sun, C. Y., Killian, C. E., Valencia, S., Mawass, M-A., Bertinetti, L., Gilbert, P.U.P.A., & Politi, Y. (2019). Growth and regrowth of adult sea urchin spines involve hydrated and anhydrous amorphous calcium carbonate precursors. *Journal of Structural Biology: X,* 1, 100004.

Asnaghi, V., Mangialajo, L., Gattuso, J. P., Francour, P., Privitera, D., & Chiantore, M. (2014). Effects of ocean acidification and diet on thickness and carbonate elemental composition of the test of juvenile sea urchins. *Marine Environmental Research*, *93*, 78–84.

Borremans, C., Hermans, J., Baillon, S., André, L., & Dubois, P. (2009). Salinity effects on the Mg/Ca and Sr/Ca in starfish skeletons and the echinoderm relevance for paleoenvironmental reconstructions. *Geology*, *37*(4), 351–354.

Chave, K. (1954). Aspects of the biogeochemistry of magnesium. 1- Calcareous marine organisms. *Journal of Geology*, *62*(3), 266–283.

Del Valls, T. A., & Dickson, A. G. (1998). The pH of buffers based on 2-amino-2-hydroxymethyl-1,3-propanediol ('tris') in synthetic sea water. *Deep Sea Research Part I: Oceanographic Research Papers*, *45*(9), 1541–1554.

Demicco, R. V., Lowenstein, T. K., Hardie, L. A., & Spencer, R. J. (2005). Model of seawater composition for the Phanerozoic. *Geology*, 33(11), 877-880.

Dery, A., Tran, P. D., Compère, P., & Dubois, P. (2018). Cidaroids spines facing ocean acidification. *Marine Environmental Research*, *138*, 9–18.

Dickson, J. A. D. (2002). Fossil Echinoderms As Monitor of the Mg/Ca Ratio of Phanerozoic Oceans. *Science*, *298*(5596), 1222–1224.

Dickson, J. A. D. (2004). Echinoderm skeletal preservation: calcite-aragonite seas and the Mg/Ca ratio of Phanerozoic oceans. *Journal of Sedimentary Research*, 74(3), 355-365.

Duquette, A., Halanych, K. M., Angus, R. A., & McClintock, J. B. (2018a). Inter and intraspecific comparisons of the skeletal Mg/Ca ratios of high latitude Antarctic echinoderms. *Antarctic Science*, 30(3), 160-169.

Duquette, A., Vohra, Y. K., McClintock, J. B., & Angus, R. A. (2018b). Near-future temperature reduces Mg/Ca ratios in the major skeletal components of the common subtropical sea urchin *Lytechinus variegatus*. *Journal of Experimental Marine Biology and Ecology*, 509, 1–7.

Gorzelak, P., Dery, A., Dubois, P., & Stolarski, J. (2017). Sea urchin growth dynamics at microstructural length scale revealed by Mn-labeling and cathodoluminescence imaging. *Frontiers in Zoology*, *14*(1), 42.

Gorzelak, P., Stolarski, J., Mazur, M., & Meibom, A. (2013). Micro- to nanostructure and geochemistry of extant crinoidal echinoderm skeletons. *Geobiology*, *11*(1), 29–43.

Hardie, L. A. (1996). Secular variation in seawater chemistry: An explanation for the coupled secular variation in the mineralogies of marine limestones and potash evaporites over the past 600 my. *Geology*, 24(3), 279-283.

Hasiuk, F. J., & Lohmann, K. C. (2010). Application of calcite Mg partitioning functions to the reconstruction of paleocean Mg/Ca. *Geochimica et Cosmochimica Acta*, *74*(23), 6751–6763.

Hermans, J., André, L., Navez, J., Pernet, P., & Dubois, P. (2011). Relative influences of solution composition and presence of intracrystalline proteins on magnesium incorporation in calcium carbonate minerals: Insight into vital effects. *Journal of Geophysical Research: Biogeosciences*, *116*(1), 1–10.

Hermans, J., Borremans, C., Willenz, P., André, L., & Dubois, P. (2010). Temperature, salinity and growth rate dependences of Mg/Ca and Sr/Ca ratios of the skeleton of the sea urchin *Paracentrotus lividus* (Lamarck): An experimental approach. *Marine Biology*, *157*(6), 1293–1300.

Kanold, J. M., Lemloh, M. L., Schwendt, P., Burghard, Z., Baier, J., Herbst, F., Bill, J., Marin, F., & Brümmer, F. (2015). In vivo enrichment of magnesium ions modifies sea urchin spicule properties. *Bioinspired, Biomimetic and Nanobiomaterials*, 4(2), 111-120.

Kołbuk, D., Dubois, P., Stolarski, J., & Gorzelak, P. (2019). Effects of seawater chemistry ($Mg^{2+}$ /$Ca^{2+}$ ratio) and diet on the skeletal Mg/Ca ratio in the common sea urchin *Paracentrotus lividus*. *Marine Environmental Research*.

Lemloh, M.-L., Burghard, Z., Forien, J.-B., Bill, J., & Brümmer, F. (2013). Low Mg/Ca ratio alters material properties in sea urchin larvae skeleton. *Bioinspired, Biomimetic and Nanobiomaterials*, *2*, 28 –34.

Ma, Y., Cohen, S. R., Addadi, L., & Weiner, S. (2008). Sea Urchin Tooth Design: An “All-Calcite” Polycrystalline Reinforced Fiber Composite for Grinding Rocks. *Advanced Materials*, *20*(8), 1555-1559.

Ma, Y., Aichmayer, B., Paris, O., Fratzl, P., Meibom, A., Metzler, R. A., Politi, Y., Addadi, L., Gilbert, P.U.P.A., & Weiner, S. (2009). The grinding tip of the sea urchin tooth exhibits exquisite control over calcite crystal orientation and Mg distribution. Proceedings of the National Academy of Sciences, 106(15), 6048-6053.

Magdans, U., & Gies, H. (2004). Single crystal structure analysis of sea urchin spine calcites: Systematic investigations of the Ca/Mg distribution as a function of habitat of the sea urchin and the sample location in the spine. *European Journal of Mineralogy*, *16*(2), 261–268.

Martino, C., Chiarelli, R., Roccheri, M. C., Matranga, V., & Byrne, M. (2019). Effects of magnesium deprivation on development and biomineralization in the sea urchin *Arbacia lixula*. *Invertebrate Reproduction and Development*, *00*(00), 1–12.

McClintock, J. B., Amsler, M. O., Angus, R. A., Challener, R. C., Schram, J. B., Amsler, C. D., Mah, C. L., Cuce, J., & Baker, B. J. (2011). The Mg-Calcite Composition of Antarctic Echinoderms: Important Implications for Predicting the Impacts of Ocean Acidification. *The Journal of Geology*, 119(5), 457–466.

Millero, F. J., & Huang, F. (2009). The density of seawater as a function of salinity (5 to 70 g kg−1) and temperature (273.15 to 363.15 K). *Ocean Science*, *5*(2), 91–100.

Millero, F. J., & Poisson, A. (1981). International one-atmosphere equation of state of seawater. *Deep Sea Research Part A. Oceanographic Research Papers*, *28*(6), 625–629.

Moureaux, C., Pérez-Huerta, A., Compère, P., Zhu, W., Leloup, T., Cusack, M., & Dubois, P. (2010). Structure, composition and mechanical relations to function in sea urchin spine. *Journal of Structural Biology*, *170*(1), 41–49.

Müller, P., Reymond, C. E., Siegel, P., & Westphal, H. (2017). Paleoenvironmental proxies in echinoid spines (*Eucidaris galapagensis*, Döderlein 1887) along a natural water temperature gradient. *Palaeogeography, palaeoclimatology, palaeoecology*, 484, 70-78.

Raz, S., Hamilton, P. C., Wilt, F. H., Weiner, S., & Addadi, L. (2003). The transient phase of amorphous calcium carbonate in sea urchin larval spicules: the involvement of proteins and magnesium ions in its formation and stabilization. *Advanced Functional Materials*, *13*(6), 480–486.

Richter, D. K., & Bruckschen, P. (1998). Geochemistry of recent tests of *Echinocyamus pusillus*: Constraints for temperature and salinity. *Carbonates and Evaporites*.

Ries, J. B. (2004). Effect of ambient Mg/Ca ratio on Mg fractionation in calcareous marine invertebrates: A record of the oceanic Mg/Ca ratio over the Phanerozoic. *Geology*, *32*(11), 981–984.

Ries, J. B., Stanley, S. M., & Hardie, L. A. (2006). Scleractinian corals produce calcite, and grow more slowly, in artificial Cretaceous seawater. *Geology*, 34(7), 525-528.

Ries, J. B. (2006). Aragonitic algae in calcite seas: effect of seawater Mg/Ca ratio on algal sediment production. *Journal of Sedimentary Research*, 76(3), 515-523.

Robach, J. S., Stock, S. R., & Veis, A. (2006). Mapping of magnesium and of different protein fragments in sea urchin teeth via secondary ion mass spectroscopy. *Journal of Structural Biology*, *155*(1), 87–95.

Russell, M. P., Gibbs, V. K., & Duwan, E. (2018). Bioerosion by pit-forming, temperate-reef sea urchins: History, rates and broader implications. *PloS One*, *13*(2),

Scheiner, F., Holcová, K., Milovský, R., & Kuhnert, H. (2018). Temperature and isotopic composition of seawater in the epicontinental sea (Central Paratethys) during the Middle Miocene Climate Transition based on Mg/Ca, δ18O and δ13C from foraminiferal tests. *Palaeogeography, palaeoclimatology, palaeoecology*, 495, 60-71.

Smith, A. M., Clark, D. E., Lamare, M. D., Winter, D. J., & Byrne, M. (2016). Risk and resilience : variations in magnesium in echinoid skeletal calcite. *Marine Ecology Progress Series*, *561*, 1–16.

Stanley, S. M., & Hardie, L. A. (1998). Secular oscillations in the carbonate mineralogy of reef-building and sediment-producing organisms driven by tectonically forced shifts in seawater chemistry. *Palaeogeography, Palaeoclimatology, Palaeoecology*, 144(1-2), 3-19.

Stock, S. R. (2014). Sea urchins have teeth? A review of their microstructure, biomineralization, development and mechanical properties. *Connective Tissue Research*, *55*(1), 41–51.

TIBCO Statistica(TM) 13.3 (2017). TIBCO Software Inc., USA.

Wang, R. Z., Addadi, L., & Weiner, S. (1997). Design strategies of sea urchin teeth: structure, composition and micromechanical relations to function. *Philosophical Transactions of the Royal Society of London. Series B: Biological Sciences*, 352(1352), 469-480.

Weber, J. N. (1969). The incorporation of magnesium into the skeletal calcites of echinoderms. *American Journal of Science*, *267*(5), 537–566.

Weber, J. N. (1973). Temperature dependence of magnesium in echinoid and asteroid skeletal calcite: a reinterpretation of its significance. *The Journal of Geology*, *81*(5), 543–556.

Wierzbowski, H., & Joachimski, M. (2007). Reconstruction of late Bajocian–Bathonian marine palaeoenvironments using carbon and oxygen isotope ratios of calcareous fossils from the Polish Jura Chain (central Poland). *Palaeogeography, Palaeoclimatology, Palaeoecology*, 254(3-4), 523-540.

Wilkinson, B. H., & Algeo, T. J. (1989). Sedimentary carbonate record of calcium-magnesium cycling. *American Journal of Science*, 289(10), 1158-1194.

SUPPLEMENTARY FILES

**Table S1.** Seawater parameters (means and standard deviations) in beakers during the experiment. Mg/Ca_sw – seawater $Mg^{2+}/Ca^{2+}$ ratio.

| Species | Nominal Mg/Ca_sw [mol/mol] | Measured MgCa_sw [mol/mol] | SD | Temperature [°C] | SD | Salinity [psu] | SD | pH | SD |
|---|---|---|---|---|---|---|---|---|---|
| *Psammechinus miliaris* | 5.2 | 5.2 | 0.07 | 13.6 | 0.38 | 32.7 | 0.26 | 8.04 | 0.06 |
| *Psammechinus miliaris* | 5.2 | 5.2 | 0.08 | 13.6 | 0.44 | 32.7 | 0.24 | 8.04 | 0.05 |
| *Psammechinus miliaris* | 5.2 | 5.22 | 0.09 | 13.6 | 0.42 | 32.7 | 0.28 | 8.03 | 0.06 |
| *Psammechinus miliaris* | 5.2 | 5.22 | 0.07 | 13.8 | 0.29 | 32.6 | 0.16 | 8.04 | 0.07 |
| *Psammechinus miliaris* | 5.2 | 5.21 | 0.07 | 13.8 | 0.27 | 32.6 | 0.16 | 8.05 | 0.07 |
| *Psammechinus miliaris* | 5.2 | 5.22 | 0.07 | 13.8 | 0.31 | 32.6 | 0.19 | 8.05 | 0.07 |
| *Psammechinus miliaris* | 2.5 | 2.43 | 0.04 | 13.6 | 0.35 | 32.7 | 0.25 | 8.03 | 0.05 |
| *Psammechinus miliaris* | 2.5 | 2.43 | 0.04 | 13.7 | 0.36 | 32.7 | 0.25 | 8.02 | 0.05 |
| *Psammechinus miliaris* | 2.5 | 2.44 | 0.04 | 13.7 | 0.37 | 32.7 | 0.25 | 8.02 | 0.06 |
| *Psammechinus miliaris* | 2.5 | 2.45 | 0.04 | 13.8 | 0.29 | 32.7 | 0.18 | 8.04 | 0.07 |
| *Psammechinus miliaris* | 2.5 | 2.45 | 0.04 | 13.8 | 0.31 | 32.7 | 0.20 | 8.04 | 0.07 |
| *Psammechinus miliaris* | 2.5 | 2.44 | 0.04 | 13.8 | 0.26 | 32.7 | 0.18 | 8.05 | 0.07 |
| *Psammechinus miliaris* | 1.5 | 1.45 | 0.02 | 13.6 | 0.50 | 32.8 | 0.30 | 8.04 | 0.06 |
| *Psammechinus miliaris* | 1.5 | 1.45 | 0.02 | 13.6 | 0.50 | 32.8 | 0.26 | 8.03 | 0.06 |
| *Psammechinus miliaris* | 1.5 | 1.45 | 0.02 | 13.6 | 0.47 | 32.8 | 0.24 | 8.03 | 0.06 |
| *Psammechinus miliaris* | 1.5 | 1.45 | 0.02 | 13.8 | 0.38 | 32.7 | 0.19 | 8.04 | 0.06 |
| *Psammechinus miliaris* | 1.5 | 1.46 | 0.03 | 13.8 | 0.39 | 32.7 | 0.19 | 8.05 | 0.06 |
| *Psammechinus miliaris* | 1.5 | 1.46 | 0.03 | 13.8 | 0.39 | 32.7 | 0.16 | 8.05 | 0.06 |
| *Prionocidaris baculosa* | 5.2 | 5.19 | 0.07 | 25.5 | 0.39 | 32.9 | 0.40 | 7.95 | 0.07 |
| *Prionocidaris baculosa* | 5.2 | 5.22 | 0.09 | 25.5 | 0.34 | 32.9 | 0.47 | 7.94 | 0.06 |
| *Prionocidaris baculosa* | 5.2 | 5.22 | 0.08 | 25.5 | 0.35 | 32.9 | 0.45 | 7.96 | 0.07 |
| *Prionocidaris baculosa* | 5.2 | 5.22 | 0.08 | 25.6 | 0.36 | 32.7 | 0.28 | 7.98 | 0.10 |
| *Prionocidaris baculosa* | 5.2 | 5.21 | 0.08 | 25.6 | 0.35 | 32.8 | 0.31 | 7.99 | 0.11 |

| | | | | | | | | | |
|---|---|---|---|---|---|---|---|---|---|
| *Prionocidaris baculosa* | 5.2 | 5.2 | 0.09 | 25.6 | 0.36 | 32.7 | 0.28 | 7.98 | 0.10 |
| *Prionocidaris baculosa* | 2.5 | 2.43 | 0.04 | 25.5 | 0.35 | 32.9 | 0.33 | 7.95 | 0.07 |
| *Prionocidaris baculosa* | 2.5 | 2.42 | 0.04 | 25.4 | 0.39 | 32.9 | 0.49 | 7.96 | 0.07 |
| *Prionocidaris baculosa* | 2.5 | 2.43 | 0.04 | 25.4 | 0.36 | 32.9 | 0.48 | 7.96 | 0.07 |
| *Prionocidaris baculosa* | 2.5 | 2.45 | 0.06 | 25.6 | 0.33 | 32.8 | 0.29 | 7.98 | 0.08 |
| *Prionocidaris baculosa* | 2.5 | 2.45 | 0.06 | 25.5 | 0.36 | 32.9 | 0.48 | 7.99 | 0.10 |
| *Prionocidaris baculosa* | 2.5 | 2.44 | 0.05 | 25.5 | 0.35 | 32.9 | 0.48 | 7.97 | 0.09 |
| *Prionocidaris baculosa* | 1.5 | 1.46 | 0.03 | 25.4 | 0.43 | 33.0 | 0.45 | 7.96 | 0.07 |
| *Prionocidaris baculosa* | 1.5 | 1.46 | 0.03 | 25.5 | 0.36 | 33.0 | 0.44 | 7.95 | 0.06 |
| *Prionocidaris baculosa* | 1.5 | 1.45 | 0.03 | 25.5 | 0.36 | 33.0 | 0.44 | 7.96 | 0.07 |
| *Prionocidaris baculosa* | 1.5 | 1.45 | 0.03 | 25.6 | 0.37 | 32.8 | 0.23 | 7.95 | 0.07 |
| *Prionocidaris baculosa* | 1.5 | 1.45 | 0.02 | 25.5 | 0.36 | 32.8 | 0.28 | 7.95 | 0.07 |
| *Prionocidaris baculosa* | 1.5 | 1.45 | 0.03 | 25.5 | 0.39 | 32.8 | 0.24 | 7.95 | 0.06 |

**Table S2.** Mean skeletal Mg/Ca ratios and growth rates (µm/day) of different types of ossicles in the experimental specimens.

| | | | Mean Mg/Ca ratio [mmol/mol] in ossicles | | | | | Growth rate [µm/day] | |
|---|---|---|---|---|---|---|---|---|---|
| Species | Nominal seawater Mg2+/Ca2+ | Diet | Test plate (galleried stereom) | Test plate (labirynthic stereom) | Teeth (primary plates) | Demipyramids | Spines | Test plates (meridional direction) | Demipyramids |
| *Psammechinus miliaris* | 5.2 | Zeigler | 0.127 | 0.102 | 0.056 | 0.115 | 0.038 | 3.31 | 0.71 |
| *Psammechinus miliaris* | 5.2 | Zeigler | 0.122 | 0.098 | 0.068 | 0.103 | 0.042 | 1.38 | 2.75 |
| *Psammechinus miliaris* | 5.2 | Zeigler | 0.117 | 0.106 | 0.062 | 0.107 | 0.044 | 1.93 | 0.51 |
| *Psammechinus miliaris* | 5.2 | Mg | 0.121 | 0.104 | 0.063 | 0.143 | 0.047 | 3.31 | 1.58 |
| *Psammechinus miliaris* | 5.2 | Mg | 0.123 | 0.106 | 0.057 | 0.127 | 0.044 | 1.62 | 0.78 |
| *Psammechinus miliaris* | 5.2 | Mg | 0.139 | 0.109 | 0.071 | 0.134 | 0.046 | 4.55 | 0.70 |
| *Psammechinus miliaris* | 2.5 | Zeigler | 0.078 | 0.073 | 0.044 | 0.065 | NA | 1.10 | 0.32 |
| *Psammechinus miliaris* | 2.5 | Zeigler | 0.078 | NA | 0.042 | NA | 0.023 | 1.26 | 0.00 |
| *Psammechinus miliaris* | 2.5 | Zeigler | 0.081 | 0.059 | 0.043 | 0.060 | 0.026 | 1.05 | 0.21 |

| | | | | | | | | | |
|---|---|---|---|---|---|---|---|---|---|
| *Psammechinus miliaris* | 2.5 | Mg | 0.109 | 0.070 | 0.039 | 0.070 | NA | 1.02 | 0.32 |
| *Psammechinus miliaris* | 2.5 | Mg | 0.094 | 0.079 | 0.049 | 0.074 | 0.035 | 0.86 | 0.97 |
| *Psammechinus miliaris* | 2.5 | Mg | 0.097 | 0.074 | 0.054 | 0.076 | 0.034 | 1.64 | 0.61 |
| *Psammechinus miliaris* | 1.5 | Zeigler | 0.076 | 0.077 | NA | NA | 0.021 | 2.00 | 0.00 |
| *Psammechinus miliaris* | 1.5 | Zeigler | 0.078 | 0.076 | 0.02 | NA | 0.023 | 1.24 | 0.00 |
| *Psammechinus miliaris* | 1.5 | Zeigler | 0.049 | NA | NA | NA | 0.008 | 0.69 | 0.00 |
| *Psammechinus miliaris* | 1.5 | Mg | 0.067 | 0.067 | 0.024 | NA | 0.019 | 1.14 | 0.00 |
| *Psammechinus miliaris* | 1.5 | Mg | 0.074 | 0.063 | 0.033 | NA | 0.024 | 1.10 | 0.00 |
| *Psammechinus miliaris* | 1.5 | Mg | 0.079 | 0.075 | 0.025 | NA | 0.02 | 0.38 | 0.00 |
| *Prionocidaris baculosa* | 5.2 | Zeigler | 0.164 | 0.138 | 0.133 | 0.169 | 0.086 | 1.50 | 3.10 |
| *Prionocidaris baculosa* | 5.2 | Zeigler | 0.153 | 0.134 | 0.121 | 0.166 | 0.079 | 5.60 | 3.73 |
| *Prionocidaris baculosa* | 5.2 | Zeigler | 0.150 | 0.135 | 0.127 | 0.163 | 0.081 | 3.86 | 5.81 |
| *Prionocidaris baculosa* | 5.2 | Mg | 0.173 | 0.153 | 0.148 | 0.176 | NA | 4.57 | 4.13 |
| *Prionocidaris baculosa* | 5.2 | Mg | 0.175 | 0.155 | 0.126 | 0.175 | 0.092 | 2.38 | 3.65 |
| *Prionocidaris baculosa* | 5.2 | Mg | 0.166 | 0.151 | 0.151 | 0.175 | 0.086 | 1.81 | 4.00 |
| *Prionocidaris baculosa* | 2.5 | Zeigler | 0.089 | 0.086 | 0.076 | 0.102 | 0.054 | 1.81 | 2.79 |
| *Prionocidaris baculosa* | 2.5 | Zeigler | 0.107 | 0.114 | 0.078 | 0.103 | 0.056 | 1.21 | 1.59 |
| *Prionocidaris baculosa* | 2.5 | Zeigler | 0.100 | 0.088 | 0.075 | 0.106 | 0.048 | 1.12 | 1.62 |
| *Prionocidaris baculosa* | 2.5 | Mg | 0.103 | 0.094 | 0.101 | 0.104 | 0.054 | 1.24 | 3.05 |
| *Prionocidaris baculosa* | 2.5 | Mg | 0.114 | 0.092 | NA | 0.121 | NA | 0.69 | 0.43 |
| *Prionocidaris baculosa* | 2.5 | Mg | NA | 0.118 | 0.09 | 0.109 | 0.053 | 1.14 | 4.37 |
| *Prionocidaris baculosa* | 1.5 | Zeigler | 0.086 | 0.054 | 0.047 | 0.066 | NA | 0.00 | 0.00 |
| *Prionocidaris baculosa* | 1.5 | Zeigler | 0.070 | NA | 0.046 | 0.065 | NA | 0.00 | 1.33 |
| *Prionocidaris baculosa* | 1.5 | Zeigler | NA | NA | 0.043 | NA | 0.043 | 0.00 | 0.00 |
| *Prionocidaris baculosa* | 1.5 | Mg | NA | 0.067 | 0.057 | NA | NA | 0.00 | 0.00 |
| *Prionocidaris baculosa* | 1.5 | Mg | 0.116 | 0.099 | 0.058 | 0.068 | NA | 1.19 | 0.00 |

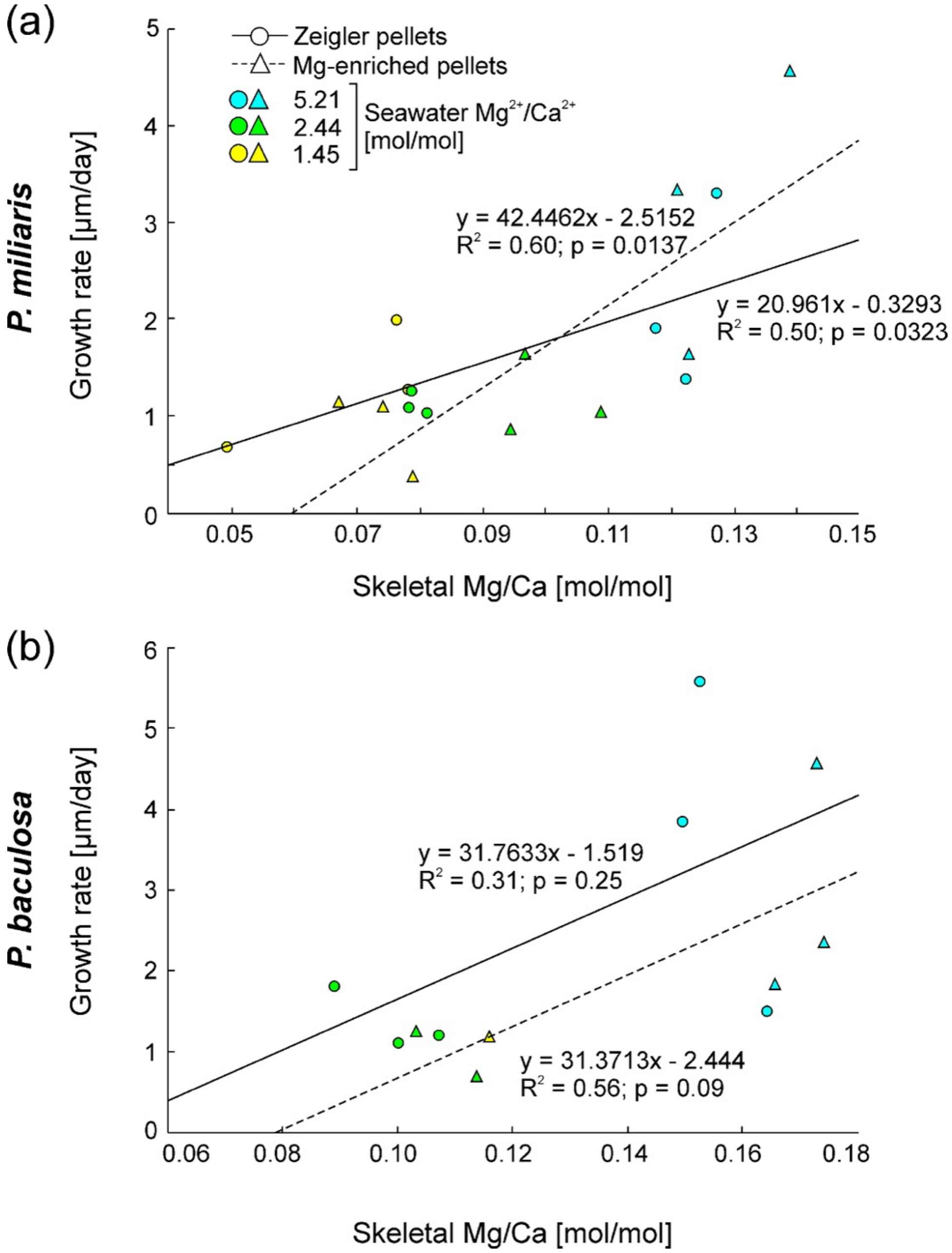

**Figure F1.** Growth rate in the meridional direction according to skeletal Mg/Ca ratio in (a) *Psammechinus miliaris* and (b) *Prionocidaris baculosa*.

# Chapter III

## Impact of seawater $Mg^{2+}/Ca^{2+}$ on Mg/Ca of asterozoan skeleton – evidence from culturing and the fossil record[5]

Dorota Kołbuk[a], Philippe Dubois[b], Jarosław Stolarski[a], Przemysław Gorzelak[a]*

[a] Institute of Paleobiology, Polish Academy of Sciences, Twarda 51/55, PL-00-818 Warsaw, Poland; *pgorzelak@twarda.pan.pl

[b] Université Libre de Bruxelles, Faculté des Sciences, Laboratoire de Biologie Marine, CP 160/15, av. F.D. Roosevelt, 50 B-1050, Bruxelles, Belgium

### Abstract

Skeletal Mg/Ca in echinoderms is thought to be related to ambient seawater $Mg^{2+}/Ca^{2+}$ ratio, which prompts the use of well-preserved fossil echinoderms as paleoseawater $Mg^{2+}/Ca^{2+}$ proxies. Nonetheless, experimental studies testing the effect of seawater $Mg^{2+}/Ca^{2+}$ ratio on echinoderm skeleton are limited to one echinoderm class, i.e., sea urchins (echinoids). Here, we investigated the effect of decreased seawater $Mg^{2+}/Ca^{2+}$ ratio on skeletal composition (Mg/Ca ratio) of a sea star *Asterias rubens* and a brittle star *Ophiocomina nigra*. Specimens were tagged with manganese and then cultured under three different $Mg^{2+}/Ca^{2+}$ molar ratios (~5.2, ~2.5, ~1.5 mol/mol) in order to simulate variations of ambient seawater $Mg^{2+}/Ca^{2+}$ ratio that existed throughout the Phanerozoic. Decreased $Mg^{2+}/Ca^{2+}$ in seawater did not affect the respiration rates or inhibit calcification of sea stars, which suggests that they were not significantly stressed by the treatment. It did, however, clearly affect growth and mortality in brittle stars, for which reliable geochemical data could not be obtained. Under decreased seawater $Mg^{2+}/Ca^{2+}$ sea stars produced a skeleton with decreased Mg/Ca ratio. This is consistent with the hypothesis that the skeletal chemistry in echinoderms is influenced by seawater chemistry and, consequently, that fossil echinoderms may preserve a record of paleoseawater $Mg^{2+}/Ca^{2+}$. Although our data from well-preserved fossil sea stars from the Middle Jurassic and Miocene are consistent with low $Mg^{2+}/Ca^{2+}$ ratio of the Jurassic "calcite sea" and high $Mg^{2+}/Ca^{2+}$ ratio of the Miocene "aragonite

---

[5] Postprint version of an article: Kołbuk, D., Dubois, P., Stolarski, J., & Gorzelak, P. (2021). Impact of seawater $Mg^{2+}/Ca^{2+}$ on Mg/Ca of asterozoan skeleton–Evidence from culturing and the fossil record. *Chemical Geology*, 120557, doi: 10.1016/j.chemgeo.2021.120557

sea”, the accuracy of paleoseawater $Mg^{2+}/Ca^{2+}$ reconstructions from fossil echinoderms is limited by the fact that Mg partition coefficients vary significantly between different echinoderm species.

**Keywords**

Echinoderms, biomineralization, magnesium, culturing, seawater $Mg^{2+}/Ca^{2+}$

## 1. Introduction

To date, studies investigating the effect of seawater $Mg^{2+}/Ca^{2+}$ on the skeletal Mg/Ca in echinoderms focused on sea urchins. It has been experimentally shown that under lowered $Mg^{2+}/Ca^{2+}$ ratio certain species of echinoids (including cidaroids: *Eucidaris tribuloides, Prionocidaris baculosa,* and euechinoids: *Paracentrotus lividus, Psammechinus miliaris*) produce skeleton with decreased Mg/Ca ratio (Ries, 2004; Kołbuk et al., 2019, 2020). Accordingly, it has been suggested that Mg/Ca ratio in well-preserved fossil echinoderms constitutes a reliable proxy for the seawater composition ($Mg^{2+}/Ca^{2+}$ ratio) in the Phanerozoic era (Dickson, 2002, 2004; Ries, 2004; Hasiuk and Lohmann, 2010). However, experimental studies on some sea urchins showed that magnesium in their skeletons can also originate from diet (Asnaghi et al., 2014; Kołbuk et al., 2019, 2020), imposing constraints on the application of fossil echinoderms as a reliable paleoseawater $Mg^{2+}/Ca^{2+}$ proxy. Furthermore, the skeletal Mg/Ca ratio in echinoderms can be also affected by temperature, salinity (Chave, 1954; Weber, 1969, 1973; Borremans et al., 2009; Hermans et al., 2010) and physiological (vital) effects (Hermans et al., 2011).

Asterozoans, i.e., a clade comprising asteroids (sea stars or starfish) and ophiuroids (brittle stars), have been more extensively studied in the context of their remarkable regeneration abilities (e.g., Dubois and Jangoux, 1990; Sköld and Rosenberg, 1996; Ben Khadra et al., 2015; 2018 and literature cited therein; Czarkwiani et al., 2016) rather than their skeletal chemistry. Some notable exceptions include field-collected specimens studied by Clarke and Wheeler (1922), who examined $MgCO_3$ content in 29 asteroid and 16 ophiuroid species from different latitudes. These authors observed a correlation between seawater temperature and skeletal magnesium content in their skeletons. Chave (1954) examined Mg concentration in a few more asterozoan specimens (9 asteroids and 6 ophiuroids from different or unidentified species) from various locations and confirmed a temperature–magnesium level dependency in their skeletons. Weber (1969, 1973) further explored the effect of environmental control (temperature) and physiological factors on skeletal composition of echinoderms on different levels: taxonomic (from class to species), within and between populations, and within single individuals. These studies showed that, compared to echinoids, within-population and within-individual variations in asterozoans are small or insignificant. However, higher taxonomic levels, including genera and orders, show considerable variation with respect to skeletal magnesium concentration. In recent years, a few field studies enabled to better document the chemical composition of asterozoans from various locations (e.g., McClintock et al., 2011; Lebrato et al., 2016; Iglikowska et al., 2017; Duquette et al., 2018), which showed that even under similar environmental conditions, skeletal magnesium concentration can vary strongly between species. Overall, these findings suggest that echinoderms can, at least to some degree, exert control over Mg incorporation.

Surprisingly few experimental studies analysed skeletal chemistry and growth dynamics of asterozoans under varying environmental conditions other than ocean acidification (the effect of the ocean acidification was tested e.g., by Gooding et al., 2009 and Wood et al., 2010). For instance, Borremans et al. (2009) detected a salinity effect on skeletal Mg/Ca and Sr/Ca ratios in the sea star *Asterias rubens*. Donachy and Watabe (1986) found that decreasing calcium concentration and salinity reduced regeneration rate in brittle star *Ophiotrix angulata.*

The effect of lowered ambient $Mg^{2+}/Ca^{2+}$ ratio on skeletal chemistry (Mg/Ca ratio) has not been tested so far on the asterozoan skeleton. Thus, the main goal of this study was to investigate the effect of decreased seawater $Mg^{2+}/Ca^{2+}$ ratio on the chemical composition (Mg/Ca ratio) of starfish *Asterias rubens* and brittle star *Ophiocomina nigra.* Furthermore, skeletal Mg/Ca ratios obtained from both extant and well-preserved fossil asteroids were compared to existing data on echinoids in order to determine whether phylogenetically distant echinoderm species should be treated as equally reliable proxies of ancient seawater $Mg^{2+}/Ca^{2+}$ ratio.

## 2. Methods

### 2.1. Collection and handling of animals

Adult sea stars *Asterias rubens* (mean arm length: 41.9 mm ± 5 SD) (Figure 1A) and brittle stars *Ophiocomina nigra* (mean disc diameter: 13.3 mm ± 0.9 SD) (Figure 2A) were collected from the North Sea (Belgian coast) and obtained from Roscoff Marine Station (France), respectively, and transported to Laboratoire de Biologie Marine (Université Libre de Bruxelles, Belgium).

Firstly, the specimens were labeled with manganese. Despite being widely used in biomineralization studies (e.g., Hawkes et al., 1996; Barbin et al., 2008; Lartaud et al., 2010), manganese only recently gained attention as a reliable labeling tool for echinoderms (Gorzelak et al., 2017; Kołbuk et al., 2020). Nonetheless, its efficiency in tagging asterozoan skeletons has not yet been determined. A low concentration of manganese (3 mg/L) was used so as not to disturb the motoric behaviour (which was previously observed at a much higher Mn concentration, i.e., 12 mg/L; Sköld et al., 2015). The solution was prepared by mixing seawater with dissolved $MnCl_2*4H_2O$ (Sigma-Aldrich). Specimens of both species were cultured in the marking solution in separate 1 L beakers for the next 24 h.

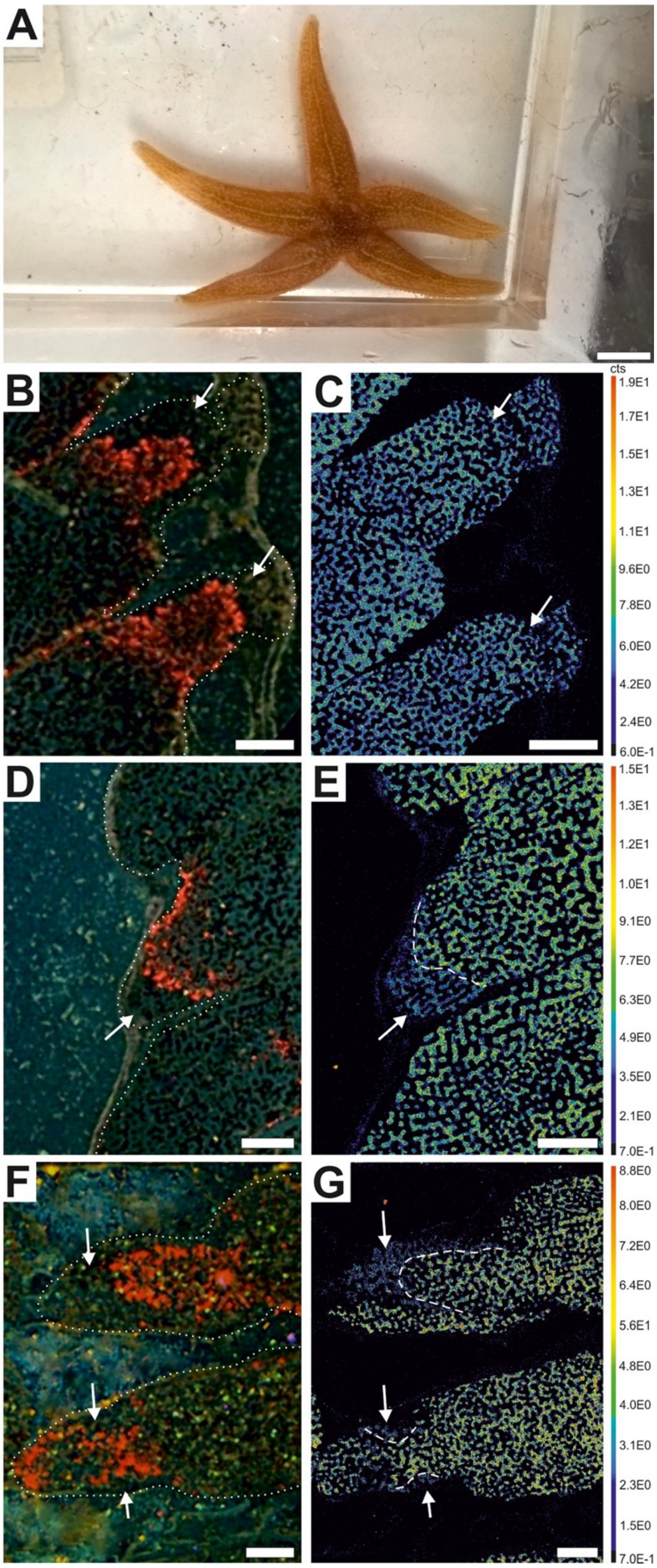

**Figure 1.** (A) Sea star *Asterias rubens* in a beaker. Scale bar 1 cm. (B, D, F) CL images (fine dotted lines delineate ossicle margins) and (C, E, G; dashed lines delineate sharp contrast in Mg content) WDS maps of Mg distribution in polished and carbon-coated *A. rubens* ossicles. Specimens were labeled with $Mn^{2+}$ and kept under three $Mg^{2+}/Ca^{2+}_{SW}$ ratios: (B-C) ~5.2

mol/mol (control group), (D-E) ~2.5 mol/mol, (F-G) ~1.5 mol/mol. White arrows indicate newly grown skeleton. Scale bar 100 μm.

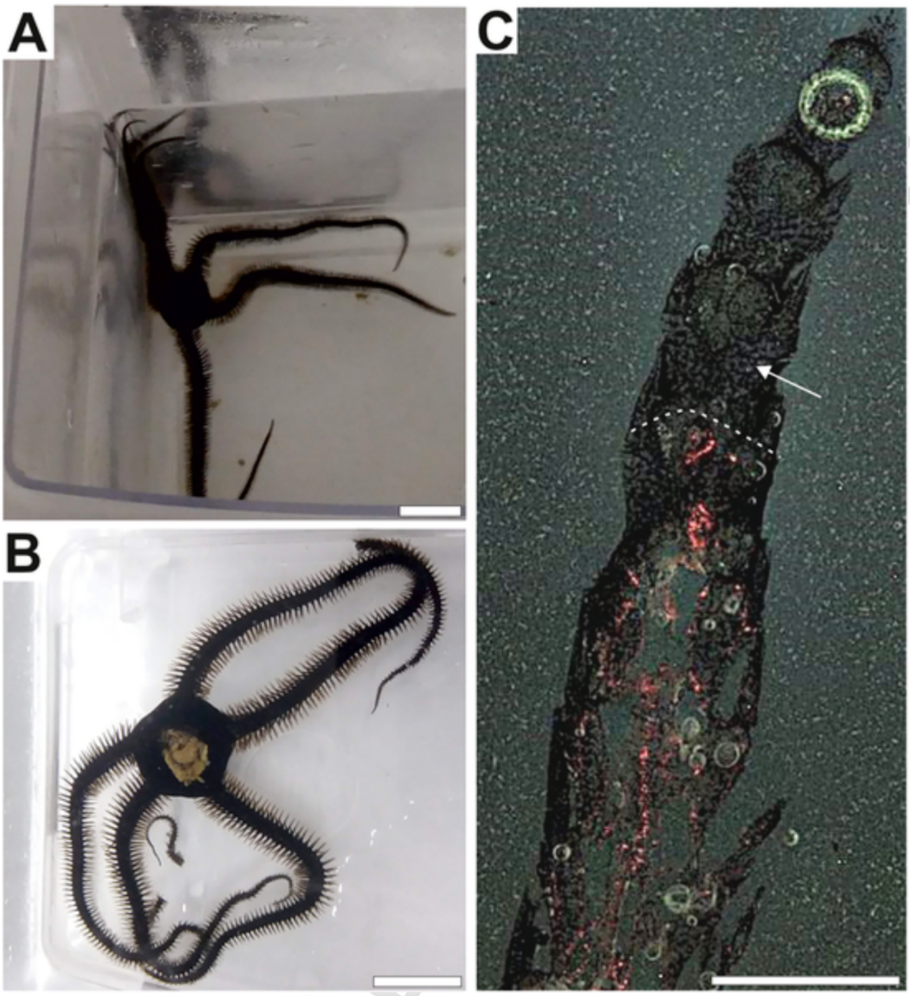

**Figure 2.** (A) Brittle star *Ophiocomina nigra* in beaker. Scale bar 1 cm. (B) Autotomized arms and central disc perforation in O. nigra cultured under lowest (~1.5 mol/ mol) $Mg^{2+}$/ $Ca^{2+}_{SW}$ ratio. Scale bar 1 cm. (C) CL image of *O. nigra* arm with traces of $Mn^{2+}$-activated luminescence (red-orange spots). White arrow indicates zone of newly grown skeleton (between the dotted line and tip of the arm). Scale bar 0.5 mm.

2.2. Experimental setup

After the labeling, 18 specimens of each species were randomly allocated to separate 1 L beakers with three different $Mg^{2+}/Ca^{2+}$ ratios [mol/mol]: ~5.2, ~2.5, and ~1.5 (6 specimens of each species per treatment), with molar sums of $Mg^{2+}$and $Ca^{2+}$ held constant. Both $Mg^{2+}$ and $Ca^{2+}$ concentrations are considered to have concomitantly changed during the Phanerozoic (e.g., Wilkinson and Algeo, 1989), therefore decreased $Mg^{2+}/Ca^{2+}$ molar ratios were obtained through lowering $Mg^{2+}$ and increasing $Ca^{2+}$ concentration (see Higuchi et al., 2017). Natural seawater from the English Channel was mixed with artificial $Ca^{2+}$-enriched seawater without $Mg^{2+}$ (prepared by dissolving NaCl, $Na_2SO_4$, $CaCl_2$, KCl, KBr, $SrCl_2$, NaF, $H_3BO_3$, and $NaHCO_3$ (Sigma-Aldrich) in ultrapure water). Individuals were kept under experimental conditions for 21 days, except for 6 brittle stars cultured under the lowest $Mg^{2+}/Ca^{2+}$, which died during the first week of the experiment.

Specimens (18 sea stars and 12 brittle stars) were kept under constant temperature (~17.8 °C), salinity (~32.9 psu), pH (~8), and $Mg^{2+}/Ca^{2+}$ molar ratios (~5.2, ~2.5, ~1.5 [mol/mol]; Table 1) in separate 1L aerated beakers. Seawater parameters (T, salinity, pH) were checked three times a day with a WTW Multi 340i multimeter, equipped with a conductivity cell and an integrated temperature sensor, and a Metrohm pH-meter (826 pH mobile) equipped with a combined glass electrode Metrohm 6.0228.010. The pH electrode was calibrated every day with Merck CertiPUR buffer solutions pH 4.00 and 7.00. All pH measurements were converted to total scale using standard buffers TRIS/AMP method (Del Valls and Dickson, 1998). Seawater in each beaker was renewed every day. Seawater samples (50 ml from each beaker; filtered through 0.45 µm membrane filters and stabilized with nitric acid) were collected every day and $Mg^{2+}$ and $Ca^{2+}$ concentrations in each sample were analysed with inductively coupled plasma-optical emission spectrometry (Thermo Scientific iCAP 6500 Duo ICP-OES spectrometer; detection limits for Mg and Ca: 0.1 mg/l) at the Central Chemical Laboratory of the Polish Geological Institute–National Research Institute (Warsaw). Stability of parameters (temperature, salinity, pH, and three levels of $Mg^{2+}/Ca^{2+}$) was additionally verified with one-way ANOVA and post-hoc Tukey's HSD tests (Table 1).

**Table 1.** Seawater parameters (means and standard deviations) in each beaker during the entire experiment (t = 21 days). Temperature, salinity and pH within individual beakers were not significantly different from each other ($p_{Tukey} > 0.05$). Three different Mg/Ca_sw (seawater $Mg^{2+}/Ca^{2+}$ ratio) levels were constant throughout the experiment ($p_{Tukey} > 0.05$)

| Species | Nominal Mg/Ca_sw [mol/mol] | Mg/Ca_sw [mol/mol] | SD | Temperature [°C] | SD | Salinity [psu] | SD | pH | SD |
|---|---|---|---|---|---|---|---|---|---|
| *Asterias rubens* | 5.2 | 5.15 | 0.02 | 17.7 | 0.45 | 32.9 | 0.33 | 8.1 | 0.08 |
| *Asterias rubens* | 5.2 | 5.16 | 0.02 | 17.7 | 0.45 | 32.9 | 0.31 | 8.1 | 0.08 |

| | | | | | | | | | |
|---|---|---|---|---|---|---|---|---|---|
| *Asterias rubens* | 5.2 | 5.15 | 0.02 | 17.7 | 0.45 | 32.9 | 0.29 | 8.1 | 0.09 |
| *Asterias rubens* | 5.2 | 5.16 | 0.02 | 17.7 | 0.43 | 32.9 | 0.28 | 8.1 | 0.09 |
| *Asterias rubens* | 5.2 | 5.16 | 0.02 | 17.7 | 0.46 | 32.9 | 0.28 | 8.1 | 0.08 |
| *Asterias rubens* | 5.2 | 5.15 | 0.02 | 17.7 | 0.45 | 32.9 | 0.31 | 8.1 | 0.09 |
| *Asterias rubens* | 2.5 | 2.44 | 0.02 | 17.8 | 0.49 | 32.9 | 0.32 | 8.0 | 0.08 |
| *Asterias rubens* | 2.5 | 2.44 | 0.02 | 17.8 | 0.47 | 32.9 | 0.27 | 8.1 | 0.08 |
| *Asterias rubens* | 2.5 | 2.44 | 0.02 | 17.8 | 0.48 | 32.9 | 0.29 | 8.1 | 0.08 |
| *Asterias rubens* | 2.5 | 2.44 | 0.02 | 17.8 | 0.47 | 32.9 | 0.29 | 8.1 | 0.08 |
| *Asterias rubens* | 2.5 | 2.44 | 0.02 | 17.8 | 0.50 | 32.9 | 0.29 | 8.1 | 0.08 |
| *Asterias rubens* | 2.5 | 2.44 | 0.01 | 17.8 | 0.48 | 32.9 | 0.29 | 8.1 | 0.08 |
| *Asterias rubens* | 1.5 | 1.44 | 0.01 | 17.8 | 0.50 | 32.9 | 0.29 | 8.0 | 0.07 |
| *Asterias rubens* | 1.5 | 1.44 | 0.01 | 17.9 | 0.48 | 32.9 | 0.25 | 8.0 | 0.07 |
| *Asterias rubens* | 1.5 | 1.44 | 0.01 | 17.9 | 0.49 | 32.9 | 0.25 | 8.0 | 0.07 |
| *Asterias rubens* | 1.5 | 1.44 | 0.01 | 17.9 | 0.49 | 32.9 | 0.24 | 8.0 | 0.07 |
| *Asterias rubens* | 1.5 | 1.44 | 0.01 | 17.9 | 0.50 | 32.8 | 0.24 | 8.0 | 0.07 |
| *Asterias rubens* | 1.5 | 1.44 | 0.01 | 17.9 | 0.48 | 32.9 | 0.27 | 8.0 | 0.07 |
| *Ophiocomina nigra* | 5.2 | 5.16 | 0.02 | 17.8 | 0.32 | 32.8 | 0.24 | 8.0 | 0.08 |
| *Ophiocomina nigra* | 5.2 | 5.16 | 0.02 | 17.8 | 0.32 | 32.8 | 0.25 | 8.0 | 0.08 |
| *Ophiocomina nigra* | 5.2 | 5.16 | 0.03 | 17.8 | 0.34 | 32.8 | 0.24 | 8.0 | 0.08 |
| *Ophiocomina nigra* | 5.2 | 5.16 | 0.02 | 17.8 | 0.32 | 32.8 | 0.23 | 8.0 | 0.08 |
| *Ophiocomina nigra* | 5.2 | 5.15 | 0.06 | 17.8 | 0.33 | 32.8 | 0.24 | 8.0 | 0.08 |
| *Ophiocomina nigra* | 5.2 | 5.17 | 0.03 | 17.8 | 0.33 | 32.8 | 0.24 | 8.0 | 0.08 |
| *Ophiocomina nigra* | 2.5 | 2.45 | 0.01 | 17.8 | 0.41 | 32.8 | 0.23 | 8.0 | 0.07 |
| *Ophiocomina nigra* | 2.5 | 2.45 | 0.02 | 17.8 | 0.42 | 32.8 | 0.23 | 8.0 | 0.07 |

| | | | | | | | | | |
|---|---|---|---|---|---|---|---|---|---|
| *Ophiocomina nigra* | 2.5 | 2.45 | 0.01 | 17.8 | 0.40 | 32.8 | 0.22 | 8.0 | 0.07 |
| *Ophiocomina nigra* | 2.5 | 2.45 | 0.01 | 17.8 | 0.44 | 32.8 | 0.23 | 8.0 | 0.08 |
| *Ophiocomina nigra* | 2.5 | 2.45 | 0.02 | 17.8 | 0.42 | 32.8 | 0.24 | 8.0 | 0.08 |
| *Ophiocomina nigra* | 2.5 | 2.45 | 0.01 | 17.8 | 0.41 | 32.8 | 0.23 | 8.0 | 0.08 |

### 2.3. Respiration rate

Brittle stars appeared to be more stress-sensitive than sea stars. Thus, the measurements of respiration rate were not attempted on *Ophiocomina nigra* due to high mortality observed during culturing under the lowest $Mg^{2+}/Ca^{2+}$ treatment. Respiration measurements were carried out on 7 random individuals of *Asterias rubens* after 7, 14 and 21 days of exposure in order to examine their metabolic response to potentially stressful conditions. Sea stars were placed in Plexiglas respiratory chambers (diameter: 5.5 cm) with an optode oxygen sensor (PreSens, Regensburg, Germany), which were filled with seawater from their respective beaker. Chambers were placed on magnetic stirring units in order to homogenize the oxygen content. Oxygen saturation was measured every five minutes for one hour with a Fibox 3 PC-controlled fiber-optic oxygen meter and registered via Fibox 3 software v602 (PreSens). After the measurements, the animals were wet weighted. The oxygen uptake rate was calculated using the slope of the linear regression of seawater oxygen concentration over time. Calculated value was corrected by seawater volume (based on the seawater density calculations by Millero and Poisson, 1981; Millero and Huang, 2009) and divided by the wet weight of the animal. The respiration rate was expressed in μmol of $O_2$ per hour and grams of wet weight.

### 2.4. Termination of the experiment, geochemical analysis, data handling

After 21 days of experiment, specimens were dissected and dried at 50°C for 48 h. Arms of *A. rubens* and *O. nigra* were selected and fixed and dehydrated in graded ethanol series (70% for 3 hours, 90% for 1 hour and 100% for 1 hour). Standard thin sections from the biological material embedded in epoxy resin were prepared through a series of diamond suspensions and carbon-coated[6].

---

[6] Sections of investigated material are housed at the Institute of Paleobiology, Polish Academy of Sciences, Warsaw (ZPALV.42 PhD).

Microscopic observations were performed at the Institute of Paleobiology of the Polish Academy of Sciences in Warsaw. To detect the presence of manganese labeling, thin sections were observed under Lumic HC5-LM cathodoluminescence (CL) microscope (hot cathode; electron energy 14 keV, beam currents 0.1-0.15 mA, exposure time 5-8 s).

Spot geochemical analyses on newly grown parts of the skeleton in each individual were conducted using CAMECA SX100 electron microprobe at the Micro-Area Analysis Laboratory, Polish Geological Institute – National Research Institute in Warsaw (accelerating voltage 15 kV, beam current 5 nA for calcium, 20 nA for magnesium, beam diameter ~5 μm, standard used: „NIST", serial number: 12570). Mean Mg/Ca ratios in the newly grown stereom for sea stars were determined from spot measurements in proximal adambulacrals, and the most distal parts of the arms (Figure 1). Selected thin sections were additionally imaged with CAMECA SX100 electron microprobe in order to obtain WDS maps of Mg distribution. Few spot analyses were also performed on the stereom grown before the experiment (the manganese labeling demarcated the pre-experimental growth and the growth during culturing). Brittle stars, cultured under control (~5.2 mol/mol) and decreased (~2.5 mol/mol) $Mg^{2+}/Ca^{2+}$ ratios, were examined for Mg/Ca ratio through spot measurements in the most distal arm vertebrae.

Skeletal Mg/Ca ratio in *Asterias rubens* (n = 14) was analysed through one-way ANOVA with seawater $Mg^{2+}/Ca^{2+}$ ratio level as a fixed factor. Remaining sea stars (n = 4), which displayed no post-tagging growth, were not considered in the statistical analysis. Due to limited growth (Figure 2) and therefore lack of reliable data, brittle stars (n = 12) were also not analysed statistically. Respiration rate in *A. rubens* as a function of time was analysed with repeated measures nested ANOVA (specimen, random factor, nested into $Mg^{2+}/Ca^{2+}$, fixed factor, and time, repeated factor). Analyses were performed in the Statistica software, with significance level set to 0.05.

In order to estimate the reconstruction error, we compared the actual seawater $Mg^{2+}/Ca^{2+}$ ratios used in the experiment with seawater $Mg^{2+}/Ca^{2+}$ values calculated with an algorithm based on echinoderm skeletal Mg/Ca ratio. To do so, we inserted the experimentally obtained values of skeletal Mg/Ca ratios in *Asterias rubens* from each treatment to the following equation by Ries (2004): $Mg/Ca_C = S(0.000719T + 0.0292)Mg/Ca_{SW}^{0.668}$, where $_{SW}$—seawater, C—calcite (skeleton), T—temperature, S—species coefficient (*sensu* Ries, 2004, i.e. actual skeletal Mg/Ca of this species living in the wild divided by the theoretical Mg/Ca at selected temperature and seawater $Mg^{2+}/Ca^{2+}$ ratio; species coefficient calculated herein for *A. rubens* S = 0.994). It should be noted, however, that Ries' equation is typically applied to echinoid test plates. Calculations performed on asteroid-derived material should be therefore treated with caution.

## 2.5. Fossil specimens

Several well-preserved fossil asteroids were sampled in order to reconstruct paleoseawater $Mg^{2+}/Ca^{2+}$ ratio based on the Ries' algorithm which utilizes skeletal Mg/Ca ratios (see paragraph above) and our equation determined in this study ($Mg/Ca_C = 0.0207\ Mg/Ca_{SW} + 0.0191$ , see below). The Middle Jurassic (Callovian; Šaltiškiai, Lithuania) ossicles ascribed to the family Astropectinidae (from the "calcite sea"; i.e., $Mg^{2+}/Ca^{2+}_{sw}$ ~1.5) were provided by Faculty of Natural Sciences, University of Silesia in Katowice. They were collected from fine-grained grey sandy clays with rich benthic fauna belonging to the Papartinė formation (Salamon 2008). Sedimentology and fossil assemblages of this formation indicate a shallow sea depositional environment, with no evidence of anoxic conditions in the water column (Marynowski and Zatoń, 2010). The Miocene (Badenian; Korytnica, Poland) ossicles belonging to the order Paxillosida ($Mg^{2+}/Ca^{2+}_{sw}$ ~ 3.5; aragonite sea conditions) were provided by the Faculty of Geology, University of Warsaw. They were collected from the so-called Korytnica clays. These sediments were formed in a shallow marine bay, semi-isolated from the open sea (northernmost part of the Paratethys), somewhat similar to calm lagoons in Recent coral-reef atolls (Zagorsek et al., 2012).

The ossicles were slightly etched in formic acid and observed under Philips XL-20 Scanning Electron Microscope (Institute of Paleobiology of the Polish Academy of Sciences, Warsaw) to determine the presence of layered stereom, which is indicative of low degree of diagenetic structural alteration (Gorzelak et al., 2016). Additional examination under cathodoluminescence (CL) microscope revealed lack or dull luminescence in the areas selected for geochemical analysis, further confirming a good preservation of stereom (Figure 3). Furthermore, CAMECA SX100 electron microprobe analyses revealed no detectable Mn or other diagenetic elements (e.g., Fe) and no diagenetic depletion of trace elements (Sr and S) in these ossicles (*cf.* Brand and Morrison, 1987).

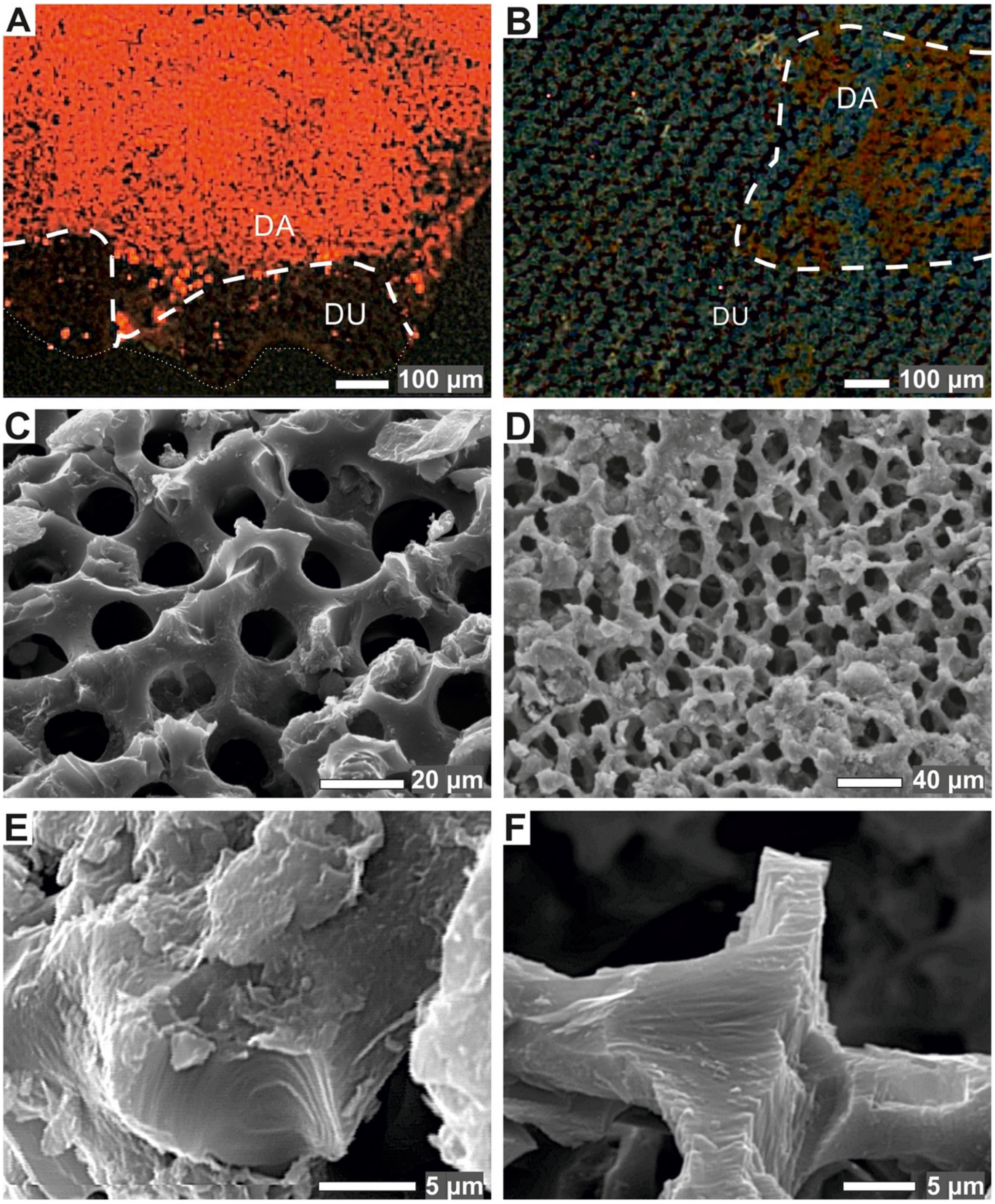

**Figure 3.** (A) Examples of CL images showing (A) dark, non-luminescent diagenetically unaltered (DU) fragment of stereom in Paxillosida indet. (Miocene, Korytnica) con- trasting with Mn-activated bright orange diagenetically altered (DA) region, (B) dark, diagenetically unaltered stereom trabeculae with Mn-activated orange blotchy structure in *Archastropecten* (?) sp. (Middle Jurassic (Callovian), Šaltiškiai). Preserved fragments of stereom trabeculae showing (C, D) meshy stereom structure and (E, F) layered growth (white arrows), observed under SEM in (C, E) Paxillosida indet. (Miocene, Korytnica), (D, F) *Archastropecten* (?) sp. (Middle Jurassic (Callovian), Šaltiškiai).

The measured Mg/Ca ratios in these ossicles were thus used for the reconstruction of paleoseawater $Mg^{2+}/Ca^{2+}$ ratios using three algorithms: (a) partition coefficient: $Mg/Ca_C = 0.03182(Mg/Ca_{SW})$ (Dickson, 2004), (b) equation determined in this study ($Mg/Ca_C = 0.0207 Mg/Ca_{SW} + 0.0191$, see below) and c) species-normalized Mg partition algorithm as a function of seawater $Mg^{2+}/Ca^{2+}$ ratio and temperature: $Mg/Ca_C = S(0.000719T + 0.0292)Mg/Ca_{SW}^{0.668}$ (Ries, 2004; where SW—seawater, C—skeletal calcite, T—temperature, S—species coefficient). For the latter equation, temperature data were taken from Brand (1986), and Scheiner et al. (2018) for the Callovian and Miocene respectively; species coefficients (*sensu* Ries, 2004) were calculated from the literature data on the skeletal Mg/Ca ratios (converted from $\%MgCO_3$) of extant relatives of the fossil taxa (Chave, 1954; Weber, 1969).

## 3. Results

### 3.1. Skeletal Mg/Ca and growth in *Ophiocomina nigra*

Mortality occurred in the first days of the experiment in all six specimens of *Ophiocomina nigra* cultured under the lowest $Mg^{2+}/Ca^{2+}$ ratio (~1.5 mol/mol). Additionally, some of the other specimens kept under lowered $Mg^{2+}/Ca^{2+}$ (~2.5 mol/mol) displayed signs of disc perforation (Figure 2B) and/or autotomy, which clearly indicated that they were stressed by the treatment (Dobson et al., 1991). Determination of new growth zones under CL was difficult in most cases due to uneven distribution of the CL-activated markers in the stereom (Figure 2C). The bright orange-red luminescence zones were often dispersed in the entire skeleton.

In two specimens, however, cultured under lowered $Mg^{2+}/Ca^{2+}$ ratio (~2.5 mol/mol) newly grown zones could be identified through abrupt decrease in Mg/Ca ratio (~0.08 mol/mol) observable in the most distal parts of the arms. Specimens grown under control $Mg^{2+}/Ca^{2+}$ ratio (~5.2 mol/mol) typically displayed higher skeletal Mg/Ca ratios (0.13-0.14 mol/mol; Table S1 in supplementary files).

However, the scarcity of geochemical data obtained from the specimens cultured under decreased $Mg^{2+}/Ca^{2+}$ ratio did not allow a reliable statistical assessment of the differences between treatments.

### 3.2. Skeletal Mg/Ca and growth in *Asterias rubens*

No mortality occurred in *Asterias rubens.* Mn-labeling and post-tagging growth fronts were detected in most of the investigated thin sections, which indicates that the sea stars grew during the experiment, although different orientation of the cut surface or uneven growth in the adjacent ossicles often did not allow the quantitative estimation of the actual growth rates.

Geochemical analyses performed on the newly grown skeleton show that sea stars cultured under lowered seawater $Mg^{2+}/Ca^{2+}$ ratio display lower skeletal Mg/Ca ratios compared with the control specimens ($p_{ANOVA} << 10^{-6}$; Figure 4).

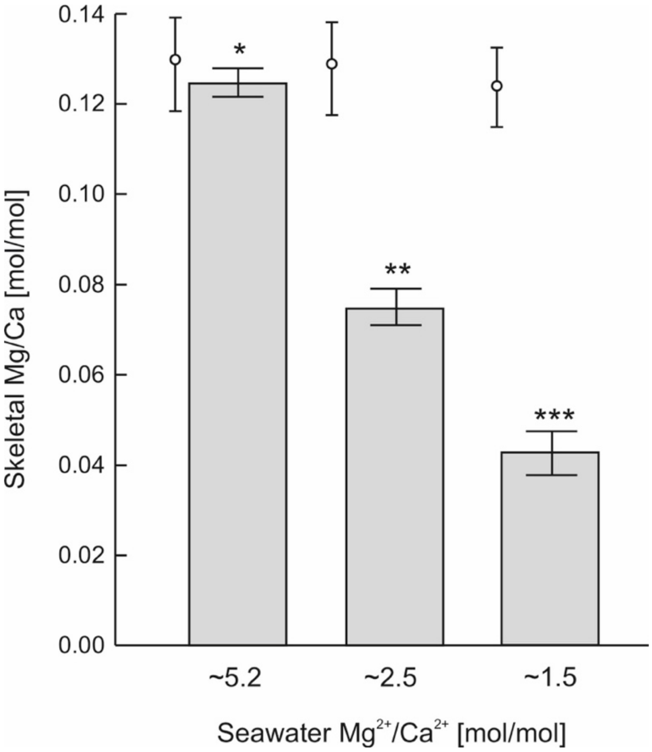

**Figure 4.** Mean Mg/Ca ratios (±SD) of skeletal components of *Asterias rubens* in three seawater $Mg^{2+}/Ca^{2+}$ treatments: ~5.2 mol/mol (n = 6), ~2.5 mol/mol (n = 5), ~1.5 mol/mol (n = 3). Asterisks denote statistically significant differences between treatments. Open circles indicate mean skeletal Mg/Ca ratios (±SD) obtained from the measurements of the pre-cultured stereom.

### 3.3. Respiration rate in *Asterias rubens*

Values measured from starfish specimens are presented in the Table 2. No significant effect of seawater $Mg^{2+}/Ca^{2+}$ ratio on respiration rate was found ($p_{ANOVA} = 0.89$). Time of exposure also had no significant effect on the respiration of individuals ($p_{ANOVA} = 0.86$).

**Table 2.** Measured respiration rates of *Asterias rubens* (n = 7) after 7, 14 and 21 days of exposure to three ambient $Mg^{2+}/Ca^{2+}$ ratios (high ~5.2, medium ~2.5, low ~1.5 [mol/mol]). No significant differences according to seawater $Mg^{2+}/Ca^{2+}$ ratio ($p_{ANOVA} = 0.89$) and time ($p_{ANOVA} = 0.86$) were recorded.

| Specimen | Seawater $Mg^{2+}/Ca^{2+}$ [mol/mol] | Respiration rate [$O_2$µmol/(h*g)] | | |
|---|---|---|---|---|
| | | Day 7 | Day 14 | Day 21 |
| 1 | ~5.2 | 0.201 | 0.219 | 0.150 |
| 2 | ~5.2 | 0.201 | 0.100 | 0.172 |
| 3 | ~5.2 | 0.313 | 0.170 | 0.174 |
| 4 | ~2.5 | 0.134 | 0.106 | 0.244 |
| 5 | ~2.5 | 0.248 | 0.182 | 0.147 |
| 6 | ~1.5 | 0.222 | 0.138 | 0.124 |
| 7 | ~1.5 | 0.098 | 0.349 | 0.221 |

### 3.4. Reconstruction error

For the experimental starfish, specimens cultured under control (~5.2 mol/mol) and lowered to ~2.5 (mol/mol) $Mg^{2+}/Ca^{2+}$ ratios, the ambient seawater reconstruction error (calculated from the algorithm involving skeletal Mg/Ca ratio, temperature and species coefficient; Ries, 2004) was very low (less than 2%). For the asteroids cultured under the lowest seawater $Mg^{2+}/Ca^{2+}$ ratio (~1.5 mol/mol), the discrepancy between the ambient and calculated theoretical values was higher, leading to a 39.7% error in the reconstruction (Table 3).

**Table 3.** Measured seawater $Mg^{2+}/Ca^{2+}$ ratios compared with the values reconstructed from skeletal Mg/Ca ratios in *Asterias rubens*. Based on Ries' (2004) algorithm for echinoid test plates: $Mg/Ca_C = S(0.000719\ T + 0.0292)Mg/Ca_{SW}^{0.668}$. SW – seawater, C – calcite, T – temperature, S – species coefficient (calculated from the known value of Mg/Ca of this specimen in the wild and T of the original environment).

| T | S | Measured $Mg/Ca_C$ (mean for treatment) | Measured $Mg^{2+}/Ca^{2}$ sw ratio (mean for treatment) | Calculated $Mg^{2+}/Ca^{2}$ sw ratio (mean for treatment) | Calculated reconstruction error (mean for treatment) |
|---|---|---|---|---|---|
| 17.7 | 0.994 | 0.125 | 5.16 | 5.16 | 0% |
| 17.8 | | 0.075 | 2.44 | 2.39 | 1.9% |
| 17.9 | | 0.043 | 1.44 | 1.03 | 39.7% |

3.5. Fossil specimens

Jurassic specimens are easily distinguishable from the Miocene ones due to their much lower Mg/Ca ratios (Table 4). Reconstructed Jurassic seawater $Mg^{2+}/Ca^{2+}$ ratios range from 1.2 to 1.82 mol/mol depending on the algorithm and specimen, whereas the Miocene $Mg^{2+}/Ca^{2+}$ ratios tend to be much higher (up to 6.48 mol/mol).

**Table 4.** Reconstructed values of seawater $Mg^{2+}/Ca^{2+}$ ratios for fossil asteroids (n specimens = 6) using different algorithms. Note that only Ries' equation is temperature-normalized. T – temperature, S – species coefficient, DcMg – Mg fractionation coefficient, SD – standard deviation. Temperature data were taken from Brand (1986), and Scheiner et al. (2018) for the Callovian and Miocene respectively, species coefficients were based on the data for *Astropecten andromeda* (from Chave, 1954) and the order Paxillosida (from Weber, 1969).

| Taxon | Sampling site | Age | T [C] | S | Skeletal Mg/Ca [mol/mol] ± SD | Seawater $Mg^{2+}/Ca^{2+}$ [mol/mol] (Dickson, 2004) | DcMg (mean skeletal Mg/Ca : sw $Mg^{2+}/Ca^{2+}$) | Seawater $Mg^{2+}/Ca^{2+}$ [mol/mol] (this study) | DcMg (mean skeletal Mg/Ca : sw $Mg^{2+}/Ca^{2+}$) | Seawater $Mg^{2+}/Ca^{2+}$ [mol/mol] including T and S (Ries, 2004) | DcMg (mean skeletal Mg/Ca : sw $Mg^{2+}/Ca^{2+}$) | Source of data for S calculation |
|---|---|---|---|---|---|---|---|---|---|---|---|---|
| Astropectinidae (*Archastropecten*?) | Šaltiškiai, Lithuania | Callovian, Middle Jurassic | 12.5 | 1.56 | 0.0567 ± 0.004 | 1.78 | 0.032 | 1.82 | 0.031 | 1.2 | 0.047 | Chave, 1954 (*Astropecten andromeda*) |
| Astropectinidae (*Archastropecten*?) | Šaltiškiai, Lithuania | Callovian, Middle Jurassic | 12.5 | 1.56 | 0.0565 ± 0.004 | 1.78 | 0.032 | 1.81 | 0.031 | 1.2 | 0.047 | Chave, 1954 (*Astropecten andromeda*) |
| Paxillosida indet. | Korytnica, Poland | Miocene, Neogene | 24.3 | 1.38 | 0.1533 ± 0.008 | 4.82 | 0.032 | 6.48 | 0.024 | 4.75 | 0.032 | Weber, 1969 (order Paxillosida) |
| Paxillosida indet. | Korytnica, Poland | Miocene, Neogene | 24.3 | 1.38 | 0.1426 ± 0.010 | 4.48 | 0.032 | 5.97 | 0.024 | 4.26 | 0.033 | Weber, 1969 (order Paxillosida) |
| Paxillosida indet. | Korytnica, Poland | Miocene, Neogene | 24.3 | 1.38 | 0.1518 ± 0.016 | 4.77 | 0.032 | 6.41 | 0.024 | 4.68 | 0.032 | Weber, 1969 (order Paxillosida) |
| Paxillosida indet. | Korytnica, Poland | Miocene, Neogene | 24.3 | 1.38 | 0.1445 ± 0.003 | 4.54 | 0.032 | 6.06 | 0.024 | 4.35 | 0.033 | Weber, 1969 (order Paxillosida) |

## 4. Discussion

Calcium carbonate polymorphs rich in magnesium dissolve faster in warmer and more acidic seawater, which suggests that magnesium can influence the dissolution rate of the skeleton post mortem in some benthic calcifiers (e.g., Ries et al., 2016). In echinoderms, magnesium participates in various processes, including skeletogenesis. For instance, it has been suggested that magnesium ions play a significant role in stabilization of amorphous calcium carbonate (ACC), the precursor to skeletal calcium carbonate (Addadi et al., 2003). Decreased magnesium concentration in sea water also affects the expression of skeletogenic genes (Martino et al., 2019) and magnesium concentration in the sea urchin tooth skeleton has an effect on the mechanical properties of calcite (Ma et al., 2008, 2009). Low ambient $Mg^{2+}/Ca^{2+}$ is also known to slow down calcification rates in sea urchins (*Prionocidaris baculosa* and *Psammechinus miliaris*; Kołbuk et al., 2020). Magnesium deprivation was expected to be also harmful for other echinoderms, including asterozoans. Indeed, the brittle star *Ophiocomina nigra* cultured under low ambient $Mg^{2+}/Ca^{2+}$ either died or commonly displayed arm autotomy, disc perforation, and growth impairment.

The manganese labeling in brittle stars proved to be less efficient than in asteroids due to the dispersed bright orange-red CL luminescence in the entire skeleton, possibly caused by increased $Mn^{2+}$ levels in the original environment. Even though Recent echinoderms are often non- or blue-luminescent (Barbin, 2000; Gorzelak et al., 2016), some echinoderm species collected from the offshore environments may occasionally display bright orange luminescent spots (e.g., Richter and Zinkernagel, 1981). Interestingly, in two specimens of brittle stars kept under lowered $Mg^{2+}/Ca^{2+}$ ratio, the new growth was observed through an abrupt change in skeletal Mg/Ca in the most distal parts of the arm, where, according to the distalization-intercalation model, new plates are formed during arm regeneration (e.g., Czarkwiani et al., 2016). Overall, all of the above suggests that brittle stars appear much more sensitive to changes in the seawater composition than sea urchins and asteroids. Although these sparse geochemical data may suggest that skeletal chemistry in brittle stars, as in the case of sea urchins and asteroids, may be also controlled by seawater chemistry, further experiments are needed to fully test this hypothesis.

Skeletal growth in sea stars is expressed mainly through the formation of the plates in the most distal parts of the arm (e.g., Fewkes 1888, Verrill, 1914; Ben Khadra et al., 2015), as well as thickening of already existing plates (Hotchkiss, 2012). This pattern was confirmed through manganese labeling (Figure 1). Newly formed skeleton of non-control specimens has significantly lower Mg/Ca ratios, thus corroborating the effect of ambient $Mg^{2+}/Ca^{2+}$ ratio on geochemical composition of the starfish skeleton.

Although the seawater composition has the prevalent role in echinoderm biomineralization, the ultimate skeletal Mg/Ca ratio is a result of a complex interplay between environmental and physiological factors. In echinoids, the Mg/Ca ratio in the stereom differs on several organizational levels, e.g., between orders, families, species, or on an individual scale (i.e., significant variation is detected between different ossicles within a single specimen or even within one ossicle; see Discussion in Gorzelak et al. 2013; Kołbuk et al., 2020). Other echinoderm classes, such as asteroids and ophiuroids, also display a wide range of Mg/Ca ratios, on higher taxonomic levels such as orders and families (Weber, 1969); additional variation can also occur between species (Duquette et al., 2018) from similar environmental conditions. Notably, comparison of Mg/Ca values obtained in a series of experiments on echinoids and asteroids showed that they displayed different magnesium fractionation curves, although it should be underlined that these specimens grew under different temperature conditions (Figure 5; Table S2 in supplementary files). Nonetheless, the skeletal Mg/Ca ratio cannot be solely ascribed to environmental conditions (Hermans et al., 2011; Asnaghi et al., 2014; Kołbuk et al., 2019, 2020). The physiological effect (“vital effect”) involved in magnesium incorporation and distribution in the skeleton can complicate reconstructions of ancient seawater $Mg^{2+}/Ca^{2+}$ ratio, and applying a single algorithm to different fossil echinoderms, without considering their physiology-based variation, may produce a significant reconstruction error (e.g., Table 3).

Interestingly, the chemical composition of seawater (concentrations of $Mg^{2+}$ and $Ca^{2+}$) of the environment in which echinoderms grow might itself be less stable than it was previously thought. Recently, Lebrato et al. (2020) challenged the long-standing assumption of a limited seawater $Mg^{2+}/Ca^{2+}$ variability. It has been long argued that the seawater $Mg^{2+}/Ca^{2+}$ ratio fluctuated on a temporal scale (in the Phanerozoic between ~1 and ~5.2 (mol/mol; e.g. Hardie, 1996)), but not on a spatial one. A uniform $Mg^{2+}/Ca^{2+}$ ratio is typically assumed for the entire global ocean due to the broad presumption that the residence times of Mg and Ca, are ∼13 Ma, and 1 Ma, respectively. However, a vast dataset collected by Lebrato et al. (2020) from various modern marine environments showed a significant variability for seawater $Mg^{2+}/Ca^{2+}$ ratio with respect to location, ecosystem and depth. For instance, in the upwelling and polar regions, shelves or river-influenced settings the seawater $Mg^{2+}/Ca^{2+}$ ratio ranges from ~4.4 to 6.4 mol/mol whereas these ratios in the open-ocean environment range from ~4.9 to ~5.3 mol/mol. This variability is explained by a complex system of removal and addition of $Ca^{2+}$ and $Mg^{2+}$ to seawater, that is strongly dependent on the spatiotemporal scale, with additional relation to other geochemical or biological parameters of the environment (e.g., total alkalinity or presence of calcifying communities). It is thus clear that such variability occurred also in the past, which may question the use of calcifying organisms as proxies of "global" $Mg^{2+}/Ca^{2+}$ trends in the Phanerozoic. Naturally, not all fossils used in paleoenvironmental studies originated from more stable, "semi-conservative" open-ocean conditions; many specimens come from the areas more prone to $Mg^{2+}/Ca^{2+}$ shifts, e.g., coasts, river-influenced areas, or shelves. such as the Jurassic or Miocene sea stars used in this study (which grew in the basins semi-isolated from open waters, i.e., in the epicontinental sea connected to the Tethys ocean or in the northernmost parts of the Paratethys basin, respectively). Herein, the reconstructions of the paleoseawater $Mg^{2+}/Ca^{2+}$ based on fossil specimens are generally consistent with low $Mg^{2+}/Ca^{2+}$ seawater ratio in the Jurassic ("calcite sea") and high $Mg^{2+}/Ca^{2+}$ ratio in the Miocene ("aragonite sea"). The variations in the temperature-normalized reconstructed $Mg^{2+}/Ca^{2+}$ ratios are lower than for the sea urchins from the same periods (see table 4 in Kołbuk et al., 2020), which may be caused by the aforementioned Mg fractionation within sea urchins, observed for instance on an individual level (between and within ossicles). In asteroids differences in Mg content between ossicles are weaker than in echinoids (Weber, 1973; Borremans et al., 2009). Differences in control abilities of the $Mg^{2+}$ concentration in the coelomic fluid (CF) between sea stars and sea urchins could also account for the lower variations recorded in asteroids. Indeed, sea urchin species significantly differ in their abilities to control magnesium concentration in their CF, with some species maintaining an almost constant concentration whatever the sea water $Mg^{2+}$ concentration (Santos et al., 2013). On the contrary the CF $Mg^{2+}$ concentration in sea stars is much closer to the sea water $Mg^{2+}$ concentration in studied species (Diehl and Lawrence, 1984). This would point to a higher control capacity in some sea urchin species. Interestingly, this is similar to the acid-base balancing abilities of sea urchins, some being able to compensate their extracellular pH (and this parallels the abilities to control the CF $Mg^{2+}$ concentration) (Collard et al., 2013, Di Giglio et al., 2020). On the contrary, sea stars studied so far are unable to compensate their extracellular pH when facing low pH sea water (Dupont and Thorndyke, 2012; Collard et al., 2013). In experimental studies, the intrapopulation variation in Mg content also appears to be larger in echinoids than in asteroids (Figure 5). Comparison of reconstructions based on asteroids and echinoids from the same geological period and using the same algorithms reveals significant discrepancy in paleoseawater $Mg^{2+}/Ca^{2+}$ ratio, which is visible especially in the case of the Miocene specimens, obtained from the same geologic formation deposited in the same part of the basin. For instance, the temperature-normalized reconstructed paleoseawater $Mg^{2+}/Ca^{2+}$ ratio based on skeletal Mg/Ca in asteroids is around 4.5 mol/mol, while the ratio reconstructed from sea urchins is generally much lower (~3-3.3 mol/mol; Kołbuk et al., 2020).

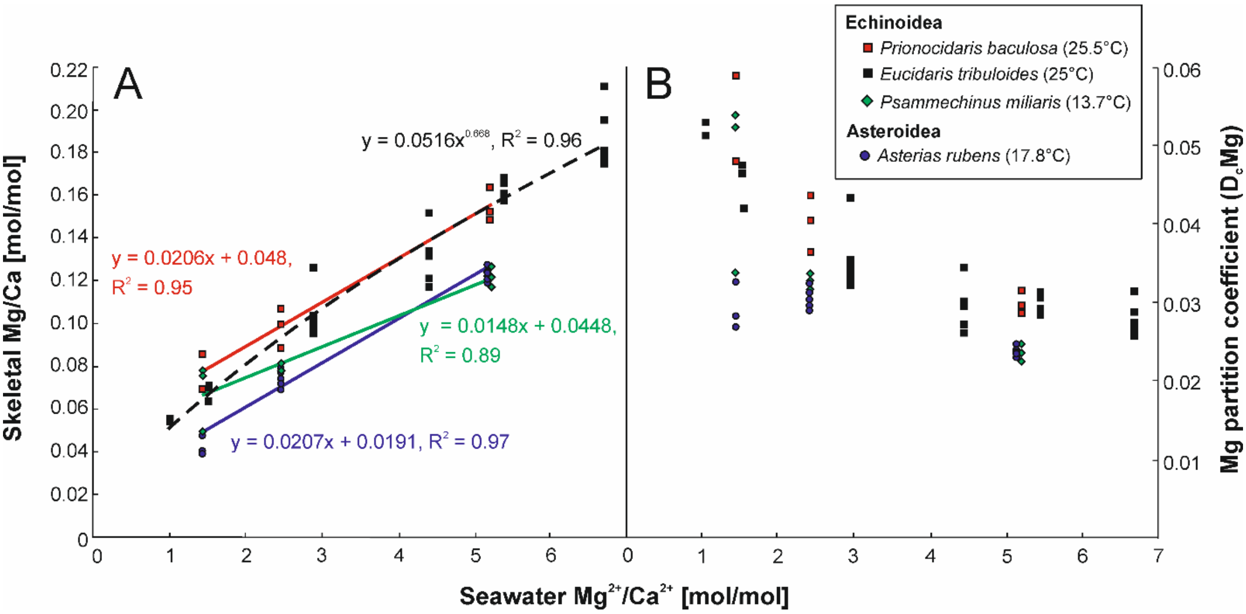

**Figure 5.** (A) Magnesium fractionation curves and (B) partition coefficients for the ossicles of four echinoderm species kept under different $Mg^{2+}/Ca^{2+}$ seawater ratios with the indication of temperature during the experiments: ambital plates (galleried stereom) of *Prionocidaris baculosa* kept in T = 25.5°C (red squares; Kołbuk et al., 2020), coronal plates of *Eucidaris tribuloides* kept in T = 25°C (black squares; Ries, 2004), ambital plates (galleried stereom) of *Psammechinus miliaris* kept in T = 13.7°C (green diamonds; Kołbuk et al., 2020), various arm ossicles of *Asterias rubens* kept in T = 17.8°C (blue circles; this study).

Notwithstanding the effects of other environmental controls (temperature, salinity) and physiology (vital effect) or diet, which may affect skeletal Mg/Ca ratio in echinoderms, geochemical data obtained from fossil echinoderms from a specific location may give an insight into the local environmental conditions at that particular time and place. Regardless, mean skeletal Mg/Ca values calculated from several well-preserved fossil species from a given period might still reflect "global" conditions, and confirm secular variation in seawater Mg/Ca during the Phanerozoic (calcite-aragonite seas).

## 5. Conclusions

In this study we confirmed for the first time the effect of ambient seawater $Mg^{2+}/Ca^{2+}$ ratio on skeletal Mg/Ca ratio in asteroids. Sea stars cultured under decreased seawater $Mg^{2+}/Ca^{2+}$ ratio exhibited lower skeletal Mg/Ca ratios compared with the control specimens. However, a comparison of several echinoderm species belonging to different classes showed a significant physiology-based variation in skeletal Mg/Ca ratios on different organizational levels (inter-class, inter- and intra-species, and inter- and intra-individual), producing different magnesium fractionation curves. The presence of the physiological factor (vital effect) imposes limitations on the use of well-preserved echinoderm fossils in paleoseawater $Mg^{2+}/Ca^{2+}$ ratio reconstructions, which themselves can be also biased with respect to the local environment.

**Acknowledgements.** We thank our colleagues from the Marine Biology Laboratory (Université Libre de Bruxelles) for aid during the experiment, Urszula Radwańska (University of Warsaw) and Mariusz Salamon (University of Silesia in Katowice) for providing fossil specimens, Michał Loba (University of Warsaw) for identifying fossil asteroids. We are grateful to the handling editor (Christian France-Lanord) and two referees (Justin Ries from Northeastern University and an anonymous reviewer) for their constructive comments.

This research was funded by the National Science Centre (NCN) grant no. 2016/23/B/ST10/00990 and was performed in part in the NanoFun laboratory co-financed by the European Regional Development Fund within the Innovation Economy Operational Programme POIG.02.02.00–00-025/09, and at the Micro-Area Analysis and Chemical Laboratories, Polish Geological Institute—National Research Institute in Warsaw. Ph. Dubois is a Research Director of the National Fund for Scientific Research (FRS-FNRS; Belgium).

All experiments on live asteroids and ophiuroids were performed in Brussels (Belgium), where no ethics approval is required for the maintenance and handling of echinoderms. Nevertheless, our research followed the ethical principles of replacement, reduction, refinement and minimization of animal suffering following the guidelines reported in the European Directive 2010/63/EU.

## References

Addadi, L., Raz, S., & Weiner, S. (2003). Taking advantage of disorder: amorphous calcium carbonate and its roles in biomineralization. *Advanced Materials*, 15(12), 959-970.

Asnaghi, V., Mangialajo, L., Gattuso, J. P., Francour, P., Privitera, D., & Chiantore, M. (2014). Effects of ocean acidification and diet on thickness and carbonate elemental composition of the test of juvenile sea urchins. *Marine Environmental Research*, 93, 78–84.

Barbin, V. (2000). Cathodoluminescence of carbonate shells: biochemical vs diagenetic process. In Cathodoluminescence in geosciences (pp. 303-329). Springer, Berlin, Heidelberg.

Barbin, V., Ramseyer, K., & Elfman, M. (2008). Biological record of added manganese in seawater: a new efficient tool to mark in vivo growth lines in the oyster species *Crassostrea gigas. International Journal of Earth Sciences*, 97(1), 193-199.

Ben Khadra, Y., Ferrario, C., Benedetto, C. D., Said, K., Bonasoro, F., Candia Carnevali, M. D., & Sugni, M. (2015). Re-growth, morphogenesis, and differentiation during starfish arm regeneration. *Wound Repair and Regeneration*, 23(4), 623-634.

Ben Khadra, Y., Sugni, M., Ferrario, C., Bonasoro, F., Oliveri, P., Martinez, P., & Carnevali, M. D. C. (2018). Regeneration in stellate echinoderms: Crinoidea, Asteroidea and Ophiuroidea. In *Marine organisms as model systems in biology and medicine* (pp. 285-320). Springer, Cham.

Borremans, C., Hermans, J., Baillon, S., André, L., & Dubois, P. (2009). Salinity effects on the Mg/Ca and Sr/Ca in starfish skeletons and the echinoderm relevance for paleoenvironmental reconstructions. *Geology*, 37(4), 351–354.

Brand, U. (1986). Paleoenvironmental analysis of Middle Jurassic (Callovian) ammonoids from Poland: trace elements and stable isotopes. *Journal of Paleontology*, 293-301.

Brand, U., & Morrison, J. O. (1987). Diagenesis and pyritization of crinoid ossicles. *Canadian Journal of Earth Sciences*, 24(12), 2486-2498.

Chave, K. (1954). Aspects of the biogeochemistry of magnesium.1- Calcareous marine organisms. *Journal of Geology*, 62(3), 266–283.

Clarke, F. W., & Wheeler, W. C. (1922). The inorganic constituents of marine invertebrates (Vol. 124). US Government Printing Office.

Collard, M., Laitat, K., Moulin, L., Catarino, A. I., Grosjean, P., & Dubois, P. (2013). Buffer capacity of the coelomic fluid in echinoderms. *Comparative Biochemistry and Physiology Part A: Molecular & Integrative Physiology*, 166(1), 199-206.

Czarkwiani, A., Ferrario, C., Dylus, D. V., Sugni, M., & Oliveri, P. (2016). Skeletal regeneration in the brittle star *Amphiura filiformis. Frontiers in Zoology*, 13(1), 18.

Del Valls, T. A., & Dickson, A. G. (1998). The pH of buffers based on 2-amino-2-hydroxymethyl-1,3-propanediol ('tris') in synthetic sea water. *Deep Sea Research Part I: Oceanographic Research Papers*, 45(9), 1541–1554.

Di Giglio, S., Spatafora, D., Milazzo, M., M'Zoudi, S., Zito, F., Dubois, P., & Costa, C. (2020). Are control of extracellular acid-base balance and regulation of skeleton genes linked to resistance to ocean acidification in adult sea urchins? *Science of the Total Environment*, 720, 137443.

Dickson, J. A. D. (2002). Fossil Echinoderms As Monitor of the Mg/Ca Ratio of Phanerozoic Oceans. *Science*, 298(5596), 1222–1224.

Dickson, J. A. D. (2004). Echinoderm skeletal preservation; calcite-aragonite seas and the Mg/Ca ratio of Phanerozoic oceans. *Journal of Sedimentary Research*, 74(3), 355–365.

Diehl, W. J., & Lawrence, J. M. (1984). The effect of salinity on coelomic fluid osmolyte concentration and intracellular water content in *Luidia clathrata* (Say)(Echinodermata: Asteroidea). *Comparative Biochemistry and Physiology Part A: Physiology,* 79(1), 119-126.

Dobson, W. E., Stancyk, S. E., Clements, L. A., & Showman, R. M. (1991). Nutrient Translocation during Early Disc Regeneration in the Brittlestar *Microphiopholis gracillima* (Stimpson) (Echinodermata: Ophiuroidea). *The Biological Bulletin*, 180(1), 167–184.

Donachy, J. E., & Watabe, N. (1986). Effects of salinity and calcium concentration on arm regeneration by *Ophiothrix angulata* (Echinodermata: Ophiuroidea). *Marine Biology*, 91(2), 253-257.

Dubois, P., & Jangoux, M. (1990). Stereom morphogenesis and differentiation during regeneration of adambulacral spines of *Asterias rubens* (Echinodermata, Asteroida). *Zoomorphology*, 109(5), 263-272.

Dupont, S., & M. Thorndyke (2012). Relationship between CO2-driven changes in extracellular acid–base balance and cellular immune response in two polar echinoderm species. *Journal of Experimental Marine Biology and Ecology* 424: 32-37.

Duquette, A., Halanych, K. M., Angus, R. A., & McClintock, J. B. (2018). Inter and intraspecific comparisons of the skeletal Mg/Ca ratios of high latitude Antarctic echinoderms. *Antarctic Science*, 30(3), 160.

*Fewkes, J. W. (1888). On the development of calcareous plates of Asterias*. Bulletin of the Museum of Comparative Zoology*, 17, 1-56.*

Gooding, R. A., Harley, C. D., & Tang, E. (2009). Elevated water temperature and carbon dioxide concentration increase the growth of a keystone echinoderm. *Proceedings of the National Academy of Sciences*, 106(23), 9316-9321.

Gorzelak, P., Dery, A., Dubois, P., & Stolarski, J. (2017). Sea urchin growth dynamics at microstructural length scale revealed by Mn-labeling and cathodoluminescence imaging. *Frontiers in Zoology*, 14(1), 42.

Gorzelak, P., Krzykawski, T., & Stolarski, J. (2016). Diagenesis of echinoderm skeletons: constraints on paleoseawater Mg/Ca reconstructions. *Global and Planetary Change*, 144, 142-157.

Gorzelak, P., Stolarski, J., Mazur, M., & Meibom, A. (2013). Micro- to nanostructure and geochemistry of extant crinoidal echinoderm skeletons. *Geobiology*, 11(1), 29–43.

Hardie, L. A. (1996). Secular variation in seawater chemistry: An explanation for the coupled secular variation in the mineralogies of marine limestones and potash evaporites over the past 600 my. *Geology*, *24*(3), 279-283.

Hasiuk, F. J., & Lohmann, K. C. (2010). Application of calcite Mg partitioning functions to the reconstruction of paleocean Mg/Ca. *Geochimica et Cosmochimica Acta*, 74(23), 6751–6763.

Hawkes, G. P., Day, R. W., Wallace, M. W., Nugent, K. W., Bettiol, A. A., Jamieson, D. N., & Williams, M. C. (1996). Analyzing the growth and form of mollusc shell layers, in situ, by cathodoluminescence microscopy and Raman spectroscopy. *Journal of Shellfish Research*, 15(3), 659-666.

Hermans, J., André, L., Navez, J., Pernet, P., & Dubois, P. (2011). Relative influences of solution composition and presence of intracrystalline proteins on magnesium incorporation in calcium carbonate minerals: Insight into vital effects. *Journal of Geophysical Research: Biogeosciences*, 116(1), 1–10.

Hermans, J., Borremans, C., Willenz, P., André, L., & Dubois, P. (2010). Temperature, salinity and growth rate dependences of Mg/Ca and Sr/Ca ratios of the skeleton of the sea urchin *Paracentrotus lividus* (Lamarck): An experimental approach. *Marine Biology*, 157(6), 1293–1300.

Higuchi, T., Shirai, K., Mezaki, T., & Yuyama, I. (2017). Temperature dependence of aragonite and calcite skeleton formation by a scleractinian coral in low mMg/Ca seawater. *Geology*, 45(12), 1087-1090.

Hotchkiss, F. H. (2012). Growth zones and extraxial-axial skeletal homologies in Asteroidea (Echinodermata). *Proceedings of the Biological Society of Washington*, 125(2), 106-121.

Iglikowska, A., Najorka, J., Voronkov, A., Chełchowski, M., & Kukliński, P. (2017). Variability in magnesium content in Arctic echinoderm skeletons. *Marine Environmental Research*, 129, 207–218.

Kołbuk, D., Dubois, P., Stolarski, J., & Gorzelak, P. (2019). Effects of seawater chemistry ($Mg^{2+}/Ca^{2+}$ ratio) and diet on the skeletal Mg/Ca ratio in the common sea urchin *Paracentrotus lividus. Marine Environmental Research,* 145, 22-26.

Kołbuk, D., Di Giglio, S., M'Zoudi, S., Dubois, P., Stolarski, J., & Gorzelak, P. (2020). Effects of seawater $Mg^{2+}/Ca^{2+}$ ratio and diet on the biomineralization and growth of sea urchins and the relevance of fossil echinoderms to paleoenvironmental reconstructions. *Geobiology*, 18(6), 710-724.

Lartaud, F., De Rafélis, M., Ropert, M., Emmanuel, L., Geairon, P., & Renard, M. (2010). Mn labelling of living oysters: artificial and natural cathodoluminescence analyses as a tool for age and growth rate determination of *C. gigas* (Thunberg, 1793) shells. *Aquaculture*, 300(1-4), 206-217.

Lebrato, M., Andersson, A. J., Ries, J. B., Aronson, R. B., Lamare, M. D., Koeve, W., Oschlies, A., Iglesias-Rodriguez, M. D., Thatje, S., Amsler, M., Vos, S. C., Jones, D. O. B., Ruhl, H. A., Gates, A. R. & McClintock, J. B. (2016). Benthic marine calcifiers coexist with CaCO3-undersaturated seawater worldwide. *Global Biogeochemical Cycles*, 30(7), 1038-1053.

Lebrato, M., Garbe-Schönberg, D., Müller, M. N., Blanco-Ameijeiras, S., Feely, R. A., Lorenzoni, L., Molinero, J.-C., Bremer, K., Jones, D. O. B., Iglesias-Rodriguez, D., Greeley, D., Lamare, M. D., Paulmier, A., Graco, M., Cartes, J., Barcelos e Ramos, J., de Lara, A., Sanchez-Leal, R., Jimenez, P., Paparazzo, F. E., Hartman, S. E., Westernströer, U., Küter, M., Benavides, R., da Silva, A. F., Bell, S., Payne, C., Olafsdottir, S., Robinson, K., Jantunen, L. M., Korablev, A., Webster, R. J., Jones, E. M., Gilg, O., Bailly du Bois, P., Beldowski, J., Ashjian, C., Yahia, N. D., Twining, B., Chen, X. G., Tseng, L. C., Hwang, J. S., Dahms, H. U. & Oschlies, A. (2020). Global variability in seawater Mg: Ca and Sr: Ca ratios in the modern ocean. *Proceedings of the National Academy of Sciences*, 117(36), 22281-22292.

Ma, Y., Cohen, S. R., Addadi, L., & Weiner, S. (2008). Sea Urchin Tooth Design: An "All-Calcite" Polycrystalline Reinforced Fiber Composite for Grinding Rocks. *Advanced Materials*, 20(8), 1555-1559.

Ma, Y., Aichmayer, B., Paris, O., Fratzl, P., Meibom, A., Metzler, R. A., Politi, Y., Addadi, L., Gilbert, P.U.P.A., & Weiner, S. (2009). The grinding tip of the sea urchin tooth exhibits exquisite control over calcite crystal orientation and Mg distribution. *Proceedings of the National Academy of Sciences*, 106(15), 6048-6053.

Martino, C., Chiarelli, R., Roccheri, M. C., Matranga, V., & Byrne, M. (2019). Effects of magnesium deprivation on development and biomineralization in the sea urchin *Arbacia lixula. Invertebrate Reproduction and Development,* 163 (3): 165-176.

Marynowski, L., & Zatoń, M. (2010). Organic matter from the Callovian (Middle Jurassic) deposits of Lithuania: compositions, sources and depositional environments. *Applied Geochemistry*, 25(7), 933-946.

McClintock, J. B., Amsler, M. O., Angus, R. A., Challener, R. C., Schram, J. B., Amsler, C. D., Mah, C. L., Cuce, J., & Baker, B. J. (2011). The Mg-calcite composition of Antarctic echinoderms: Important implications for predicting the impacts of ocean acidification. *The Journal of Geology*, 119(5), 457-466.

Millero, F. J., & Huang, F. (2009). The density of seawater as a function of salinity (5 to 70 g kg−1) and temperature (273.15 to 363.15 K). *Ocean Science*, 5(2), 91–100.

Millero, F. J., & Poisson, A. (1981). International one-atmosphere equation of state of seawater. *Deep Sea Research Part A. Oceanographic Research Papers*, 28(6), 625–629.

Richter, D. K., & Zinkernagel, U. (1981). Zur Anwendung der Kathodolumineszenz in der Karbonatpetrographie. *Geologische Rundschau*, 70(3), 1276-1302.

Ries, J. B. (2004). Effect of ambient Mg/Ca ratio on Mg fractionation in calcareous marine invertebrates: A record of the oceanic Mg/Ca ratio over the Phanerozoic. *Geology*, 32(11), 981–984.

Ries, J. B., Ghazaleh, M. N., Connolly, B., Westfield, I., & Castillo, K. D. (2016). Impacts of seawater saturation state (ΩA= 0.4–4.6) and temperature (10, 25 C) on the dissolution kinetics of whole-shell biogenic carbonates. *Geochimica et Cosmochimica Acta*, 192, 318-337.

Salamon, M. A. (2008). The Callovian (Middle Jurassic) crinoids from northern Lithuania. Paläontologische Zeitschrift, 82(3), 269-278.

Santos, I. A., Castellano, G. C., & Freire, C. A. (2013). Direct relationship between osmotic and ionic conforming behavior and tissue water regulatory capacity in echinoids. *Comparative Biochemistry and Physiology Part A: Molecular & Integrative Physiology*, 164(3), 466-476.

Scheiner, F., Holcová, K., Milovský, R., & Kuhnert, H. (2018). Temperature and isotopic composition of seawater in the epicontinental sea (Central Paratethys) during the Middle Miocene Climate Transition based on Mg/Ca, δ18O and δ13C from foraminiferal tests. *Palaeogeography, Palaeoclimatology, Palaeoecology*, 495, 60-71.

Sköld, H. N., Baden, S. P., Looström, J., Eriksson, S. P., & Hernroth, B. E. (2015). Motoric impairment following manganese exposure in asteroid echinoderms. *Aquatic Toxicology*, 167, 31-37.

Sköld, M., & Rosenberg, R. (1996). Arm regeneration frequency in eight species of Ophiuroidea (Echinodermata) from European sea areas. *Journal of Sea Research*, 35(4), 353-362.

Verrill, A. E. (1914). Monograph of the shallow-water starfishes of the North Pacific coast from the Arctic Ocean to California. Smithsonian Institution.

Weber, J. N. (1969). The incorporation of magnesium into the skeletal calcites of echinoderms. *American Journal of Science*, 267(5), 537–566.

Weber, J. N. (1973). Temperature dependence of magnesium in echinoid and asteroid skeletal calcite: a reinterpretation of its significance. *The Journal of Geology*, 81(5), 543–556.

Wilkinson, B. H., & Algeo, T. J. (1989). Sedimentary carbonate record of calcium-magnesium cycling. *American Journal of Science*, 289(10), 1158-1194.

Wood, H. L., Spicer, J. I., Lowe, D. M., & Widdicombe, S. (2010). Interaction of ocean acidification and temperature; the high cost of survival in the brittlestar *Ophiura ophiura*. *Marine Biology*, 157(9), 2001-2013.

Zagorsek, K., Radwańska, U., & Radwański, A. (2012). Bryozoa from the Korytnica Basin (Middle Miocene; Holy Cross Mountains, Central Poland). Bulletin of Geosciences, 87(2), 201-218.

SUPPLEMENTARY FILES

**Table S1.** List of specimens used in the experiment. Nominal $Mg^{2+}/Ca^{2+}$_sw represent three treatments, mean Mg/Ca ratios in ossicles – mean Mg/Ca values measured in the newly formed skeleton of the experimental specimens. SD – standard deviation. Asterisk indicates data collected from the pre-cultured asteroid skeletons (mean skeletal Mg/Ca ± SD).

| Specimen | Species | Nominal $Mg^{2+}/Ca^{2+}$_sw [mol/mol] | Mean Mg/Ca ratio [mol/mol] in ossicles | SD |
|---|---|---|---|---|
| A1 | *Ophiocomina nigra* | 5.2 | 0.142 | 0.009 |
| A2 | *Ophiocomina nigra* | 5.2 | 0.135 | 0.012 |
| A3 | *Ophiocomina nigra* | 5.2 | 0.139 | 0.004 |
| A4 | *Ophiocomina nigra* | 5.2 | 0.140 | 0.01 |
| A5 | *Ophiocomina nigra* | 5.2 | NA | NA |
| A6 | *Ophiocomina nigra* | 5.2 | 0.146 | 0.003 |
| B1 | *Ophiocomina nigra* | 2.5 | NA | NA |
| B2 | *Ophiocomina nigra* | 2.5 | 0.084 | 0.004 |
| B3 | *Ophiocomina nigra* | 2.5 | NA | NA |
| B4 | *Ophiocomina nigra* | 2.5 | NA | NA |
| B5 | *Ophiocomina nigra* | 2.5 | 0.081 | 0.003 |
| B6 | *Ophiocomina nigra* | 2.5 | NA | NA |
| D1-6* | *Asterias rubens* | 5.2 | 0.129 | 0.011 |
| D1 | *Asterias rubens* | 5.2 | 0.119 | 0.006 |
| D2 | *Asterias rubens* | 5.2 | 0.122 | 0.008 |
| D3 | *Asterias rubens* | 5.2 | 0.127 | 0.009 |
| D4 | *Asterias rubens* | 5.2 | 0.128 | 0.005 |
| D5 | *Asterias rubens* | 5.2 | 0.127 | 0.007 |
| D6 | *Asterias rubens* | 5.2 | 0.125 | 0.008 |
| E1-6* | *Asterias rubens* | 2.5 | 0.128 | 0.010 |
| E1 | *Asterias rubens* | 2.5 | 0.080 | 0.002 |
| E2 | *Asterias rubens* | 2.5 | 0.075 | 0.004 |
| E3 | *Asterias rubens* | 2.5 | 0.073 | 0.009 |
| E4 | *Asterias rubens* | 2.5 | 0.069 | 0.006 |
| E5 | *Asterias rubens* | 2.5 | 0.077 | 0.003 |
| E6 | *Asterias rubens* | 2.5 | NA | NA |
| F1-6* | *Asterias rubens* | 1.5 | 0.123 | 0.009 |
| F1 | *Asterias rubens* | 1.5 | NA | NA |
| F2 | *Asterias rubens* | 1.5 | NA | NA |
| F3 | *Asterias rubens* | 1.5 | NA | NA |
| F4 | *Asterias rubens* | 1.5 | 0.040 | 0.04 |
| F5 | *Asterias rubens* | 1.5 | 0.048 | 0.048 |
| F6 | *Asterias rubens* | 1.5 | 0.039 | 0.039 |

**Table S2.** Environmental conditions (T – temperature, sal – salinity, MgCa_sw – seawater $Mg^{2+}/Ca^{2+}$) in sea urchin experiments, including geochemical data on measured skeletal Mg/Ca and calculated DcMg - partition coefficients (cf. Figure 5B).

| Species | T [*C] | Sal | Mg/Ca_sw [mol/mol] | Mg/Ca_skeleton_mean [mol/mol] | DcMg |
|---|---|---|---|---|---|
| *Psammechinus miliaris* (details in Kołbuk et al., 2020) | 13.6 | 32.7 | 5.2 | 0.127 | 0.024 |
| | 13.6 | 32.7 | 5.2 | 0.122 | 0.024 |
| | 13.6 | 32.7 | 5.22 | 0.117 | 0.022 |
| | 13.6 | 32.7 | 2.43 | 0.078 | 0.032 |
| | 13.7 | 32.7 | 2.43 | 0.078 | 0.032 |
| | 13.7 | 32.7 | 2.44 | 0.081 | 0.033 |
| | 13.6 | 32.8 | 1.45 | 0.076 | 0.052 |
| | 13.6 | 32.8 | 1.45 | 0.078 | 0.054 |
| | 13.6 | 32.8 | 1.45 | 0.049 | 0.034 |
| *Prionocidaris baculosa* (details in Kołbuk et al., 2020) | 25.5 | 32.9 | 5.2 | 0.164 | 0.032 |
| | 25.5 | 32.9 | 5.2 | 0.153 | 0.029 |
| | 25.5 | 32.9 | 5.2 | 0.150 | 0.029 |
| | 25.5 | 32.9 | 2.45 | 0.089 | 0.036 |
| | 25.4 | 32.9 | 2.45 | 0.107 | 0.044 |
| | 25.4 | 32.9 | 2.45 | 0.100 | 0.041 |
| | 25.4 | 33 | 1.45 | 0.086 | 0.059 |
| | 25.5 | 33 | 1.45 | 0.070 | 0.048 |
| *Asterias rubens* (this study) | 17.7 | 32.9 | 5.2 | 0.119 | 0.023 |
| | 17.7 | 32.9 | 5.2 | 0.122 | 0.024 |
| | 17.7 | 32.9 | 5.2 | 0.127 | 0.024 |
| | 17.7 | 32.9 | 5.2 | 0.128 | 0.025 |
| | 17.7 | 32.9 | 5.2 | 0.127 | 0.024 |
| | 17.7 | 32.9 | 5.2 | 0.125 | 0.024 |
| | 17.8 | 32.9 | 2.44 | 0.080 | 0.033 |
| | 17.8 | 32.9 | 2.44 | 0.075 | 0.031 |
| | 17.8 | 32.9 | 2.44 | 0.073 | 0.030 |
| | 17.8 | 32.9 | 2.44 | 0.070 | 0.029 |
| | 17.8 | 32.9 | 2.44 | 0.077 | 0.032 |
| | 17.9 | 32.9 | 1.44 | 0.040 | 0.028 |
| | 17.9 | 32.8 | 1.44 | 0.048 | 0.033 |
| | 17.9 | 32.9 | 1.44 | 0.039 | 0.027 |
| *Eucidaris tribuloides* | 25 | NA | for high-resolution graph of Mg/Ca calcite vs Mg/Ca sw please refer to Ries (2004, 2010) | | |

# Conclusions

- Representatives of echinoderm classes (echinoids, ophiuroids and asteroids) cultured in artificial seawater with decreased $Mg^{2+}/Ca^{2+}$ ratio produced skeleton with decreased Mg/Ca ratio.

- Additionally, echinoids fed on Mg-enriched diet displayed higher skeletal Mg content in their skeleton.

- These results have potential consequences for paleoenvironmental reconstructions of ancient seawater $Mg^{2+}/Ca^{2+}$ ratio from echinoderm skeletal Mg/Ca ratio. Seawater was often considered the only source of ions in biomineralization, which prompted the use of well-preserved fossil echinoderm ossicles as a reliable proxy of secular $Mg^{2+}/Ca^{2+}$ changes of the Phanerozoic seawater. This work shows for the first time that the bias introduced by diet in the seawater $Mg^{2+}/Ca^{2+}$ reconstructed from sea urchins can reach up to 64.5%.

- Due to low Mg/Ca variation in the skeleton of sea stars, they appear to be a more precise seawater $Mg^{2+}/Ca^{2+}$ proxy than sea urchins.

- The Mg/Ca ratio in the skeletal calcite of echinoderms can vary on various taxonomic levels (between class, family, species), within a single specimen (depending on the ossicle type), or even within a single ossicle (depending on the type of stereom). This implies that the reconstruction of the seawater $Mg^{2+}/Ca^{2+}$ ratio based on Mg/Ca obtained from the echinoderm skeleton may be affected by errors resulting not only from the diet effect, but also from physiological variation (vital effects). Thus, application of a single Mg fractionation algorithm to all echinoderms (in particular to extinct groups) is problematic.

## Future perspectives

1) In addition to short-term experiments, typically revealing phenotypic plasticity, long-term experiments can be planned in order to observe the long-term effect of seawater $Mg^{2+}/Ca^{2+}$ on the biomineralization and minimize the effect of “shock” of the treatment. Increased experimental duration allows more time for shifts in gene-expression, revealing more chronic (perhaps even evolutionary) responses. Additionally, since the paleoseawater chemical variations involved not only fluctuations in $Mg^{2+}/Ca^{2+}$ ratio, but also in $Sr^{2+}$ and $SO_4^{2-}$ concentrations, it would be interesting to test the synergistic effect of these parameters on echinoderm biomineralization. Experiments with geologically adequate levels of these ions can be further developed.

2) In order to expand and generalize the results obtained in this PhD thesis to the phylum Echinodermata, additional experiments on other echinoderm classes may be performed. For instance, due to their importance and abundance in the fossil record, crinoids are worth investigating. However, their culturing is still much more difficult than in the case of echinoids or asterozoans.

3) Considering the effect of the Mg-enriched diet on echinoderm skeleton, labeling experiments with tagged diet and subsequent cryofixation and scanning electron microscopy observations are worth performing in order to visualize the cellular pathways of dietary magnesium transport to the mineralization sites.

# Declarations

Name and surname: Dorota Kołbuk

Affiliation: Instytut Paleobiologii im. R. Kozłowskiego Polskiej Akademii Nauk

The undersigned co-author hereby confirms her contribution to the work as stated below:

- ☐ Paper: Kołbuk, D., Dubois, P., Stolarski, J., & Gorzelak, P. (2019). Effects of seawater chemistry ($Mg^{2+}/Ca^{2+}$ ratio) and diet on the skeletal Mg/Ca ratio in the common sea urchin *Paracentrotus lividus. Marine Environmental Research*, 145, 22-26.

  Description of the contribution: Data analysis, interpretation of the results, writing the early draft of the manuscript, preparation of the illustrations.

  Estimated contribution in percentage: 55%

- ☐ Paper: Kołbuk, D., Di Giglio, S., M'Zoudi, S., Dubois, P., Stolarski, J., & Gorzelak, P. (2020). Effects of seawater $Mg^{2+}/Ca^{2+}$ ratio and diet on the biomineralization and growth of sea urchins and the relevance of fossil echinoderms to paleoenvironmental reconstructions. *Geobiology*, 18(6), 710-724.

  Description of the contribution: Concept/design, conducting the experiment, data analysis/interpretation, drafting of the manuscript, preparation of the illustrations.

  Estimated contribution in percentage: 60%

- ☐ Paper: Kołbuk, D., Dubois, P., Stolarski, J., & Gorzelak, P. (2021). Impact of seawater $Mg^{2+}/Ca^{2+}$ on Mg/Ca of asterozoan skeleton–Evidence from culturing and the fossil record. *Chemical Geology*, 584, 120557. (previous title: Impact of seawater $Mg^{2+}/Ca^{2+}$ ratio on Mg/Ca composition of asterozoan skeleton – evidence from recent experiments and the fossil record).

  Description of the contribution: Concept/design, conducting the experiment, data analysis/interpretation, drafting of the manuscript, preparation of the illustrations.

  Estimated contribution in percentage: 70%

08.10.2021
**Data**

Dorota Kołbuk
**Podpis**

# Co-author statement

Name and surname: Przemysław Gorzelak

Affiliation: Instytut Paleobiologii im. R. Kozłowskiego Polskiej Akademii Nauk

The undersigned co-author hereby confirms his contribution to the work as stated below:

☐ Paper: Kołbuk, D., Dubois, P., Stolarski, J., & Gorzelak, P. (2019). Effects of seawater chemistry ($Mg^{2+}/Ca^{2+}$ ratio) and diet on the skeletal Mg/Ca ratio in the common sea urchin *Paracentrotus lividus. Marine Environmental Research*, 145, 22-26.

Description of the contribution: Concept/design, assistance in conducting experiment, planning, intellectual contribution, draft editing

Estimate contribution in percentage: 20%

☐ Paper: Kołbuk, D., Di Giglio, S., M'Zoudi, S., Dubois, P., Stolarski, J., & Gorzelak, P. (2020). Effects of seawater $Mg^{2+}/Ca^{2+}$ ratio and diet on the biomineralization and growth of sea urchins and the relevance of fossil echinoderms to paleoenvironmental reconstructions. *Geobiology*, 18(6), 710-724.

Description of the contribution: Concept/design, supervision, intellectual contribution, draft editing

Estimate contribution in percentage: 15%

☐ Paper: Kołbuk, D., Dubois, P., Stolarski, J., & Gorzelak, P. (2021). Impact of seawater $Mg^{2+}/Ca^{2+}$ on Mg/Ca of asterozoan skeleton–Evidence from culturing and the fossil record. *Chemical Geology*, 584, 120557. (previous title: Impact of seawater $Mg^{2+}/Ca^{2+}$ ratio on Mg/Ca composition of asterozoan skeleton – evidence from recent experiments and the fossil record).

Description of the contribution: Concept/design, supervision, intellectual contribution, draft editing

Estimate contribution in percentage: 15%

20.10.2021
**Date**

**Signature**

# Co-author statement

Name and surname: Jarosław Stolarski

Affiliation: Instytut Paleobiologii im. R. Kozłowskiego Polskiej Akademii Nauk

The undersigned co-author hereby confirms his contribution to the work as stated below:

☐ Paper: Kołbuk, D., Dubois, P., Stolarski, J., & Gorzelak, P. (2019). Effects of seawater chemistry ($Mg^{2+}/Ca^{2+}$ ratio) and diet on the skeletal Mg/Ca ratio in the common sea urchin *Paracentrotus lividus. Marine Environmental Research*, 145, 22-26.

Description of the contribution: Intellectual contribution, editing

Estimate contribution in percentage: 10%

☐ Paper: Kołbuk, D., Di Giglio, S., M'Zoudi, S., Dubois, P., Stolarski, J., & Gorzelak, P. (2020). Effects of seawater $Mg^{2+}/Ca^{2+}$ ratio and diet on the biomineralization and growth of sea urchins and the relevance of fossil echinoderms to paleoenvironmental reconstructions. *Geobiology*, 18(6), 710-724.

Description of the contribution: Intellectual contribution, editing

Estimate contribution in percentage: 5%

☐ Paper: Kołbuk, D., Dubois, P., Stolarski, J., & Gorzelak, P. (2021). Impact of seawater $Mg^{2+}/Ca^{2+}$ on Mg/Ca of asterozoan skeleton–Evidence from culturing and the fossil record. *Chemical Geology*, 584, 120557. (previous title: Impact of seawater $Mg^{2+}/Ca^{2+}$ ratio on Mg/Ca composition of asterozoan skeleton – evidence from recent experiments and the fossil record).

Description of the contribution: Intellectual contribution, editing

Estimate contribution in percentage: 5%

21 November 2021

**Date** **Signature**

# Co-author statement

Name and surname: Philippe Dubois

Affiliation: Université Libre de Bruxelles

The undersigned co-author hereby confirms his contribution to the work as stated below:

- ☐ Paper: Kołbuk, D., Dubois, P., Stolarski, J., & Gorzelak, P. (2019). Effects of seawater chemistry ($Mg^{2+}/Ca^{2+}$ ratio) and diet on the skeletal Mg/Ca ratio in the common sea urchin *Paracentrotus lividus. Marine Environmental Research*, 145, 22-26.

  Description of the contribution: mentorship and consultation, paper revision prior to submission

  Estimate contribution in percentage: 15%

- ☐ Paper: Kołbuk, D., Di Giglio, S., M'Zoudi, S., Dubois, P., Stolarski, J., & Gorzelak, P. (2020). Effects of seawater $Mg^{2+}/Ca^{2+}$ ratio and diet on the biomineralization and growth of sea urchins and the relevance of fossil echinoderms to paleoenvironmental reconstructions. *Geobiology*, 18(6), 710-724.

  Description of the contribution: mentorship and consultation, paper revision prior to submission

  Estimate contribution in percentage: 10%

- ☐ Paper: Kołbuk, D., Dubois, P., Stolarski, J., & Gorzelak, P. Impact of seawater $Mg^{2+}/Ca^{2+}$ ratio on Mg/Ca composition of asterozoan skeleton – evidence from recent experiments and the fossil record (in review, *Chemical Geology*).

  Description of the contribution: mentorship and consultation, paper revision prior to submission

  Estimate contribution in percentage: 10%

**Date** **Signature**

May 11th, 2021

# Co-author statement

Name and surname: Sarah Di Giglio

Affiliation: Université Libre de Bruxelles

The undersigned co-author hereby confirms her contribution to the work as stated below:

☐ Paper: Kołbuk, D., Di Giglio, S., M'Zoudi, S., Dubois, P., Stolarski, J., & Gorzelak, P. (2020). Effects of seawater $Mg^{2+}/Ca^{2+}$ ratio and diet on the biomineralization and growth of sea urchins and the relevance of fossil echinoderms to paleoenvironmental reconstructions. *Geobiology*, 18(6), 710-724.

Description of the contribution: Assistance in conducting experimental research

Estimate contribution in percentage: 5%

Bruxelles, 14th May 2021

**Date** **Signature**

# Co-author statement

Name and surname: Saloua M'Zoudi

Affiliation: Université Libre de Bruxelles

The undersigned co-author hereby confirms her contribution to the work as stated below:

☐ Paper: Kołbuk, D., Di Giglio, S., M'Zoudi, S., Dubois, P., Stolarski, J., & Gorzelak, P. (2020). Effects of seawater $Mg^{2+}/Ca^{2+}$ ratio and diet on the biomineralization and growth of sea urchins and the relevance of fossil echinoderms to paleoenvironmental reconstructions. *Geobiology*, 18(6), 710-724.

Description of the contribution: Assistance in conducting experimental research

Estimate contribution in percentage: 5%

12. 05. 2021

**Date**

**Signature**